December 2013

www.arctic.noaa.gov/reportcard

Citing the complete report:
Jeffries, M. O., J. A. Richter-Menge, and J. E. Overland, Eds., 2013: Arctic Report Card 2013, http://www.arctic.noaa.gov/reportcard.

Citing an essay (example):
Derksen, C. and R. Brown, 2013: Snow [in Arctic Report Card 2013], http://www.arctic.noaa.gov/reportcard.

Table of Contents

Authors and Affiliations

A. Arendt, Geophysical Institute, University of Alaska Fairbanks, Fairbanks, AK, USA

I. Ashik, Arctic and Antarctic Research Institute, St. Petersburg, Russia

G. Bernhard, Biospherical Instruments, San Diego, CA

U.S. Bhatt, Geophysical Institute, University of Alaska Fairbanks, Fairbanks, AK, USA

P.A. Bieniek, International Arctic Research Center, University of Alaska Fairbanks, AK, USA

B.A. Bluhm, School of Fisheries and Ocean Sciences, University of Alaska Fairbanks, Fairbanks, AK, USA

J.E. Box, Geological Survey of Denmark and Greenland, Copenhagen, Denmark

M.S. Bret-Harte, Institute of Arctic Biology, University of Alaska Fairbanks, Fairbanks, AK, USA

L.C. Brown, Climate Research Division, Environment Canada, Downsview, ON, Canada

R. Brown, Climate Research Division, Environment Canada, Montreal, PQ, Canada

D. Burgess, Geological Survey of Canada, Ottawa, ON, Canada

J.F. Burkhart, University of Oslo, Department of Geosciences, 0316 Oslo, Norway

Y. Cao, Ocean University of China, Qingdao, China

J. Cappelen, Danish Meteorological Institute, Copenhagen, Denmark

E. Chan, Environment Canada, Atmospheric Science and Technology Directorate, Toronto, ON, Canada

H.H. Christiansen, Geology Department, University Centre in Svalbard, UNIS, Norway
Institute of Geography and Geology, University of Copenhagen, Denmark

J.S. Christiansen, Department of Arctic and Marine Biology, UiT The Arctic University of Norway, Tromsø, Norway

B.W. Coad, Canadian Museum of Nature, P.O. Box 3443, Station D, Ottawa, ON, Canada

J.G. Cogley, Department of Geography, Trent University, Peterborough, ON, Canada

J. Comiso, Cryospheric Sciences Branch, NASA Goddard Space Flight Center, Greenbelt, MD, USA

C. Cox, Cooperative Institute for Research in Environmental Sciences, University of Colorado, Boulder, CO, USA

M. Daase, Norwegian Polar Institute, Fram Centre, Tromsø, Norway

A. Dahlback, Department of Physics, University of Oslo, Norway

C. Derksen, Climate Research Division, Environment Canada, Toronto, ON, Canada

D.S. Drozdov, Earth Cryosphere Institute, Tyumen, Russia

C. Duguay, Interdisciplinary Centre on Climate Change & Department of Geography and Environmental Management, University of Waterloo, Waterloo, ON, Canada

J. Eamer, Eamer Science Services, Jackpine Street, Gabriola Island, BC, Canada

K. Eleftheriadis, Institute of Nuclear and Radiological Science & Technology, Energy & Safety N.C.S.R. "Demokritos" 15310 Ag. Paraskevi, Attiki, Greece

H.E. Epstein, Department of Environmental Sciences, University of Virginia, Charlottesville, VA, USA

X. Fettweis, Department of Geography, University of Liege, Liege, Belgium

V. Fioletov, Environment Canada, Toronto, Ontario, Canada

B.C. Forbes, Arctic Centre, University of Lapland, Rovaniemi, Finland

I. Frolov, Arctic and Antarctic Research Institute, St. Petersburg, Russia

G.V. Frost, Department of Environmental Sciences, University of Virginia, Charlottesville, VA, USA

M.-L. Geai, Department of Earth and Atmospheric Science, University of Alberta, Edmonton, AB, Canada

S. Gerland, Norwegian Polar Institute, Fram Centre, Tromsø, Norway

R. Gradinger, School of Fisheries and Ocean Sciences, University of Alaska Fairbanks, Fairbanks, AK, USA

J.-U. Grooß, Forschungszentrum Jülich, Jülich, Germany

A.R. Gruzdev, Wrangel Island State Nature Reserve, Pevek, Chukchi Autonomous Region, Russia

A. Gunn, Roland Road, Salt Spring Island, BC, Canada

H.K. Ha, Korea Polar Research Institute, Incheon, Republic of Korea

E. Hanna, Department of Geography, University of Sheffield, Sheffield, UK

I. Hanssen-Bauer, Norwegian Meteorological Institute, Blindern, 0313 Oslo, Norway

K.J. Hedges, Department of Arctic and Marine Biology, UiT The Arctic University of Norway, Tromsø, Norway

A. Heikkilä, Finnish Meteorological Institute, Helsinki, Finland

S. Hendricks, Alfred Wegener Institute, Bremerhaven, Germany

H. Hop, Norwegian Polar Institute, Fram Centre, Tromsø, Norway

K. Iken, School of Fisheries and Ocean Sciences, University of Alaska Fairbanks, Fairbanks, AK, USA

R. Ingvaldsen, Institute of Marine Research, Bergen, Norway

A. Jefferson, NOAA ESRL, Boulder, CO, USA

T. Jensen, Geological Survey of Denmark and Greenland, Copenhagen, Denmark

G.J. Jia, Institute of Atmospheric Physics, Chinese Academy of Sciences, Beijing, China

B. Johnsen, Norwegian Radiation Protection Authority, Østerås, Norway

K.-K. Kang, Interdisciplinary Centre on Climate Change & Department of Geography and Environmental Management, University of Waterloo, Waterloo, ON, Canada

O.V. Karamushko, Murmansk Marine Biological Institute, Kola Science Centre, Russian Academy of Sciences, Murmansk, Russia

J. Key, Center for Satellite Applications and Research, NOAA/NESDIS, Madison, WI, USA

H. Kheyrollah Pour, Interdisciplinary Centre on Climate Change & Department of Geography and Environmental Management, University of Waterloo, Waterloo, ON, Canada

A.L. Kholodov, Geophysical Institute, University of Alaska Fairbanks, Fairbanks, Alaska, USA

T. Kikuchi, Japan Agency for Marine-Earth Science and Technology, Tokyo, Japan

B.-M. Kim, Korea Polar Research Institute, Incheon, Republic of Korea

S.-J. Kim, Korea Polar Research Institute, Incheon, Republic of Korea

T.W. Kim, Korea Polar Research Institute, Incheon, Republic of Korea

T. Koskela, Finnish Meteorological Institute, Helsinki, Finland

R. Krishfield, Woods Hole Oceanographic Institution, Woods Hole, MA, USA

K. Lakkala, Finnish Meteorological Institute, Arctic Research Centre, Sodankylä, Finland

R.R. Lauth, Alaska Fisheries Science Center, National Marine Fisheries Service, NOAA, 7600 Sand Point Way NE, Seattle, WA, U.S.A.

Y. Liu, Cooperative Institute for Meteorological Satellite Studies, University of Wisconsin, Madison, WI, USA

H. Loeng, Institute of Marine Research, Bergen, Norway

K. Luojus, Arctic Research Centre, Finnish Meteorological Institute, 99600 Sodankylä, Finland

A. Lynghammar, Department of Arctic and Marine Biology, UiT The Arctic University of Norway, Tromsø, Norway

M. Macias-Fauria, Department of Zoology, University of Oxford, Oxford, UK

M.C. Mack, Department of Biology, University of Florida, Gainesville, FL, USA

S.A. MacPhee, Fisheries and Oceans Canada, 501 University Crescent, Winnipeg, MB, Canada

A.R. Majewski, Fisheries and Oceans Canada, 501 University Crescent, Winnipeg, MB, Canada

G. Manney, Jet Propulsion Laboratory, California Institute of Technology, Pasadena, CA, U.S.A.
New Mexico Institute of Mining and Technology, Socorro, NM, U.S.A.

S.S. Marchenko, Geophysical Institute, University of Alaska Fairbanks, Fairbanks, Alaska, USA

C.W. Mecklenburg, California Academy of Sciences, San Francisco, CA & Point Stephens Research, Auke Bay, AK, USA

W. Meier, NASA Goddard Space Flight Center, Greenbelt, MD, USA

T. Mote, Department of Geography, University of Georgia, Athens, GA, USA

F.J. Mueter, University of Alaska Fairbanks, School of Fisheries and Ocean Sciences, Fairbanks, AK, USA

R. Müller, Forschungszentrum Jülich, Jülich, Germany

R. Myneni, Department of Earth and Environment, Boston University, Boston, MA, USA

M. Nicolaus, Alfred Wegener Institute, Bremerhaven, Germany

S. Nishino, Japan Agency for Marine-Earth Science and Technology, Tokyo, Japan

N.G. Oberman, MIRECO Mining Company, Syktyvkar, Russia

J.A. Ogren, NOAA ESRL, Boulder, CO, USA

J. Overland, NOAA/PMEL, Seattle, WA, USA

D. Perovich, ERDC - CRREL, 72 Lyme Road, Hanover USA
Thayer School of Engineering, Dartmouth College, Hanover, NH, USA

R. Pickart, Woods Hole Oceanographic Institution, Woods Hole, MA, USA

J. Pinzon, Biospheric Science Branch, NASA Goddard Space Flight Center, Greenbelt, MD, USA

I.V. Polyakov, International Arctic Research Center, University of Alaska Fairbanks, Fairbanks, AK, USA
Department of Atmospheric Sciences, University of Alaska Fairbanks, Fairbanks, AK, USA

M. Poulin, Research and Collections Division, Canadian Museum of Nature, Ottawa, ON, Canada

P.K. Quinn, NOAA PMEL, Seattle, WA, USA

B. Rabe, Alfred Wegener Institute, Bremerhaven, Germany

M.K. Raynolds, Institute of Arctic Biology, University of Alaska Fairbanks, Fairbanks, AK, USA

J.D. Reist, Fisheries and Oceans Canada, 501 University Crescent, Winnipeg, MB, Canada

A.K. Rennermalm, Department of Geography, Rutgers, The State University of New Jersey, New Brunswick, NJ, USA

P. Reynolds, Fairbanks, AK, USA

J. Richter-Menge, ERDC - CRREL, 72 Lyme Road, Hanover USA

A.V. Rocha, Department of Biological Sciences, University of Notre Dame, Notre Dame, IN, USA

V.E. Romanovsky, Geophysical Institute, University of Alaska Fairbanks, Fairbanks, Alaska, USA

D.E. Russell, Yukon College, Whitehorse, YT, Canada

C.D. Sawatzky, Fisheries and Oceans Canada, 501 University Crescent, Winnipeg, MB, Canada

U. Schauer, Alfred Wegener Institute, Bremerhaven, Germany

P. Schlosser, Lamont-Doherty Earth Observatory of Columbia University, Palisades, NY, USA

I. Semiletov, International Arctic Research Center, University of Alaska Fairbanks, Fairbanks, AK, USA

N. Shakhova, International Arctic Research Center, University of Alaska Fairbanks, Fairbanks, AK, USA

S. Sharma, Environment Canada, Atmospheric Science and Technology Directorate, Toronto, ON, Canada

M. Sharp, Department of Earth and Atmospheric Science, University of Alberta, Edmonton, AB, Canada

G.R. Shaver, The Ecosystems Center, Marine Biological Laboratory, Woods Hole, MA, USA

N. I. Shiklomanov, Department of Geography, George Washington University, Washington, DC, USA

T.P. Sipko, Institute of Ecology and Evolution, Russian Academy of Sciences, Moscow, Russia

W.M. Smethie, Lamont-Doherty Earth Observatory of Columbia University, Palisades, NY, USA

L.C. Smith, Department of Geography, University of California Los Angeles, CA, USA

S.L. Smith, Geological Survey of Canada, Natural Resources Canada, Ottawa, ON, Canada

V. Sokolov, Arctic and Antarctic Research Institute, St. Petersburg, Russia

J.E. Søreide, The University Centre in Svalbard, Norway

M. Steele, Applied Physics Laboratory, University of Washington, Seattle, WA, USA

R. Stone, Global Monitoring Division, NOAA/ESRL, Boulder, CO, USA
Cooperative Institute for Research in Environmental Sciences, University of Colorado, Boulder, CO, USA

D.A. Streletskiy, Department of Geography, George Washington University, Washington, DC, USA

J. Su, Ocean University of China, Qingdao, China

T. Svendby, Norwegian Institute for Air Research, Kjeller, Norway

M. Tedesco, The City College of New York, New York, NY, USA

M.-L. Timmermans, Yale University, New Haven, CT, USA

J. Toole, Woods Hole Oceanographic Institution, Woods Hole, MA, USA

M. Tschudi, Aerospace Engineering Sciences, University of Colorado, Boulder, CO, USA

C.J. Tucker, Biospheric Science Branch, NASA Goddard Space Flight Center, Greenbelt, MD, USA

R.S.W. van de Wal, Institute for Marine and Atmospheric Research Utrecht, Utrecht University, The Netherlands

J. Wahr, Department of Physics and CIRES, University of Colorado, Boulder, CO, USA

V. Walden, Department of Civil and Environmental Engineering, Washington State University, Pullman, WA, USA

D.A. Walker, Institute of Arctic Biology, University of Alaska Fairbanks, Fairbanks, AK, USA

J. Walsh, International Arctic Research Center, University of Alaska Fairbanks, Fairbanks, AK, USA

M. Wang, Joint Institute for the Study of the Atmosphere and Ocean, University of Washington, Seattle, WA, USA

W. Williams, Institute of Ocean Sciences, Sidney, BC, Canada

G. Wolken, Alaska Division of Geological and Geophysical Surveys, Fairbanks, AK, USA

R. Woodgate, Applied Physics Laboratory, University of Washington, Seattle, WA, USA

B. Wouters, School of Geographical Sciences, University of Bristol, Bristol, UK

L. Xu, Institute of the Environment and Sustainability, University of California Los Angeles, Los Angeles, C.A., USA

H. Zeng, Institute of Atmospheric Physics, Chinese Academy of Sciences, Beijing, China

J. Zhao, Ocean University of China, Qingdao, China

W. Zhong, Ocean University of China, Qingdao, China

S. Zimmermann, Institute of Ocean Sciences, Sidney, BC, Canada

Executive Summary

November 21, 2013

Overview

The Arctic Report Card (www.arctic.noaa.gov/reportcard/) considers a wide range of environmental observations throughout the Arctic, and is updated annually. The 2013 update to the Report Card illustrates the significant effects of year-to-year and regional variability, which overlie the impacts of the persistent warming trend that began over 30 years ago. For instance, after a record-setting year in 2012, relatively cool air temperatures in summer 2013 across the central Arctic Ocean, Greenland and northern Canada facilitated an increase in the summer sea ice extent and a decrease in the extent and duration of melting at the surface of the Greenland ice sheet. In contrast, summer 2013 was one of the warmest on record in Alaska, where new record high temperatures were set at some permafrost observatories, and Fairbanks, in the center of the state, experienced a record 36 days with temperatures of 27°C or higher.

A second key point in Report Card 2013 is that the longer-term impacts of the warming climate on the physical environment are influencing the Arctic terrestrial and marine ecosystems. Evidence is seen from the foundations through the upper levels of the food web. The ability to more effectively measure, monitor, document and attribute these changes depends on a continued increase in the number of comprehensive research surveys and sustained long-term observing programs.

Highlights

In early 2013, the Northern Hemisphere-wide spring snow cover extent (SCE) was lower than the observed average for the period 1967-2013. In May, a new record low SCE occurred in Eurasia and in June the North American SCE was the fourth lowest on record. These conditions were driven by rapid snow melt, rather than anomalously low snow accumulation prior to melt onset, and can be linked to the regional distribution of surface air temperature and circulation patterns. New record high permafrost temperatures at a depth of 20 meters below the surface were also set in summer 2013 at permafrost observatories on the North Slope of Alaska, in the Brooks Range, Alaska, and in the High Canadian Arctic, where measurements began in the late 1970s.

While fewer new record-setting events occurred in 2013 compared to 2012, the impacts of the persistent warming trend of over 30 years remain clearly evident. For instance, while the minimum summer extent of the Arctic sea ice cover in September 2013 exceeded the record low of 2012, it still ranked as the sixth lowest summer minimum extent since observations began in 1979, and the seven lowest ice extents since 1979 have occurred in the last seven years (2007-2013). In the upper Arctic Ocean, relatively high freshwater and heat contents continued to be observed in 2013 in the Beaufort Gyre region of the Canada Basin. Immediately adjacent to the Arctic Ocean, in regions where there are large areas of summer open water and widespread above-average sea surface temperatures, tundra vegetation greenness (a measure of productivity) and growing season length have continued to increase since observations began in 1982. Also on land, lake ice break-up in spring 2013 was earlier than average throughout much of the Arctic, and ice duration was shorter than average in many regions. In Greenland, further extensive melting occurred at the surface of the ice sheet, where the

maximum melt extent and average melt extent were at or above the average over the 30-year period of record.

The response of the physical environment system to the persistent warming temperatures is having an impact on the marine ecosystem. Responses of Arctic benthic communities to climate and anthropogenic factors are being observed as shifts in species distribution patterns and in the appearance of new (to the Arctic) species. Some of the changes in the characteristics of the Arctic benthic and community structure are likely related to recent changes in food supplied via primary production, which can be linked to the rapid and dramatic loss of the sea ice cover. New fish species have also been reported in several areas, especially the Canadian Beaufort Sea, which likely represents both altered distributions resulting from climate change and previously occurring but undetected species.

As with the marine environment, the assessment of climate change impacts on arctic wildlife is complicated because these land-based communities respond to a host of other factors, including disease, hunting rates and changes to management regimes. Consequently, studies of large land mammals convey a mixed message. Regional surveys of muskoxen indicate that their numbers have mostly stabilized or increased since the 1970s, following strategic introductions and conservation efforts. In contrast, many caribou and reindeer herds are currently at relatively low numbers. Recovery of these herds is difficult to predict, given the cyclic nature of the abundance of these herds and their complex interactions in a warming climate.

Acknowledgments

The Arctic Report Card is supported by the Arctic Research Program in the NOAA Climate Program Office. The preparation of Arctic Report Card 2013 was directed by a U.S. inter-agency editorial team of representatives from NOAA, the Cold Regions Research and Engineering Laboratory and the U.S. Arctic Research Commission. The 18 essays in Report Card 2013, representing the collective effort of an international team of 147 researchers in 14 countries, are based on published and ongoing scientific research. Independent, peer-review of the scientific content of the Report Card was facilitated by the Arctic Monitoring and Assessment (AMAP) Program of the Arctic Council. The Circumpolar Biodiversity Monitoring Program (CBMP), the cornerstone program of the Conservation of Arctic Flora and Fauna (CAFF) Working Group of the Arctic Council, provides leadership on the ecosystem elements of the Report Card.

Atmosphere Summary

Section Coordinator: James E. Overland

National Oceanographic and Atmospheric Administration,
Pacific Marine Environmental Laboratory, Seattle, WA, USA

November 21, 2013

The Atmosphere section includes reports on Air Temperature, Cloud Cover and Surface Radiation, Ozone, UV Radiation and Black carbon (soot). Surface Radiation and Black Carbon are new topics that appear for the first time in the Arctic Report Card.

The Arctic atmosphere showed considerable spatial and seasonal variability during the period from fall 2012 through summer 2013. For January-August 2013, air temperatures in the Arctic relaxed from the high extremes seen during the last five years, but remained warmer than all but one year since the beginning of the 20th century.

Fall 2012 was anomalously warm over the Arctic Ocean and adjacent lands after the record sea ice loss in summer 2012. Spring 2013 temperatures were cooler than normal in North America and Greenland, and warmer than average in Eurasia, leading to record early snow loss in Eurasia. Except for Alaska, air temperatures in summer were anomalously low across most of the Arctic, consistent with more sea ice and less melting at the surface of the Greenland ice sheet than occurred in the extraordinary summer of 2012. Increased summer cloud cover and its effect on surface radiation had an overall cooling effect, and may have contributed to the larger sea ice extent in 2013.

At several locations in the high Arctic, UV levels were below the long-term average for prolonged periods between February and May of 2013. This was primarily due to high ozone levels, which were higher than the average of the last decade because of a very early stratospheric sudden warming event in January 2013. Black carbon (a short-lived climate forcer that affects the radiation balance in the Arctic by absorbing solar radiation when suspended in the atmosphere) has declined by 55% and 45% since the early 1990s at Alert (Nunavut, Canada) and Barrow (Alaska, USA), respectively, which have the longest records of atmospheric black carbon concentrations in the Arctic. These declines are related to decreasing emissions due to the economic collapse in the former Soviet Union during the early 1990s.

Air Temperature

J. Overland[1], E. Hanna[2] , I. Hanssen-Bauer[3], B.-M. Kim[4], S.-J. Kim[4], J. Walsh[5], M. Wang[6], U. Bhatt[7]

[1]NOAA/PMEL, Seattle, WA, USA
[2]Department of Geography, University of Sheffield, Sheffield, UK
[3]Norwegian Meteorological Institute, Blindern, 0313 Oslo, Norway
[4]Korea Polar Research Institute, Incheon, Republic of Korea
[5]International Arctic Research Center, University of Alaska Fairbanks, Fairbanks, AK, USA
[6]Joint Institute for the Study of the Atmosphere and Ocean, University of Washington, Seattle, WA, USA
[7]Geophysical Institute, University of Alaska Fairbanks, Fairbanks, AK, USA

November 26, 2013

Highlights

- Fall 2012 was anomalously warm over the Arctic Ocean and adjacent lands after the record sea ice loss in summer 2012.
- Anomalously low winter temperatures in Eurasia were followed by anomalously high spring temperatures in Eurasia and the adjacent Arctic Ocean, while anomalously high winter temperatures over the central Arctic Ocean, Greenland and Baffin Bay were followed by anomalously low spring temperatures in Greenland, northern Canada and Alaska.
- The summer 2013 mean sea level pressure field was characteristic of a positive Arctic Oscillation/North Atlantic Oscillation. Consequently, relative to the previous six years, air temperatures were anomalously low across the central Arctic Ocean, Greenland and northern Canada. In contrast, summer 2013 in Alaska was one of the warmest on record.

Mean Annual Surface Air Temperature

Calendar year 2012 is the most recent year for which data are available for all months. The mean annual air temperature in 2012 was slightly lower than in 2011, but it was still sixth warmest year observed in the Arctic since the early 20th Century (**Fig. 1**). At the time of writing, the period January-August 2013 was the second warmest such period on record since the beginning of the 20th Century.

The first twelve years of the 21st Century (2001-2012) have been much warmer than the 1971-2000 baseline period at the end of the 20th Century (**Fig. 2**). Positive (warm) anomalies occurred in all parts of the Arctic, an indication that the early 21st Century temperature increase is due to global warming rather than natural regional variability (Jeffries et al. 2013). Over a longer time interval, the annual mean surface air temperature over Arctic land areas has experienced a warming of about +2°C since the mid-1960s (**Fig. 1**). This temperature increase is a manifestation of "Arctic Amplification", which is characterized by increases 1.5°C greater than (more than double) the increases at lower latitudes (Overland et al. 2011, Stroeve et al. 2012).

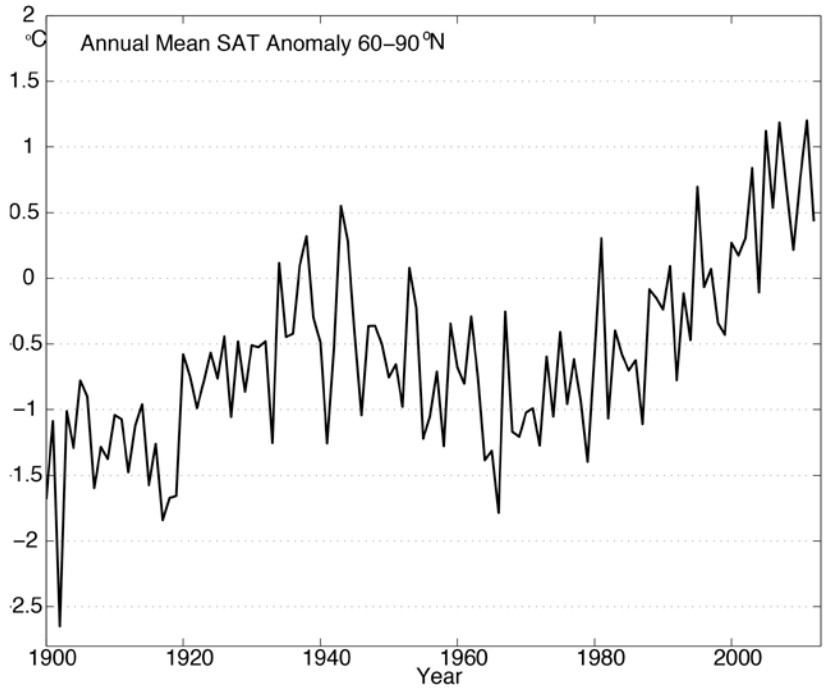

Fig. 1. Arctic-wide annual mean surface air temperature (SAT) anomalies (in ◦C) for the period 1900-2012 relative to the 1981-2010 mean value, based only on land stations north of 60°N. Data are from the CRUTEM4v dataset at www.cru.uea.ac.uk/cru/data/temperature/.

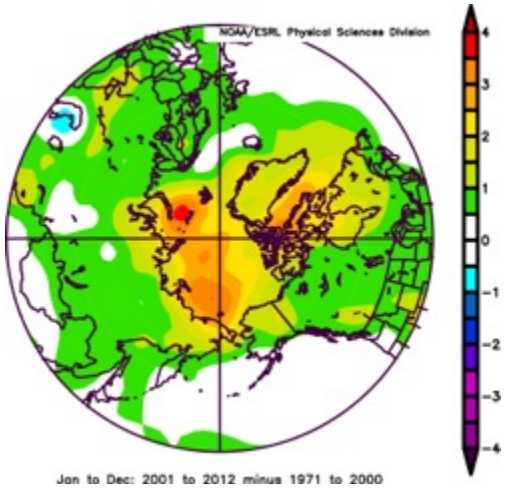

Fig. 2. Annual average near-surface air temperature anomalies (in °C) for the twelve years (2001-2012) of the 21st Century relative to the baseline period 1971-2000. Data are from NOAA/ESRL, Boulder, CO, at http://www.esrl.noaa.gov/psd/.

Seasonal Surface Air Temperature Variability, October 2012 to August 2013

Seasonal air temperature variations are described for the period October 2012 to August 2013, i.e., the period since temperatures were last reported in Arctic Report Card 2012 (Jeffries et al. 2012), and the last month for which data were available at the time this essay was written. This

11-month period is divided into fall 2012 (October, November, December), winter (January, February, March), spring (April, May) and summer (June, July, August) of 2013.

In fall 2012 there were anomalously high air temperatures over the Arctic Basin and adjacent lands, particularly Eurasia (**Fig. 3a**) and northernmost Canada. This is consistent with a large release of heat associated with the cooling and freezing of the very extensive area of open water that occurred in summer 2012, when there was a record low sea ice extent (Perovich et al. 2012).

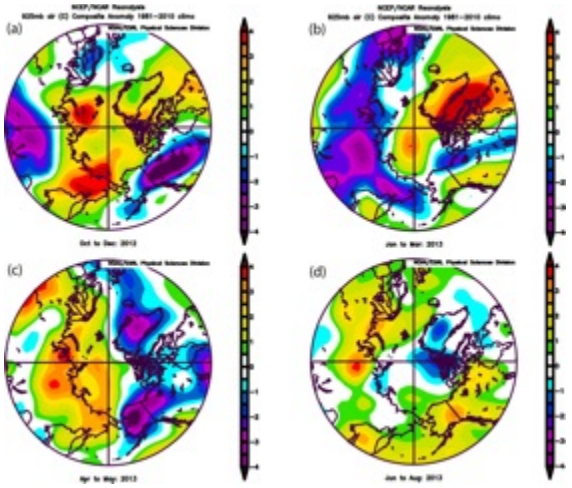

Fig. 3. Seasonal anomaly patterns for near surface air temperatures (in °C) in 2013 relative to the baseline period 1981-2010 in (a) fall 2012, (b) winter 2013, (c) spring 2013, and (d) summer 2013. Temperature analyses are from slightly above the surface layer (at 925 mb level) that emphasizes large spatial patterns rather than local features. Data are from NOAA/ESRL, Boulder, CO, at http://www.esrl.noaa.gov/psd/.

In contrast, an elliptically shaped region of low temperature anomalies stretched from central Canada to Alaska (**Fig. 3a**), where the temperature in parts of Interior Alaska was more than 6°C lower than normal in November. Subsequently, in winter 2013, Alaska enjoyed above normal winter temperatures and the Arctic Basin also remained anomalously warm (**Fig. 3b**). A very strong winter high temperature anomaly developed over the Baffin Bay region, with record high temperatures in March along the coast of west Greenland (see the essay on the *Greenland Ice Sheet*). In contrast, winter was particularly cold in Eurasia, from Scandinavia all the way across the continent to easternmost Siberia (**Fig. 3b**).

In spring 2013, the temperature anomaly pattern (**Fig. 3c**) was almost the opposite of the winter pattern (**Fig. 3b**). An area of anomalously low temperatures stretched from Iceland through Greenland and northern Canada to Alaska, where the Interior experienced the coldest April since 1924 and budburst/green-up of birch and aspen was the latest (26 May) since observations began in 1972 (Alaska Climate Research Center, 2013). In contrast, anomalously high temperatures occurred over much of the Arctic Basin and Eurasia (**Fig. 3c**), where a record low snow cover extent occurred in May (see the essay on *Snow*).

Eurasia remained anomalously warm in summer 2013 (**Fig. 3d**) and, in Alaska, an abrupt transition in late May to much-above normal temperatures heralded one of the hottest summers on record. For example, Fairbanks, in the Interior, experienced a record 36 days with temperatures of 27°C or higher. In contrast to Eurasia and Alaska, anomalously low

temperatures occurred over northernmost Canada and Greenland (**Fig. 3d**). These conditions were associated with a geographically extensive low pressure field that is characteristic of a positive Arctic Oscillation/North Atlantic Oscillation (AO/NAO) (**Fig. 4**).

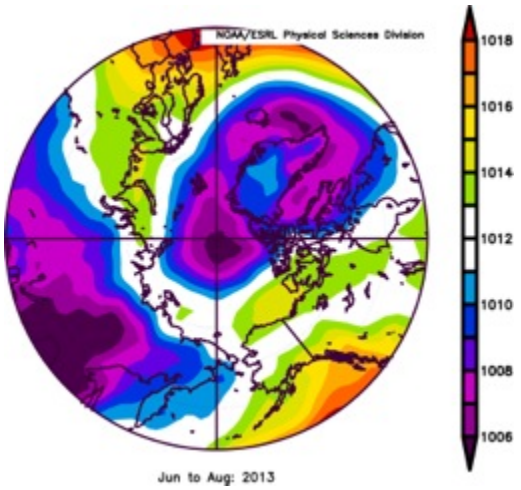

Fig. 4. Mean sea level pressure (in millibars, mb) field for summer (JJA) 2013. Data are from NOAA/ESRL, Boulder, CO, at http://www.esrl.noaa.gov/psd/.

Summer 2013 Relative to the Summer Average of 2007-2012

The relative coolness of Greenland, northernmost Canada and the adjacent high Arctic Ocean in summer 2013 (**Fig. 3d**) is particularly evident when air temperature is compared to that of the period 2007-2012 (**Fig. 5**), when the six lowest minimum sea ice extents in the satellite record occurred (Perovich et al. 2012). The air temperatures across a broad swathe of the Arctic Ocean were 1-3°C lower than they were during 2007-2012 (**Fig. 5**). These relatively low temperatures are likely to have contributed to a notable increase in the minimum extent of the 2013 summer sea ice cover, relative to the record low in 2012. The 2013 minimum sea ice extent was the largest since 2006 (see the essay on *Sea Ice*). Similarly, 1-2°C lower temperatures over Greenland in summer 2013 (**Fig. 5**) contributed to lower surface melt extent and duration, and surface mass balance and river discharge (see the essay on the *Greenland Ice Sheet*).

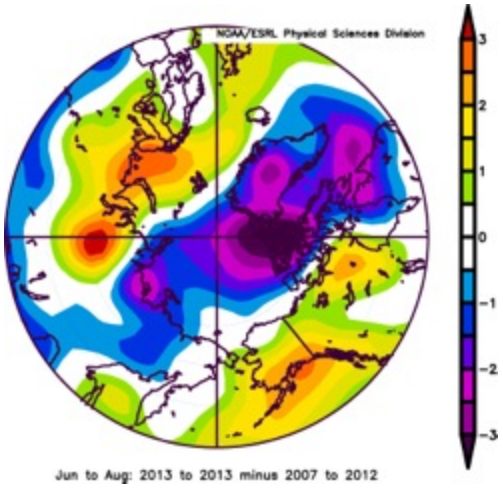

Fig. 5. Near-surface air temperature (in °C) anomalies for summer 2013 relative to 2007-2012. Temperature analyses are from slightly above the surface layer (at 925 mb level) that emphasizes large spatial patterns rather than local features. Data are from NOAA/ESRL, Boulder, CO, at http://www.esrl.noaa.gov/psd/.

References

Alaska Climate Research Center, 2013: May 2013 statewide summary. http://climate.gi.alaska.edu/Summary/Statewide/2013/May.

Jeffries, M. O., J. Richter-Menge and J. E. Overland (editors). 2012: Arctic Report Card 2012. http://www.arctic.noaa.gov/report12/.

Overland, J. E., K. R. Wood and M. Wang, 2011: Warm Arctic-cold continents: Impacts of the newly open Arctic Sea. *Polar Res.*, 30, 15787, doi: 10.3402/polar.v30i0.15787.

Perovich, D. K., W. Meier, M. Tschudi, S. Gerland and J. Richter-Menge, 2012: Sea Ice, in *Arctic Report Card 2012*. http://www.arctic.noaa.gov/report12/sea_ice.html.

Stroeve, J. C., M. C. Serreze, M. M. Holland, J. E. Kay, J. Maslanik and A. P. Barrett, 2012: The Arctic's rapidly shrinking sea ice cover: A research synthesis. *Climatic Change*, doi 10.1007/s10584-011-0101-1.

Cloud Cover and Surface Radiation Budget

J. Key[1], Y. Liu[2], R. Stone[3,4], C. Cox[4], V. Walden[5]

[1]Center for Satellite Applications and Research, NOAA/NESDIS, Madison, WI, USA
[2]Cooperative Institute for Meteorological Satellite Studies, University of Wisconsin, Madison, WI, USA
[3]Global Monitoring Division, NOAA/ESRL, Boulder, CO, USA
[4]Cooperative Institute for Research in Environmental Sciences, University of Colorado, Boulder, CO, USA
[5]Department of Civil and Environmental Engineering, Washington State University, Pullman, WA, USA

November 21, 2013

Highlights

- There was considerably less winter cloud cover in early 2013 over the western Arctic Ocean relative to the last decade, and above average cloud cover in late spring/early summer.
- The cloud cover anomalies had a cooling effect on the surface, particularly where sea ice persisted during summer 2013.

Winter 2012-2013 was characterized by below average cloud cover over the western Arctic Ocean, particularly in January (**Fig. 6a**) and February. In contrast, late spring and early summer cloud cover was above average. (**Fig. 6b**). The cloud cover anomalies are consistent with large-scale pressure and circulation patterns, where positive 850 hPa geopotential height anomalies (**Fig. 7**) occurred in winter (January-March 2013) and negative anomalies occurred in the late spring and early summer (May-June). Positive wintertime geopotential height anomalies generally result in less cloud cover, while negative anomalies are associated with increased cyclonic activity and greater cloud cover (Liu et al. 2007).

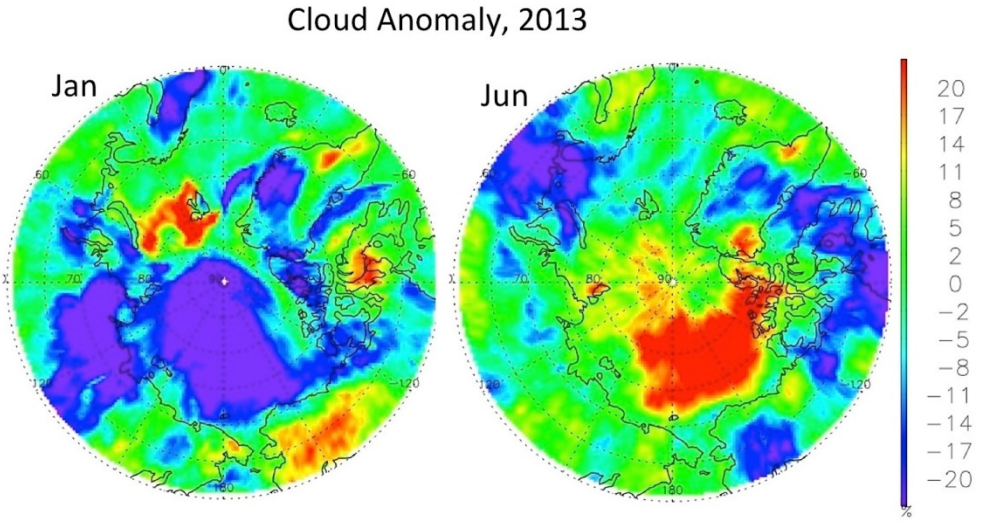

Fig. 6. Cloud cover anomalies (%) in (a, left) January and (b, right) June 2013. The anomalies are calculated relative to the long-term (2002-2011) mean for each month from observations by the Moderate Resolution Imaging Spectroradiometer (MODIS) on the Aqua satellite. Data are from the MODIS L1 and Atmosphere Archive and Distribution System (LAADS) of the Goddard Space Flight Center.

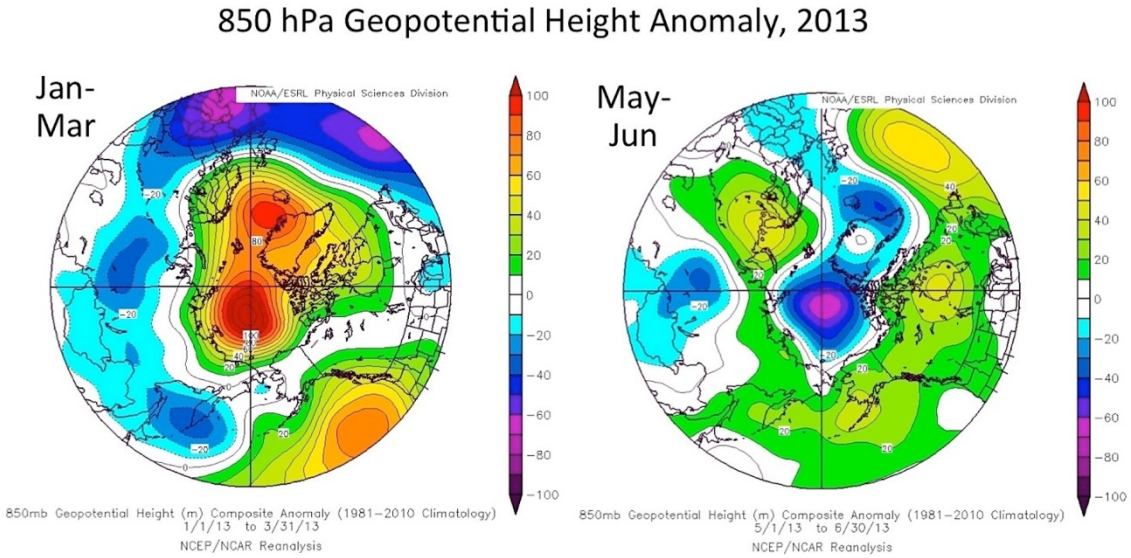

Fig. 7. The 850 mb geopotential height anomalies for (a, left) January-March 2013, and (b, right) May-June 2013. The anomalies are calculated relative to the long-term (1981-2000) mean for each month. Data are from the National Centers for Environmental Prediction (NCEP).

Over the Arctic Ocean, clouds warm the surface during winter and cool the surface in mid-summer (e.g., Stone 1997). The effect of the observed cloud cover anomalies on the radiation budget is one of decreased net longwave radiation during winter that results in cooling at the surface, and decreased solar insolation during summer, which also results in cooling. This can be seen in the January net radiation at the surface from the European Centre for Medium-range Weather Forecasts (ECMWF) Reanalysis project (ERA-Interim; **Fig. 8a**), when relatively low net radiation prevailed over the entire Arctic Basin. There is empirical evidence of a decrease in net radiation in response to reduced cloud cover (**Fig. 6a**) at Barrow, Alaska, where the surface radiation budget has been monitored for many years. During January 2013, for instance, there was a reduction in net radiation at the surface of approximately 12 W/m^{-2} (**Fig. 9**), consistent with the ERA-Interim analysis for that location (**Fig 8a**).

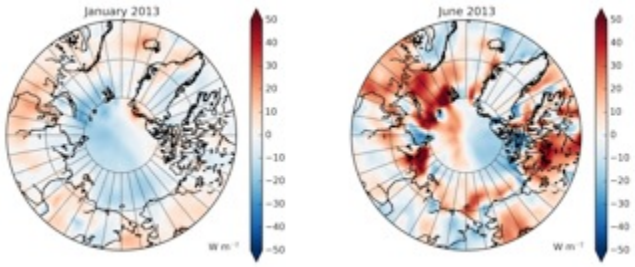

Fig. 8. (a, left) January 2013 and (b, right) June 2013 anomalies of net radiation (in W m^{-2}) at the surface (downwelling longwave - upwelling longwave + downwelling shortwave - upwelling shortwave) derived from the ERA-Interim (Dee et al. 2011). The anomalies are calculated relative to the long-term (2002-2011) mean for each month, consistent with the cloud anomalies in **Fig. 6**.

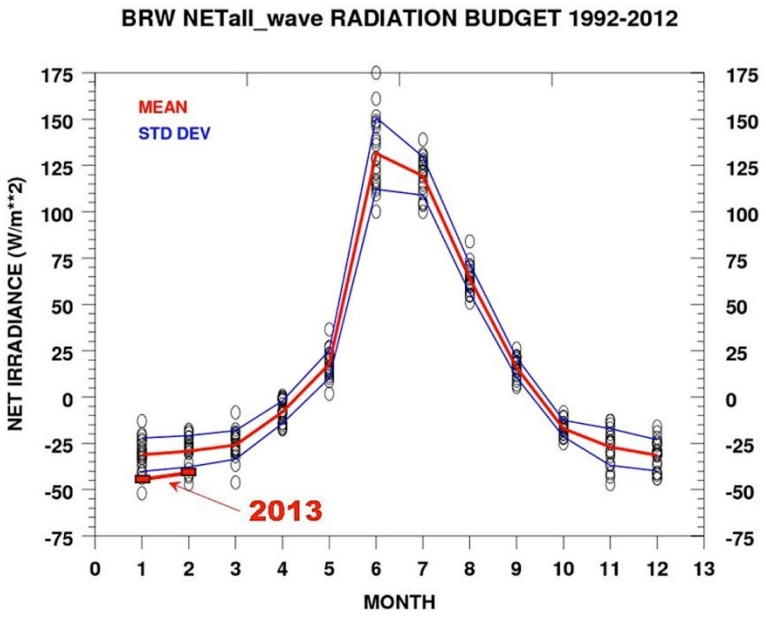

Fig. 9. Mean and standard deviation of net surface radiation (in W m^{-2}) at the NOAA Baseline Observatory, Barrow, Alaska, over the period 1992-2012. Net radiation in January and February 2013 is also shown.

In June, the net surface radiation distribution (**Fig. 8b**) is consistent with the cloud cover (**Fig. 6b**) and the sea ice distribution, with high net radiation around the margins of the Arctic Basin, where the sea ice retreated away from the coast, and low net radiation where sea ice persisted all summer (see the essays on *Air Temperature* and *Sea Ice*). Overall, however, the cloud radiative effect on the surface energy budget is larger in January than in June.

References

Dee, D. P., and 35 others, 2011: The ERA-Interim reanalysis: configuration and performance of the data assimilation system. *Q. J. Roy. Met. Soc.*, 137, 553-597.

Liu, Y., J. Key, J. Francis, and X. Wang, 2007: Possible causes of decreasing cloud cover in the Arctic winter, 1982-2000. *Geophys. Res. Lett.*, 34, L14705, doi:10.1029/2007GL030042.

Stone, R. S., 1997: Variations in western Arctic temperature in response to cloud radiative and synoptic-scale influences. *J. Geophys. Res.*, 102(D18), 21769-21776.

Ozone

G. Bernhard[1], G. Manney[2,3], V. Fioletov[4], J.-U. Grooß[5], R. Müller[5]

[1]Biospherical Instruments, San Diego, CA, U.S.A.
[2]Jet Propulsion Laboratory, California Institute of Technology, Pasadena, CA, U.S.A.
[3]New Mexico Institute of Mining and Technology, Socorro, NM, U.S.A.
[4]Environment Canada, Toronto, ON, Canada
[5]Forschungszentrum Jülich, Jülich, Germany

November 26, 2013

Highlights

- The amount of ozone measured in the Arctic atmosphere during March and April of 2013 was larger than the average of the last decade due to a stratospheric sudden warming event in January that halted chemical destruction of ozone.
- The total ozone column for March 2013, averaged over the equivalent latitude band of 63°-90°N, exceeded the average ozone column for 2000-2010 by 47 Dobson Units or 13%.

The amount of ozone measured in the Arctic atmosphere during March and April 2013 was larger than the average of the last decade. The minimum total ozone column[1] for March 2013, averaged over the "equivalent latitude[2]" band 63°-90°N, was 414 Dobson Units (DU[3]) (**Fig. 10**). This value is 47 DU above the average for 2000-2010 (367 DU) and is comparable to observations in previous warm winters that did not have significant ozone depletion, e.g., 1999, 2001 & 2006. The 2011 record-low was 308 DU (**Fig. 10**) and the average for the "baseline" period of 1979-1988 is 397 DU.

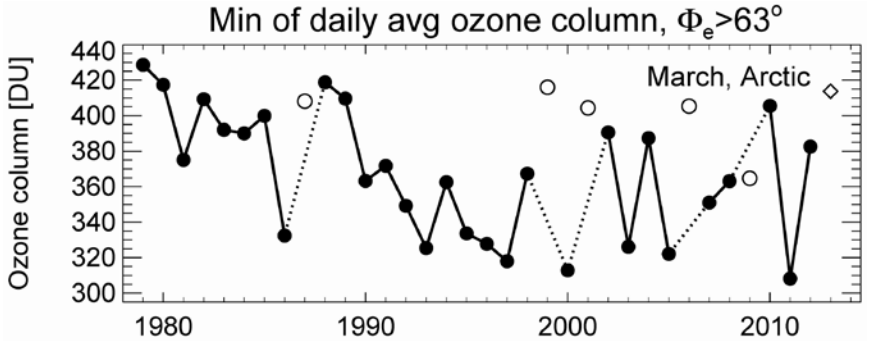

Fig. 10. Time series of minimum total ozone for March in the Arctic, calculated as the minimum of the daily average column ozone poleward of 63° equivalent latitude[2]. Open circles are also for March, but represent years (1987, 1999, 2001, 2006, 2009 and 2013) in which the polar vortex[4] broke up before March. Polar ozone in those years was relatively high because of mixing with air from lower latitudes or higher altitudes, and the lack of significant chemical ozone depletion. The figure is an updated version of that published by Müller et al. (2008) in which the state of the atmosphere is characterized by the ERA-Interim reanalysis (Dee et al. 2011). Ozone data from 1979-2012 are based on the combined total column ozone database produced by Bodeker Scientific, available at http://www.bodekerscientific.com/data/total-column-ozone. The Bodeker Scientific ozone data set for 2013 was incomplete at the time of writing. Consequently, the March 2013 ozone value (open diamond) is based on measurements by the Ozone Monitoring Instrument (OMI) aboard the NASA Aura satellite.

The relatively high ozone concentrations in 2013 were triggered by a large increase in stratospheric temperatures during the first half of January 2013. While such a "stratospheric sudden warming" (SSW) is a common dynamical event in the Arctic winter, in most years over the last two decades the SSWs have occurred in the late winter and early spring. The early winter timing of the SSW in January 2013 halted the chemical destruction of ozone in the stratosphere by chlorine activation. Transport of ozone from higher to lower altitudes also contributed to the relatively large ozone amounts in the spring of 2013.

During a SSW the strong westerly winds that define the polar vortex[4] boundary reverse to easterly winds, and polar stratospheric temperatures rise abruptly, sometimes increasing by more than 30 K (30°C) over 2-3 days. Such events have historically occurred on average about once every two winters, but are irregular; many years can elapse without any SSWs (e.g., in most of the 1990s), while other periods (such as the past decade) have many more SSWs than average. The contrast between the meteorological conditions in 2012-13 and 2011-12 (when there was also a strong, prolonged SSW) with those in 2010-11 (when a persistently cold stratosphere and high chlorine activation caused ozone destruction) highlights the large range of inter-annual variability in Arctic winter conditions, and hence in Arctic ozone loss (**Fig. 10**).

There were no extended areas with large deviations from historical measurements of the monthly mean total ozone columns for February through May 2013 (**Fig. 11**). During February, a comparison with "baseline" data for 1979-1988 indicates that the total ozone was more than 30% below the baseline value over the Atlantic Ocean, east of Canada and south of Greenland. A region with slightly elevated total ozone was centered over northern Scandinavia. In March, areas with below-average total ozone encompassed northernmost Canada and the North Pole. Positive ozone anomalies were centered over the Kola Peninsula, Russia, and northern Scandinavia. Monthly average ozone anomalies for April remained below ±10% throughout the Arctic. Average total ozone for May was elevated by about 15% over Iceland. In contrast to the monthly mean values, departures from the baseline were larger for individual days.

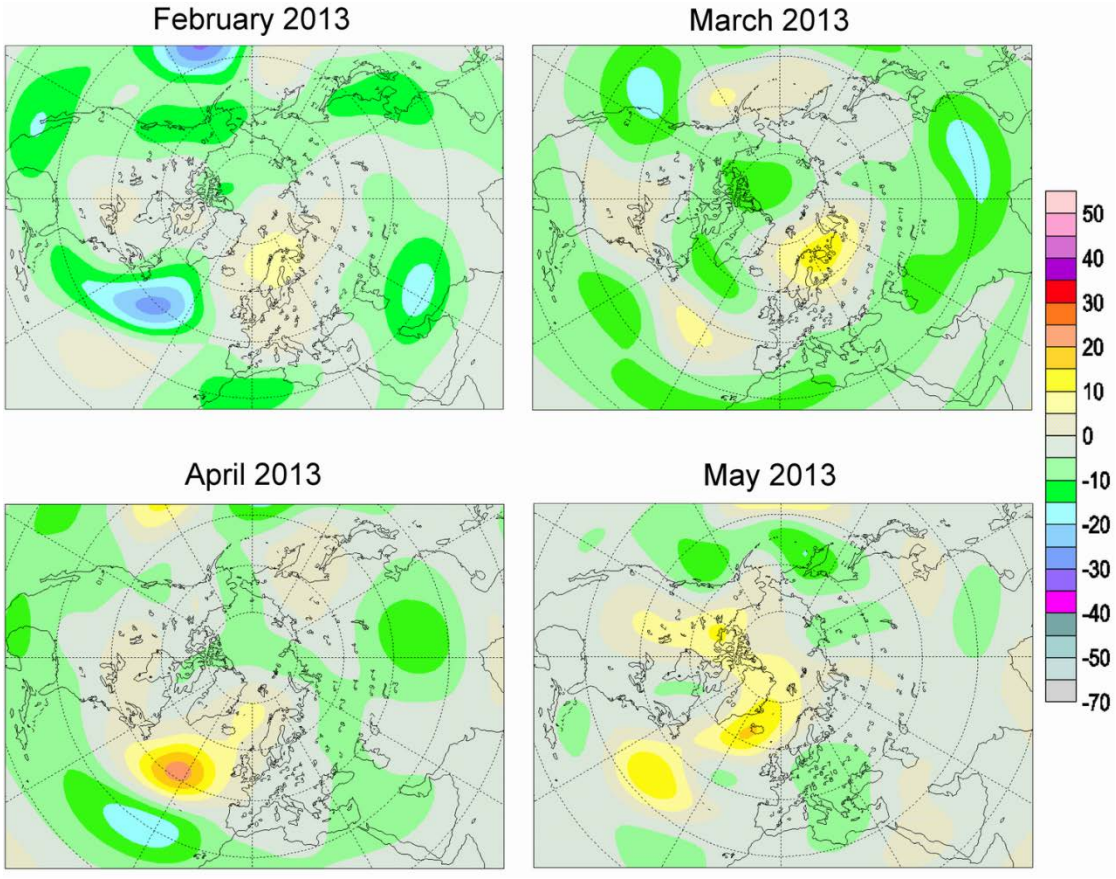

Fig. 11. Deviation (in %) of monthly average total ozone for February, March, April, and May 2013 from the 1979-1988 level. Maps were provided by Environment Canada and are available at http://es-ee.tor.ec.gc.ca/cgi-bin/selectMap. 2013 data are based on ground-based measurements and OMI and GOME-2 satellite data. NOAA Stratosphere Monitoring Ozone Blended Analysis (SMOBA) data were used for the polar night area in February. Reference data for 1979-1988 were estimated using Total Ozone Mapping Spectrometer (TOMS) observations and are available at http://ozoneaq.gsfc.nasa.gov/nimbus7Ozone.md.

Chemical ozone loss resulting from chlorine activation is most effective in years when there is a long-lasting, cold vortex, such as occurred in 2011. This is illustrated in **Fig. 12**, which compares the distribution of total ozone column over the Arctic on 3 April of the years 1981 (a year with a long-lasting and cold Arctic vortex[4], and relatively low stratospheric chlorine concentrations), 2002 (long-lasting warm vortex, high total chlorine loading), 2011 (long-lasting cold vortex, high chlorine), and 2013 (warm vortex, high chlorine). Years with a warm vortex such as 2002 and 2013 have little ozone loss.

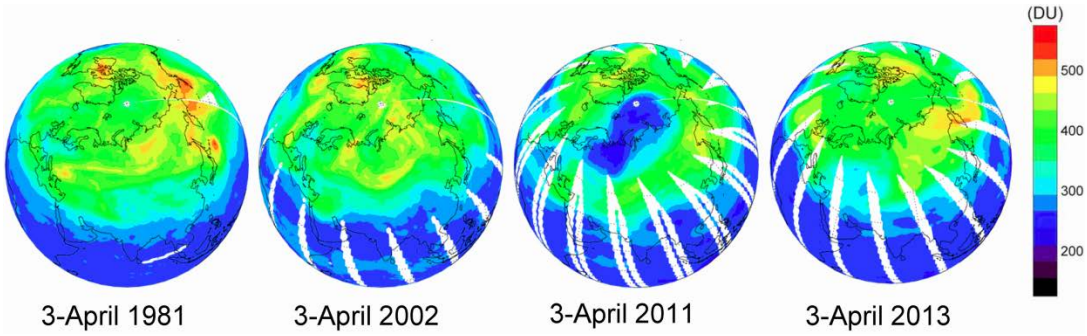

Fig. 12. Comparison of total ozone column measured by satellites on 3 April in 1981, 2002, 2011, and 2013. Data are from the Total Ozone Mapping Spectrometer (TOMS) aboard the Nimbus-7 (1981) and Earth Probe (2002) satellites, and the Ozone Monitoring Instrument (OMI) aboard the AURA spacecraft (2011 and 2013).

The temporal evolution of several variables that were crucial for the rate and extent of stratospheric ozone chemistry and ozone loss during the winter/spring of 2012-13 is illustrated in **Fig. 13** using data from the Microwave Limb Sounder (MLS) on the NASA Aura satellite.

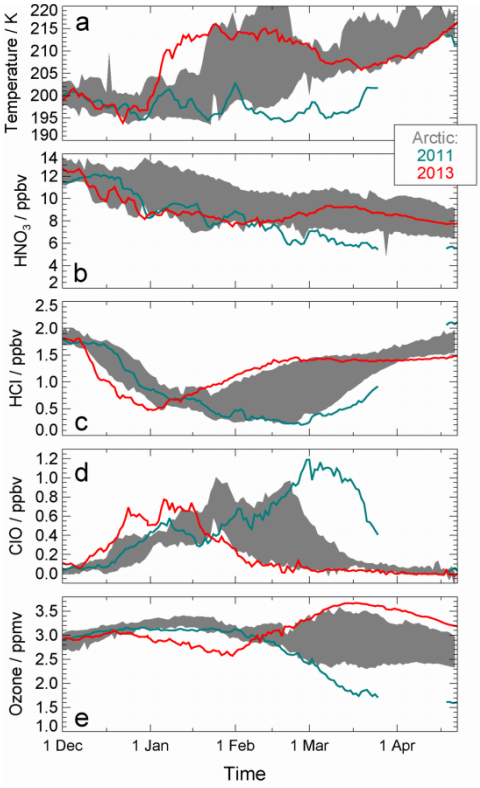

Fig. 13. Averages of high latitude (a) temperatures, (b) nitric acid (HNO_3), (c) hydrogen chloride (HCl), (d) chlorine monoxide (ClO) and (e) ozone from the NASA Aura Microwave Limb Sounder (MLS) measurements. Measurements made during Arctic winter 2012-2013 (red lines) are compared with those of Arctic winter 2010-2011 (blue-green lines), when unprecedented chemical ozone loss occurred in March 2011 (see the essay on *Ozone and UV Radiation* in Arctic Report Card 2011). The shaded areas indicate the range of values observed between winter 2004-2005 and winter 2011-2012 (excluding 2010-2011). Concentrations of trace gases are expressed as "mixing ratios" in units of "parts per billion by volume" (ppbv) for HNO_3, HCl, and ClO, and "parts per million by volume" (ppmv) for ozone. Temperature and mixing ratios refer to the 485 K potential temperature surface (note that the Kelvin [K] unit is always used for potential temperature), at an altitude of ~18 km and pressure of ~50 hPa, and were averaged over the area of the polar vortex.

Stratospheric temperatures in December 2012 were among the lowest on record (**Fig. 13a**). Low temperatures below 195 K (about -78.°C) facilitated the formation of polar stratospheric clouds (PSC), which consist of nitric acid (HNO_3) and water and occur at altitudes between about 15 and 25 km. The onset of PSC occurrence is reflected in the large decrease in gas-phase HNO_3 in early to mid-December as HNO_3 was being converted to PSC particles (**Fig. 13b**). Chemical reactions on PSC cloud particles transform inactive forms of chlorine, such as chlorine nitrate ($ClONO_2$) and hydrogen chloride (HCl), to active, ozone-destroying forms of chlorine such as chlorine monoxide (ClO). The conversion of inactive to active forms is indicated by the decrease in HCl (**Fig. 13c**) and the increase in ClO (**Fig. 13d**) following the start of PSC occurrence.

In contrast to previous Arctic winters in which early SSW events occurred, HNO_3 concentrations did not increase in early January 2013 when temperatures rose above the threshold temperature for PSC existence (compare **Figs. 13a** and **13b**). This indicates that large enough PSC particles had been present for a long enough time to drop to lower altitude by gravitational forces, permanently removing HNO_3 from the stratosphere. The removal of HNO_3 from the stratosphere is important because the conversion of active chlorine (ClO) into the inactive form $ClONO_2$ is delayed when the stratosphere is depleted of HNO_3 (Fahey and Hegglin 2011). As a consequence, chlorine did not return to its inactive forms for about one month after the start of the SSW event (compare **Figs. 13a** and **13d**).

Ozone destruction occurs as long as chlorine is activated in regions that experience sunlight. However, even with chlorine activated, ozone destruction is typically small in December and January when the polar regions are in darkness. Owing to the large SSW event, the polar vortex in late 2012 and early 2013 was shifted away from the North Pole and was exposed to more sunlight than usual. The steady decrease in ozone between late December and late January (**Fig. 13e**) indicates that significant chemical ozone loss occurred during this period.

Chlorine was finally deactivated in early February (**Fig. 13d**) and ozone increased because of an influx of ozone from higher altitudes. After mid-February, ozone concentrations in the Arctic stratosphere were the highest since 2005 (**Fig. 13e**). Thus, the SSW in January and the associated rise in stratospheric temperatures prevented extensive ozone losses in 2013, in stark contrast to the situation in 2011, when low temperatures persisted into spring, resulting in unprecedented ozone destruction during that year (Manney et al. 2011).

Footnotes

[1]Total ozone column is the height of a hypothetical layer that would result if all ozone molecules in a vertical column above the Earth's surface were brought to standard pressure (1013.25 hPa) and temperature (273.15 K (0°C)).

[2]Equivalent latitude is a latitude-like coordinate aligned with the polar vortex (Butchart and Remsberg 1986).

[3]Dobson Unit, the standard unit for measuring the total ozone column. 1 DU equals a column height of 0.01 mm and corresponds to 2.69×10^{16} molecules cm^{-2}.

[4]The polar vortex is the band of strong westerly winds in the stratosphere that encircle the North Pole in winter and within which chemical ozone destruction occurs.

References

Butchart, N., and E. E. Remsberg, 1986: The area of the stratospheric polar vortex as a diagnostic for tracer transport on an isentropic surface. *J. Atmos. Sci.*, 43, 1319-1339.

Dee, D. P., and 35 others, 2011: The ERA-Interim reanalysis: configuration and performance of the data assimilation system. *Q. J. R. Meteorol. Soc.*, 137, 553-597, doi:10.1002/qj.828, available at: http://onlinelibrary.wiley.com/doi/10.1002/qj.828/full.

Fahey, D. W., and M. I. Hegglin, 2011: Twenty Questions and Answers About the Ozone Layer: 2010 Update, *Scientific Assessment of Ozone Depletion: 2010*, 72 pp., World Meteorological Organization, Geneva, Switzerland, available at: http://www.wmo.int/pages/prog/arep/gaw/ozone_2010/documents/twentyquestions.pdf.

Manney, G. L., and 28 others, 2011: Unprecedented Arctic ozone loss in 2011 echoed the Antarctic ozone hole. *Nature*, 478, 469-475, available at: http://www.nature.com/nature/journal/v478/n7370/full/nature10556.html.

Müller, R., J.-U. Grooß, C. Lemmen, D. Heinze, M. Dameris, and G. Bodeker, 2008: Simple measures of ozone depletion in the polar stratosphere. *Atmos. Chem. Phys.*, 8, 251-264, available at: http://www.atmos-chem-phys.org/8/251/2008/acp-8-251-2008.pdf.

UV Radiation

G. Bernhard[1], V. Fioletov[2], A. Heikkilä[3], B. Johnsen[4], T. Koskela[3], K. Lakkala[5], T. Svendby[6], A. Dahlback[7]

[1]Biospherical Instruments, San Diego, CA
[2]Environment Canada, Toronto, Ontario, Canada
[3]Finnish Meteorological Institute, Helsinki, Finland
[4]Norwegian Radiation Protection Authority, Østerås, Norway
[5]Finnish Meteorological Institute, Arctic Research Centre, Sodankylä, Finland
[6]Norwegian Institute for Air Research, Kjeller, Norway
[7]Department of Physics, University of Oslo, Norway

November 26, 2013

Highlights

- At several locations in the high Arctic, UV levels were below the climatological mean for prolonged periods between February and May of 2013 primarily due to high ozone levels.
- In Scandinavia, UV levels were mostly controlled by cloud variability. Elevated UV intensities were observed in northern Scandinavia in late May and early June, partly because of advection of low-ozone air masses from lower latitudes.

Ozone molecules in the Earth's atmosphere greatly attenuate the part of the Sun's ultraviolet (UV) radiation that is harmful to life. Reductions in the atmospheric ozone amount will always lead to increased UV levels, but other factors such as the Sun angle, cloud cover, and aerosols also play important roles. Here we report UV radiation data for 2013 relative to historical records.

UV levels are described here by the UV Index (UVI)[1], a measure of the ability of UV radiation to cause erythema (sunburn) in human skin. The analysis is based on ground-based radiometers because UV radiation levels at the ground are also modified by surface conditions (e.g., variability in snow cover) and cloudiness. The effect of the two variables on UV is difficult to quantify from satellite observations at high latitudes (Tanskanen et al. 2007).

The magnitude and timing of UV anomalies is illustrated in **Fig. 14**, which compares the UVI at 11 Arctic and sub-Arctic stations in 2013 with historical measurements. Changes in the UVI tend to anti-correlate with changes in total ozone. This can be seen by comparing the center panels of **Fig. 14** (showing UVI measurements in 2013 relative to the climatological average) with the bottom panels (presenting a similar analysis for total ozone). For example, at Alert (first site in Fig. 14), UV measurements between 7 and 9 May 2013 were below the long-term average by approximately 20%, while the total ozone column during this period exceeded the long-term average by about the same amount. Because UV radiation levels are also greatly affected by changes in cloudiness, the anti-correlation between ozone and UV radiation can be masked by cloud variability, which is evident for most Scandinavian sites in **Fig. 14**.

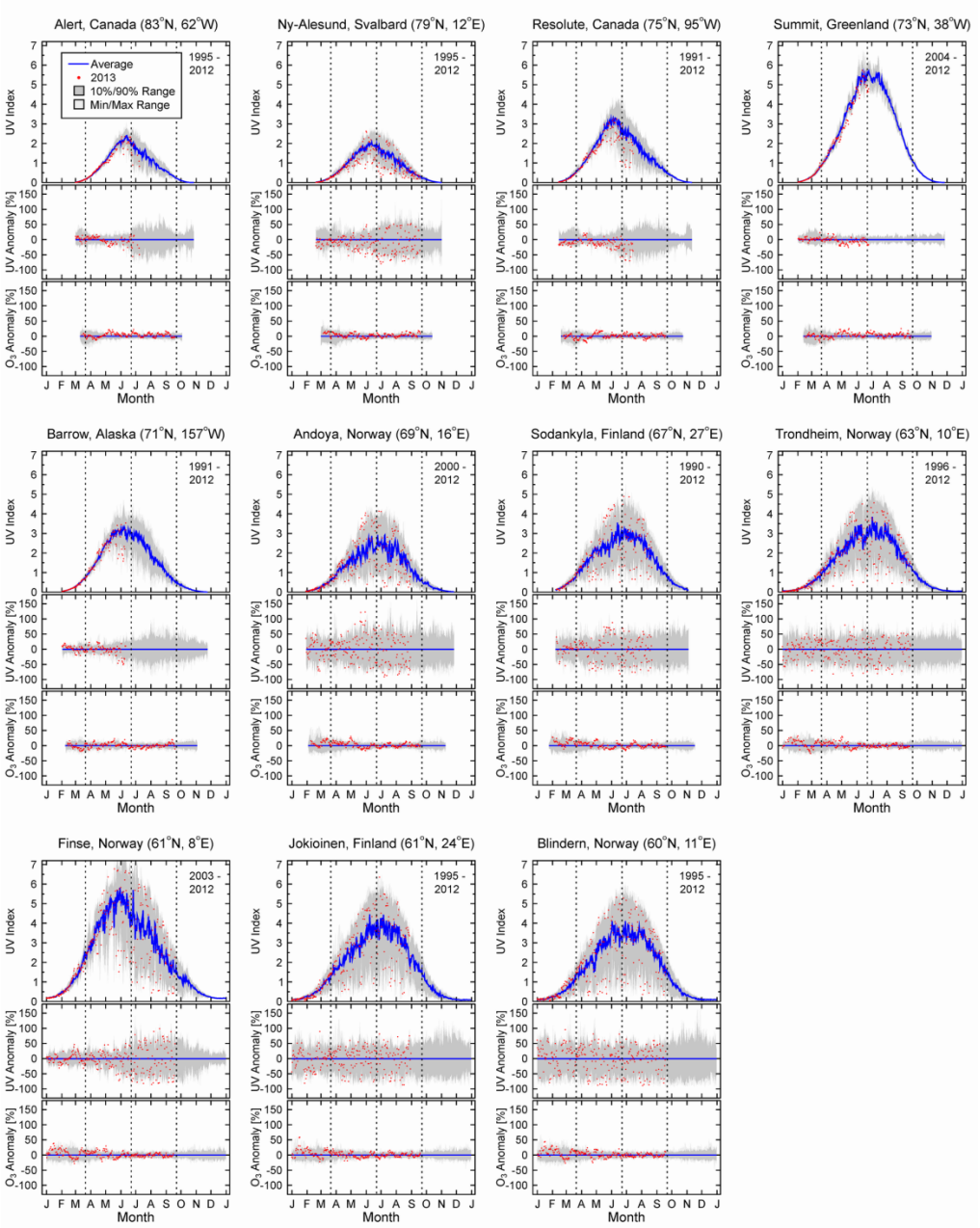

Fig. 14. Seasonal variation of the UV Index for eleven Arctic and sub-Arctic sites measured by ground-based radiometers. Data are based on the UV Index averaged over a period of two hours centered at solar noon. The top panel for each site compares UVI measurements performed in 2013 (red dots) with the average noontime UVI (blue line), the range between the 10th and 90th percentile (dark shading), and the range of historical minima and maxima (light shading). Average (the climatological mean) and ranges were calculated from measurements of the years indicated in the top-right corner of the panel. The center panel shows the relative UVI anomaly calculated as the percentage departure from the climatological mean. The bottom panel shows a similar anomaly analysis for total ozone derived from measurements of the following satellites: TOMS/Nimbus7 (1991-1992), TOMS/Meteor3 (1993-1994), TOMS/EarthProbe (1996-2004), and OMI (2005-2013). The shaded ranges for the ozone data set is based on data for the years 1991-2012 (1996-2012 for Trondheim and Finse). Ozone data are available at http://ozoneaq.gsfc.nasa.gov/ and http://avdc.gsfc.nasa.gov/index.php?site=1593048672&id=28. Vertical broken lines indicate the times of the vernal equinox, summer solstice and autumnal equinox, respectively. Additional geographical and meteorological information on the 11 sites is provided by Bernhard et al. (2013).

Because of the above-average ozone amounts observed in spring 2013 (see the essay on *Ozone*), UV levels measured in the high Arctic were below the climatological mean for prolonged periods at several stations. However, the timing of these low-UV episodes was not uniform across the Arctic. For example at Alert, a station located in the Canadian high Arctic at 83°N and approximately 700 km from the North Pole, UVI between 28 April and 27 May 2013 remained continuously below the climatological mean. In contrast, UVI measurements at Ny-Ålesund, located on the Svalbard archipelago north of Scandinavia and approximately 1,000 km from the North Pole, were below the climatological mean during February and March 2013.

UV intensities in southern Scandinavia (e.g., Trondheim, Jokioinen and Blindern) were mostly controlled by cloud variability. Enhanced UV levels were observed in northern Scandinavia during May and early June. For instance, UV levels at Sodankylä, located in northern Finland, were close to historical maxima between 16 May and 7 June 2013. On average, the UVI was elevated by 38% compared to the climatological mean. In absolute terms, the enhancement was 0.9 UVI units on average, and the maximum enhancement, observed on 3 June 2013, was 2.0 UVI units. The enhancement was mostly caused by low cloudiness, but satellite observations provided by the Tropospheric Emission Monitoring Internet Service (TEMIS, http://www.temis.nl/) suggest that advection of low-ozone air from lower latitudes also was a contributing factor.

In addition to atmospheric ozone concentrations, UV radiation is affected by the Sun angle, clouds, aerosols (liquid and solid particles suspended in air), the reflectivity of the surface (high, when snow or ice covered), and other factors (Weatherhead et al. 2005). The main driver of the annual cycle is the position of the Sun. Sites closest to the North Pole (Alert, Ny-Ålesund and Resolute in **Fig. 14**) have the smallest peak radiation, with the UVI remaining below 4 all year. Although UV Indices below 5 are considered "low" or "moderate" (WHO 2002), people involved in certain outdoor activities may receive higher-than-expected UV doses if their faces and eyes are oriented towards the low Sun or if they are exposed to UV radiation reflected off snow.

Clouds lead to a large variability in UV levels on time scales of minutes to days, but the effect is largely reduced when the ground is covered by fresh snow (Bernhard et al. 2008). Measurements at Alert and Barrow—and to a lesser extent at Ny-Ålesund, Resolute and Finse—show a large asymmetry between spring (low variability) and fall (high variability) because the surface at these sites is covered by snow until about June and free of snow thereafter until the beginning of winter. During summer and fall, the variability introduced by clouds is substantially larger than that related to ozone variations (compare shaded ranges in center and bottom panels of **Fig. 14**).

Footnotes

[1]UVI is calculated by weighting UV spectra with the action spectrum for erythema (McKinlay and Diffey 1987) and multiplying the result by 40 m^2/W.

References

Bernhard, G., C. R. Booth, and J. C. Ehramjian, 2008: Comparison of UV irradiance measurements at Summit, Greenland; Barrow, Alaska; and South Pole, Antarctica. *Atmos. Chem. Phys.*, 8, 4799-4810, available at: http://www.atmos-chem-phys.net/8/4799/2008/acp-8-4799-2008.html.

Bernhard, G., A. Dahlback, V. Fioletov, A. Heikkilä, B. Johnsen, T. Koskela, K. Lakkala, and T. M. Svendby, 2013: High levels of ultraviolet radiation observed by ground-based instruments below the 2011 Arctic ozone hole. *Atmos. Chem. Phys.*, 13, 10573-10590, doi:10.5194/acp-13-10573-2013, available at http://www.atmos-chem-phys.net/13/10573/2013/acp-13-10573-2013.html.

McKinlay, A. F., and B. L. Diffey, 1987: A reference action spectrum for ultraviolet induced erythema in human skin, *CIE Res. Note*, 6(1), 17- 22.

Tanskanen, A., and 16 others, 2007: Validation of daily erythemal doses from Ozone Monitoring Instrument with ground-based UV measurement data. *J. Geophys. Res.*, 112, D24S44, doi:10.1029/2007JD008830.

Weatherhead B., A. Tanskanen, and A. Stevermer, 2005: Ozone and Ultraviolet Radiation, Chapter 5, *Arctic Climate Impact Assessment*, Cambridge University Press, New York, 1042 pp, available at: http://www.acia.uaf.edu/PDFs/ACIA_Science_Chapters_Final/ACIA_Ch05_Final.pdf.

WHO, 2002: *Global Solar UV Index: A Practical Guid*e. World Health Organization (WHO), World Meteorological Organization (WMO), United Nations Environment Programme (UNEP), and the International Commission on Non-Ionizing Radiation Protection (ICNIRP), WHO, Geneva, Switzerland, 28 pp., ISBN 9241590076, available at: http://www.who.int/uv/publications/en/GlobalUVI.pdf.

Black Carbon in the Arctic

S. Sharma[1], J.A. Ogren[2], A. Jefferson[2], K. Eleftheriadis[3], E. Chan[1], P.K. Quinn[4], J.F. Burkhart[5]

[1]Environment Canada, Atmospheric Science and Technology Directorate, Toronto, ON, Canada
[2]NOAA ESRL, Boulder, CO, USA
[3]Institute of Nuclear and Radiological Science & Technology, Energy & Safety N.C.S.R. "Demokritos" 15310 Ag. Paraskevi, Attiki, Greece
[4]NOAA PMEL, Seattle, WA, USA
[5]University of Oslo, Department of Geosciences, 0316 Oslo, Norway

December 2, 2013

Highlights

- Average equivalent black carbon (soot) concentrations in 2012 at Alert (Nunavut, Canada), Barrow (Alaska, USA) and Ny-Ålesund (Svalbard, Norway) were similar to average concentrations during the decade 2002-2012.
- Annual equivalent black carbon has declined by 55% and 45% since the early 1990s at Alert and Barrow, respectively.

Introduction

Aerosol black carbon (soot) is released during the incomplete combustion of fossil fuels, biofuels and biomass burning. The largest black carbon emission sources that affect the Arctic are agricultural burning, wildfires and on-road diesel vehicles, followed by residential burning, off-road diesel and industrial combustion, including gas flaring. The burden of atmospheric black carbon north of 70°N in the Arctic is the result of long-range transport from the former Soviet Union, Europe, North America and east Asia (Sharma et al. 2013) (**Fig. 15**).

Fig. 15. Map showing the location of high Arctic, long-term, black carbon measurement sites at Alert (82°N, 62.3°W), Barrow (71°N, 156.6°W) and Ny-Ålesund (79°N, 12°E), and the source regions for black carbon in the Arctic: Europe (EU), former Soviet Union (FSU), North America (NA) and east Asia (EA).

Black carbon is a short-lived climate forcer that affects the radiation balance in the Arctic by absorbing solar radiation when suspended in the atmosphere (Charlson et al. 1991; Jacobson 2000, IPCC 2001), by altering cloud properties (IPCC 2007, Liu et al. 2011) and, when deposited on snow and ice, by darkening the surface and enhancing the absorption of solar radiation and melt rates (Flanner et al. 2007, Hegg et al. 2009, Bond et al. 2013). A large proportion of the Arctic climate response to an increase in surface temperature is due to the snow/albedo effect (Fletcher et al. 2009, Serreze and Barry 2011).

Long-term monitoring of black carbon in the Arctic is critical to understanding sources, transport pathways and environmental impacts in the Arctic, and to provide essential information for the development and implementation of mitigation options. Here we report black carbon observations at three high Arctic locations with the longest records: Alert (Nunavut, Canada), Barrow (Alaska, USA) and Ny-Ålesund (Svalbard, Norway) (**Fig. 15**).

Measuring Black Carbon

In the Arctic, the longest records of black carbon concentration are measured by Aethalometer. This instrument uses a filter-based optical technique changes, which measures light attenuation over time as the amount of black carbon-containing aerosol increases on the filter matrix (Hansen et al. 1984). Black carbon derived from Aethalometer measurements is referred to as Equivalent Black Carbon (EBC) (Petzold et al. 2013). The change in optical transmission is assumed to be due solely to black carbon; no corrections have been applied to account for other aerosols (Weingartner et al. 2003, Collaud Coen et al. 2010, Müller et al. 2013). By not applying the correction, artifacts can affect the EBC measurements by a factor of 2 (Louisse et al. 1993, Sharma et al. 2002, Weingartner et al. 2003). At Barrow, a Particle Soot Absorption Photometer (PSAP) has been used since the Aethalometer broke down in 2002. A good comparison between the two instruments (Sharma, unpublished data) gives us the confidence to continue the Barrow EBC time series with the PSAP data after 2002.

Equivalent Black Carbon (EBC) Observations

EBC in 2012. In 2012, annual average EBC concentrations were 36±36, 32±31 and 23±32 ng m^{-3} (arithmetic mean ± 1 standard deviation of daily averages in nanograms per cubic meter) at Alert, Barrow and Ny-Ålesund. These values are very similar to the averages (40±45, 30±36 and 27±40 ng m^{-3}) for the decade 2002-2012. This decade is used for the comparison because the continuous Ny-Ålesund record goes back only as far as 2002 (**Fig. 16**).

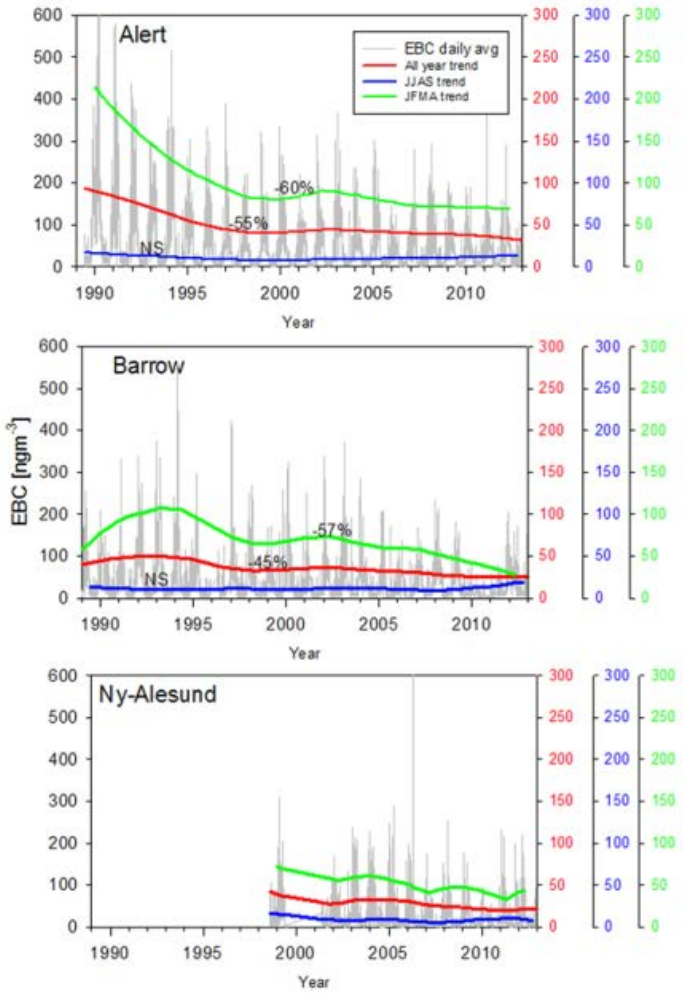

Fig. 16. Daily-average surface equivalent black carbon (EBC) at Alert, Barrow and Ny-Ålesund. Trend lines (green, red, blue) were determined using the LOWESS technique (LOcally Weighted Exponentially Scatterplot Smoothing). The red line includes all EBC data, the green line is the average for January to April (JFMA), and the blue line is the average for June to September (JJAS). The % change in EBC between 1990-1993 and 2009-2012 is given for each trend line for Alert and Barrow. No significant (NS) change occurred in summer at those locations.

Long-Term EBC Trends and Variability. Alert and Barrow have the longest measurement records (1989-present, **Fig. 16**), which allows meaningful trends to be determined. EBC measurements did not begin at Ny-Ålesund until 1998 and trends there can not be compared directly to the other two sites. However, for the period 2002-2012, daily average EBC concentrations at Ny-Ålesund are similar to those at Barrow and Alert (**Fig. 16**), in spite of their large geographical separation. This is an indication of the ubiquity of black carbon in the high Arctic.

Overall, there has been a 55% decline in EBC at Alert and a 45% decline in EBC at Barrow between 1990-1993 and 2009-2012 (**Fig. 16**). The declines are related to decreasing emissions due to the economic collapse in the former Soviet Union during the early 1990s (Sharma et al. 2004, 2006, 2013, Quinn et al. 2008, Hirdman et al. 2010). EBC has not increased since 2000 at Alert, Barrow and Ny-Ålesund, despite rising fossil fuel black carbon emissions in the source

regions (Sharma et al. 2013), especially in East Asia. Black carbon from East Asia contributes a small proportion of total deposition in the Arctic (Hegg et al. 2009) because it is transported at higher altitudes than black carbon from Europe and the former Soviet Union (Stohl et al. 2006, Sharma et al. 2013).

Monthly EBC anomalies (**Fig. 17**) at Alert and Barrow were determined by calculating the difference between monthly EBC concentrations and the monthly mean values for the period 1989-2012. Monthly EBC anomalies at Ny-Ålesund were calculated only for the period of continuous record from 2002 to 2012. At Alert and Barrow, anomalies in the 1990s were significantly higher ($P(t<0.01)$) than post-2000 anomalies, indicating that prior to 2000 monthly EBC concentrations were significantly higher than the 23 year mean for a given month. These temporal differences at Alert and Barrow are largely due to changes in black carbon source strength and depositional losses rather than changes in transport patterns. EBC anomalies at Ny-Ålesund are significantly different than those at Alert and Barrow for the same period (2002-2012); at Ny-Ålesund, site-specific influences on EBC concentrations, e.g., elevation (500 m above sea level, a.s.l.) are superimposed on larger scale influences such more frequent cyclones and cloud cover that lead to more efficient scavenging.

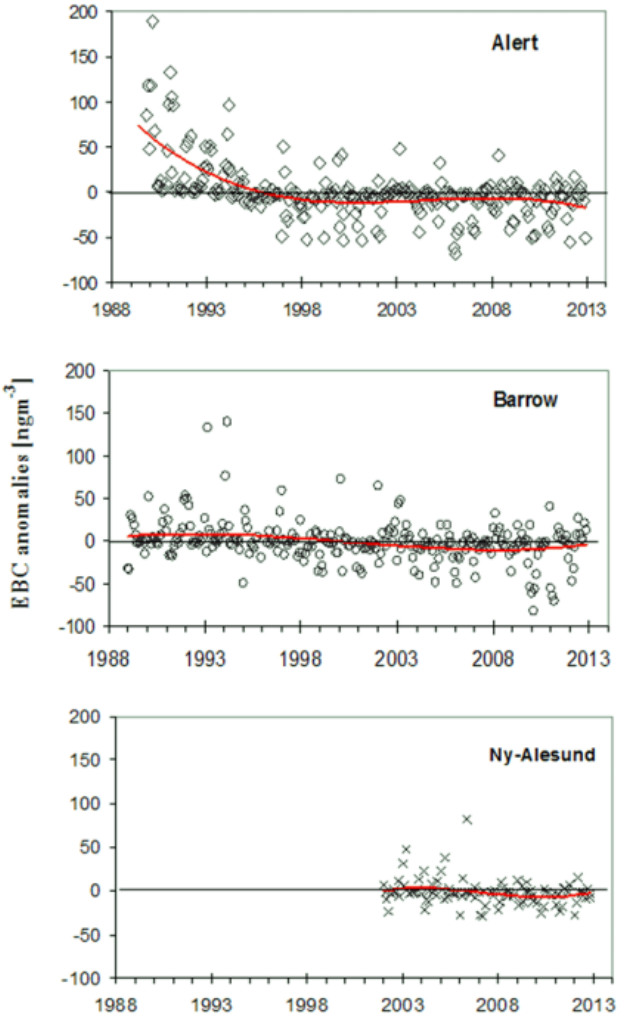

Fig. 17. Equivalent black carbon (EBC) anomalies at Alert, Barrow and Ny-Ålesund.

Seasonal Cycle of EBC. Seasonal EBC variability is evident at Alert, Barrow and Ny-Ålesund (**Fig. 16**), but is most pronounced at Alert and least pronounced at Ny-Ålesund (**Fig. 18**). This reflects spatial and inter-annual variability in EBC concentration, which is a function of black carbon source strength, transport pathways from source to receptor, and black carbon deposition (e.g., Stohl 2006, Garrett et al. 2010, Sharma et al. 2013). Also, Barrow (0 m a.s.l.) and Ny-Ålesund (575 m a.s.l.) have Pacific and Atlantic Ocean influences, resulting in higher EBC losses due to deposition than Alert (250 m a.s.l.).

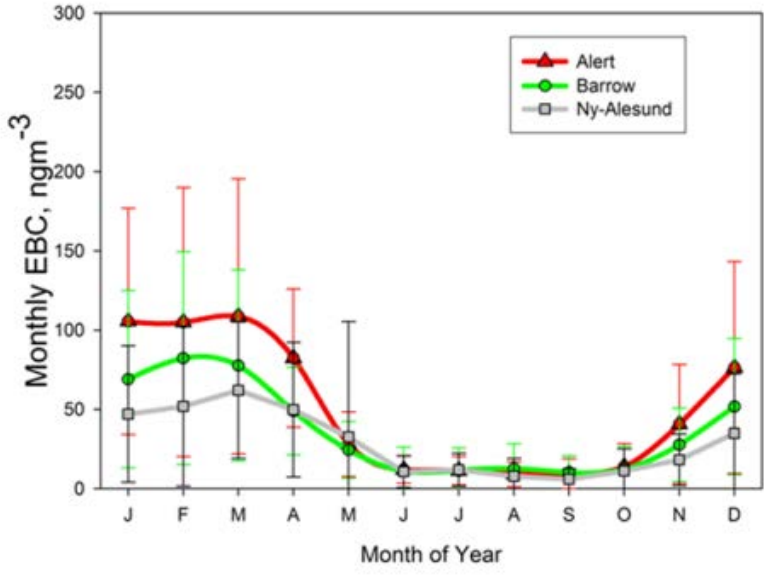

Fig. 18. Seasonal variations in monthly average equivalent black carbon (EBC) at Alert (1989-2012), Barrow (1989-2012) and Ny-Ålesund (1998-2011) show higher EBC values during the winter-spring Arctic haze period. The error bars represent one standard deviation of each mean EBC value.

Maximum EBC concentrations occur in winter and spring (**Figs. 16** and **18**) due to the seasonal influence of Arctic haze, which is transported from mid-latitude source regions (Barrie 1986, Rahn 1981, Sirois and Barrie 1999), with higher transport frequency during winter and spring as the Arctic front extends to lower latitudes. Lower summer values are due to less frequent BC transport into the Arctic and higher wet deposition (Garrett et al. 2011).

References

Barrie, L. A., 1986: Arctic air pollution: An overview of current knowledge, *Atmos. Environ.*, 20, 643-663.

Bond, T. C., and 30 others, 2013: Bounding the role of black carbon in the climate system: A scientific assessment, *J. Geophys. Res.*, 118, 5380-5552.

Charlson, R. J., J. Langner, H. Rodhe, C. B. Leovy and S. G. Warren, 1991: Perturbation of the northern hemisphere radiative balance by backscattering from anthropogenic sulfate aerosols, *Tellus, Ser. A and B*, 43, 152-163.

Collaud Coen, M., and 11 others, 2010: Minimizing light absorption measurement artifacts of the Aethalometer: evaluation of five correction algorithms, *Atmos. Meas. Tech.*, 3, 457-474.

Flanner, M. G., C. S. Zender, J. T. Randerson, and P. J. Rasch, 2007: Present-day climate forcing and response from black carbon in snow, *J. Geophys. Res.*, 112(D11202), doi:10.1029/2006JD008003.

Fletcher, C. G., P. J. Kushner, A. Hall, and X. Qu, 2009: Circulation responses to snow albedo feedback in climate change, *Geophys. Res. Lett.*, 36, L09702.

Garrett, T. J, S. Brattstrom, S. Sharma, D. E. J. Worthy, 2011: The role of scavenging in the seasonal transport of black carbon and sulfate to the Arctic, *Geophys. Res. Lett.*, 38, L16805, doi:10.1029/2011GL048221.

Hansen, A., H. Rosen and T. Novakov, 1984: The Aethalometer: an instrument for the real-time measurement of optical absorption by aerosol particles, *The Science of the Total Environment*, 36, 191-196.

Hegg, D. A., S. G. Warren, T. C. Grenfell, S. J. Doherty, T. V. Larson, and A. D. Clarke, 2009: Source attribution of black carbon in Arctic snow, *Environ. Sci. Technol.*, 43(11), 4016-4021, doi:10.1021/es803623f.

Hirdman, D., H. Sodemann, S. Eckhardt, J. F. Burkhart, A. Jefferson, T. Mefford, P. K. Quinn, S. Sharma, J. Strom, and A. Stohl, 2010: Source identification of short-lived air pollutants in the Arctic using statistical analysis of measurement data and particle dispersion model output, *Atmos. Chem. Phys.*, 10, 669-693.

IPCC (2001) Climate Change, 2001: The Scientific Basis. Contribution of Working Group I to the Third Assessment Report of the Intergovernmental Panel on Climate Change, edited by J.T. Houghton, Cambridge Univ. Press, New York.

IPCC (2007), Climate Change, 2007: The Physical Science Basis. Contribution of Working Group I to the Fourth Assessment, Report of the Intergovernmental Panel on Climate Change, 996 pp., Cambridge University Press, Cambridge, United Kingdom, and New York, NY, USA.

Jacobson, M. Z., 2000: A physically-based treatment of elemental carbon optics: Implications for global direct forcing of aerosols, *Geophys. Res. Lett.*, 27(2), 217-220, doi:10.1029/1999GL010968.

Liousse, C., H. Cachier, and S. G. Jennings, 1993: Optical and thermal measurements of black carbon aerosol content in different environments: Variation of the specific attenuation cross-section, sigma (σ), *Atmos. Environ.*, Part A, 27, 1203-1211.

Liu, Y, W. Wu, M. P. Jensen, and T. Toto, 2011: Relationship between cloud radiative forcing, cloud fraction and cloud albedo, and new surface-based approach for determining cloud albedo, *Atmos. Chem. Phys.*, 11, 7155-7170.

Müller, T., and 38 others, 2013: Characterization and intercomparison of aerosol absorption photometers: result of two intercomparison workshops, *Atmos. Meas. Tech.*, 4, 245-268.

Petzold, A., and 12 others, 2013: Recommendations for reporting "black carbon" measurements, *Atmos. Chem. Phys.*, 13, 8365-8379.

Quinn, P. K., and 12 others, 2008: Short-lived pollutants in the Arctic: Their climate impact and possible mitigation strategies, *Atmos. Chem. Phys.*, 8, 1732-1735, doi:10.5194/acp-8-1723-2008.

Rahn, K. A., 1981: Arctic Air chemistry, *Atmos. Environ.*, 1.5, 1345-1516.

Serreze, M. C., and R. G. Barry, 2011: Processes and impacts of Arctic amplification: A research synthesis, *Global Planet. Change*, 77, 85-96, doi.org/10.1016/j.gloplacha.2011.03.004.

Sharma, S., M. Ishizawa, D. Chan, D. Lavoué, E. Andrews, K. Eleftheriadis, and S. Maksyutov, 2013: 16-year simulation of Arctic black carbon: transport, source contribution, and sensitivity analysis on deposition, *J. Geophys. Res.*, 118, 1-22, doi:10.1029/2012JD017774.

Sharma, S., E. Andrews, L. A. Barrie, J. A. Ogren, and D. Lavoué, 2006: Variations and sources of the equivalent black carbon in the high Arctic revealed by long-term observations at Alert and Barrow: 1989-2003, *J. Geophys. Res.*, 111(D14208), doi:10.1029/2005JD006581.

Sharma, S., D. Lavoué, H. Cachier, L. A. Barrie and S. L. Gong, 2004: Long-term trends of the black carbon concentrations in the Canadian Arctic, *J. Geophys. Res.*, 109(D15203), doi:10.1029/2003JD004331.

Sharma, S., J. R. Brook, H. Cachier, J. Chow, A. Gaudenzi, and G. Lu, 2002: Light absorption and thermal measurements of black carbon in different regions of Canada, *J. Geophys. Res.*, 107(D24), 4771, doi:10.1029/2002JD002496.

Sirois, A., and L. A. Barrie, 1999: Arctic lower tropospheric aerosol trends and composition at Alert, Canada: 1980-1995, *J. Geophys. Res.*, 104(D9), 11,599-11,618.

Stohl, A., 2006: Characteristics of atmospheric transport into the Arctic troposphere, *J. Geophys. Res.*, 111(11), D11306, doi:10.1029/2005JD006888.

Weingartner, E., H. Saathoff, M. Schnaiter, N. Streit, B. Bitnar and U. Baltensperger, 2003: Absorption of light by soot particles: determination of the absorption coefficient by means of aethalometers, *J. Aerosol. Sci.*, 34, 1445-1463.

Sea Ice and Ocean Summary

Section Coordinator: Mary-Louise Timmermans

Department of Geology & Geophysics, Yale University, New Haven, CT, USA

November 8, 2013

The Arctic sea ice extent annual minimum in September 2013 was a little over 50% greater than the September 2012 record low of the period of satellite observations (1979-2013). Nevertheless, the annual minimum areal extent in 2013 was still almost 20% less than the 1981-2010 average. The ice cover continues to be dominated by first-year ice; 78% in March 2013 compared to 58% a quarter century ago in March 1988. Less-extensive sea-ice retreat in 2013 was linked to lower summer sea-surface temperatures in the Chukchi and East Siberian seas relative to recent years. However, anomalously warm sea-surface temperatures (relative to recent decades) persisted in most Arctic Ocean boundary regions in summer 2013. In the upper ocean, relatively high freshwater and heat contents continued to be observed in 2013 in the Beaufort Gyre region of the Canada Basin, although with slight reductions relative to the preceding year.

Sea Ice

D. Perovich[1,2], S. Gerland[3], S. Hendricks[4], W. Meier[5], M. Nicolaus[4], J. Richter-Menge[1], M. Tschudi[6]

[1]ERDC - CRREL, 72 Lyme Road, Hanover USA
[2]Thayer School of Engineering, Dartmouth College, Hanover, NH, USA
[3]Norwegian Polar Institute, Fram Centre, Tromsø, Norway
[4]Alfred Wegener Institute, Bremerhaven, Germany
[5]NASA Goddard Space Flight Center, Greenbelt, MD, USA
[6]Aerospace Engineering Sciences, University of Colorado, Boulder, CO, USA

December 5, 2013

Highlights

- The September 2013 Arctic sea ice minimum extent was 5.10 million km^2. This was 1.69 million km^2 greater than the record minimum set in 2012, but was still the sixth smallest ice extent of the satellite record (1979-2013).
- The amount of first year sea ice continues to increase, accounting for 78% of the ice cover in March 2013.
- A satellite-derived, Arctic Ocean-wide decrease in sea ice freeboard, from 0.23 m in March 2011 to 0.19 m in March 2013, implies a 0.32 m decrease in ice thickness, from 2.26 m to 1.94 m.

Sea Ice Extent

Sea ice extent is used as the basic description of the state of the Arctic sea ice cover. Satellite-based passive microwave instruments have been used to determine sea ice extent since 1979. There are two months each year that are of particular interest: September, at the end of summer, when the sea ice reaches its annual minimum extent, and March, at the end of winter, when the ice is at its maximum extent. The sea ice extent in March 2013 and September 2013 are presented in **Fig. 19**.

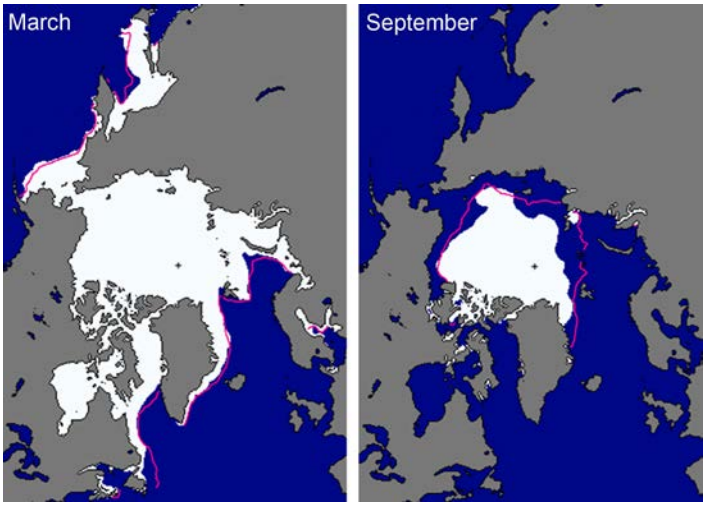

Fig. 19. Sea ice extent in March 2013 (left) and September 2013 (right), illustrating the respective monthly averages during the winter maximum and summer minimum extents. The magenta lines indicate the median ice extents in March and September, respectively, during the period 1981-2010. Note that the median ice extents are computed over a different time interval than the one (1979-2000) used in previous Arctic Report Cards, as explained by NSIDC at http://nsidc.org/data/seaice_index/baseline-change.html. Maps are from NSIDC at nsidc.org/data/seaice_index.

Based on estimates produced by the National Snow and Ice Data Center (NSIDC) the sea ice cover reached a minimum annual extent of 5.10 million km^2 on September 13, 2013. This was substantially higher (1.69 million km^2) than the record minimum of 3.41 million km^2 set in 2012 (**Fig. 20**), making it the largest September minimum ice extent since 2006. However, the 2013 summer minimum extent was still 1.12 million km^2 below the 1981-2010 average minimum ice extent. In March 2013 ice extent reached a maximum value of 15.04 million km^2 (**Fig. 20**), 3% below the 1981-2010 average. This was slightly less than the March 2012 value, but was typical of the past decade.

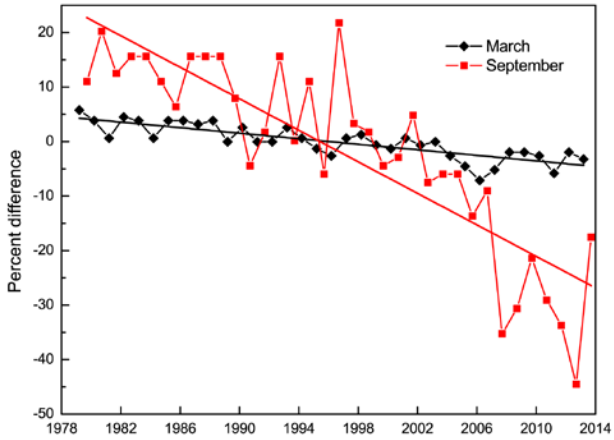

Fig. 20. Time series of ice extent anomalies in March (the month of maximum ice extent) and September (the month of minimum ice extent). The anomaly value for each year is the difference (in %) in ice extent relative to the mean values for the period 1981-2010. The black and red lines are least squares linear regression lines. The slopes of these lines indicate ice losses of -2.6% and -13.7% per decade in March and September, respectively.

Sea ice extent has decreasing trends in all months and virtually all regions (the exception being the Bering Sea during winter). As of 2013, the September monthly average trend is -13.7% per decade relative to the 1981-2010 average (**Fig. 20**). This is slightly lower than the trend (-14% per decade relative to the 1981-2010 average) in 2012, which was the twelfth consecutive year of progressively larger trends of summer ice retreat. Trends are smaller during March (-2.4% per decade, **Fig. 20**), but are still decreasing and statistically significant.

There was a loss of 9.69 million km^2 of sea ice between the March and September extents. This is the smallest seasonal decline since 2006. After reaching the March maximum extent, the seasonal decline began at a rate comparable to the 30-year average (not shown). Through the end of June the 2013 ice extent was just slightly less than the 30-year average values. For a few weeks in late-June and early-July the decrease in ice extent was greater than average. Subsequently, the 2013 ice extent tracked the shape of the average ice extent curve for the remainder of the summer melt season, but at a value about one million km^2 less than the average curve.

Age of The Ice

The age of the sea ice is another key descriptor of the state of the sea ice cover. The age of the ice is an indicator for its physical properties including surface roughness, melt pond coverage, and ice thickness. Older ice tends to be thicker and thus more resilient to changes in atmospheric and oceanic forcing than younger ice. The age of the ice can be determined using satellite observations and drifting buoy records to track ice parcels over several years (Tschudi et al. 2010). This method has been used to provide a record of ice age since the early 1980s (**Fig. 21**). The distribution of ice of different ages illustrates the extensive loss in recent years of the older ice types (Maslanik et al. 2011).

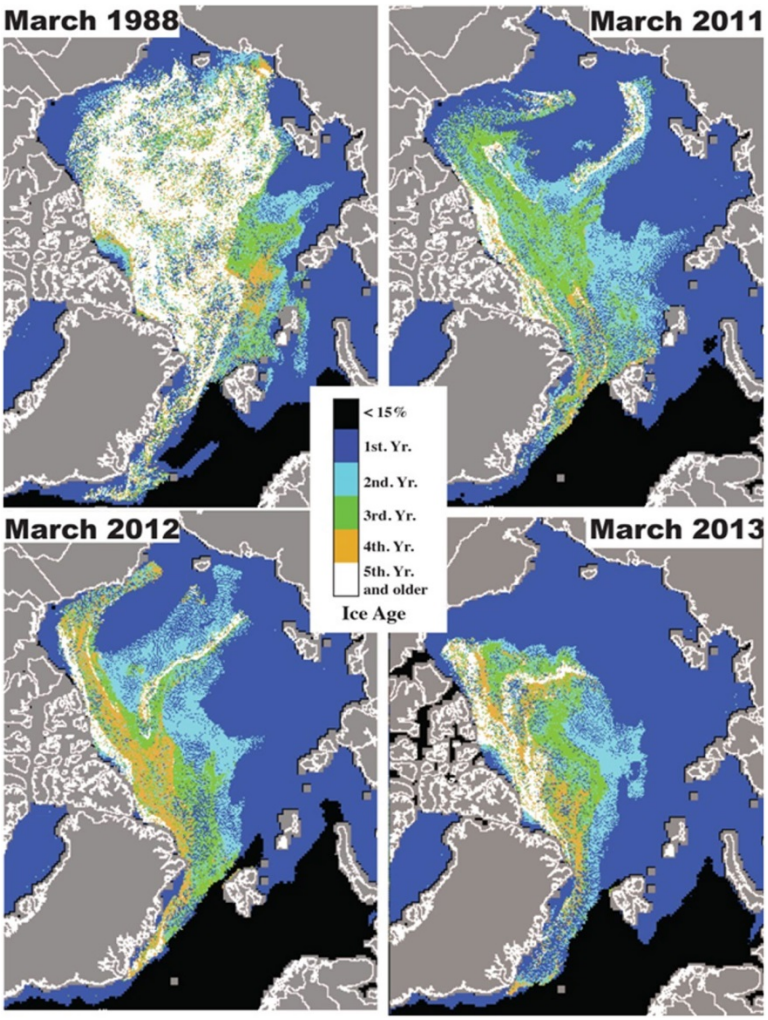

Fig. 21. Sea ice age in March 1988, 2011, 2012 and 2013, determined using satellite observations and drifting buoy records to track the movement of ice floes.

Although the minimum sea ice extent rebounded somewhat in 2013, the distribution of ice age continued to favor first-year ice (FYI, ice that has not survived a melt season), which is the thinnest ice type (e.g., Maslanik et al. 2007). In March 2013, FYI comprised 78% of the ice, up slightly from 75% in 2012. In March 1988, 58% of the ice pack was composed of first-year ice. Meanwhile, the trends continue for the recent loss of the oldest ice types, which accelerated starting in 2005 (Maslanik et al. 2011). For the month of March, the oldest ice (4 years and older) has decreased from 26% of the ice cover in 1988 to 19% in 2005 and to 7% in 2013.

At the end of winter 2013 little multiyear ice was detected in much of the Beaufort Sea (**Fig. 21**, lower right; and Richter-Menge and Farrell 2013). There is no precedent in the satellite-derived record of ice age for the near-absence of old ice in this region, which appears to have been due to a combination of the previous year's record sea ice retreat and a lack of subsequent transport of multiyear ice into the Beaufort Sea during winter 2012-2013. Negligible multiyear ice transport into the Beaufort Sea continued during summer 2013. Nor did multiyear ice drift into Siberian Arctic waters, which is also very rare. Multiyear ice remained confined to the region north of Greenland and northernmost Canada during 2013.

Ice Thickness

The key state variable for the Arctic sea ice cover is ice thickness. In recent years, ice thickness has been estimated over limited regions by aircraft, e.g., the NASA Operation IceBridge (Richter-Menge and Farrell 2013), and over large regions by satellite. The CryoSat-2 satellite, operated since 2011 by the European Space Agency, measures ice freeboard, the height of ice floes above the water line. Preliminary analysis indicates that the Cryosat-2 freeboard estimates are comparable to *in situ* field measurements, with a level of uncertainty that is comparable to other airborne and satellite-based observations. A more detailed error analysis of the freeboard estimates is currently in progress. Calculation of the actual sea-ice thickness from freeboard requires knowledge of snow depth, but in general higher freeboard indicates thicker sea ice. Therefore, freeboard maps in spring in the period from 2011 to 2013 are a proxy for sea ice thickness at the time of maximum ice extent (**Fig. 22**). During the three years of observation by Cryosat-2, the average freeboard has decreased by 0.04 m, from 0.23 m in 2011 to 0.19 m in 2013 (Laxon et al. 2013). Assuming no significant change in snow depth, the decline in freeboard amounts to a mean sea ice thinning of 0.32 m, from 2.26 m in 2011 to 1.94 m in 2013. As with the ice age maps (**Fig. 21**), the Cryosat-2 freeboard maps indicate that most of the thickest and oldest ice occurs to the north of Greenland and northernmost Canada, and it is a small proportion of the total sea ice cover at the end of winter (**Fig. 22**).

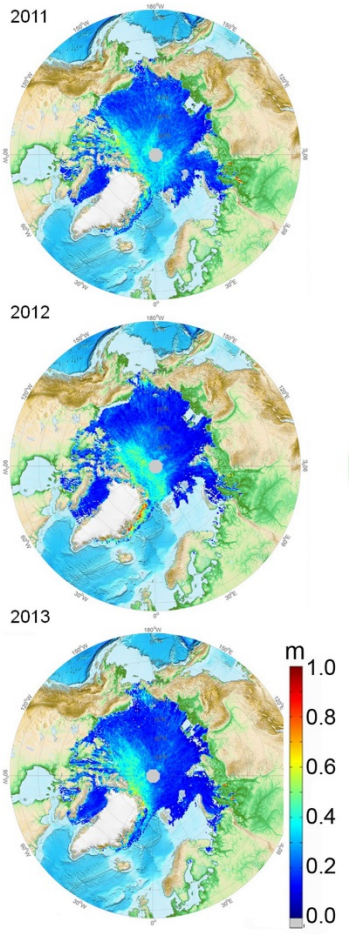

Fig. 22. Ice freeboard (in meters) estimates from Cryosat-2 in March 2011, 2012 and 2013.

References

Laxon, S. W., and 14 others, 2013: CryoSat-2 estimates of Arctic sea ice thickness and volume, *Geophys. Res. Lett.*, 40, doi: 10.1002/grl50193.

Maslanik J. A., C. Fowler, J. Stroeve, S. Drobot, J. Zwally, D. Yi, and W. Emery, 2007: A younger, thinner Arctic ice cover: Increased potential for rapid, extensive sea ice loss, *Geophys. Res. Lett.*, 34, doi:10.1029/2007GL032043.

Maslanik, J., J. Stroeve, C. Fowler, and W. Emery, 2011: Distribution and trends in Arctic sea ice age through spring 2011. *Geophys. Res. Lett.*, 38, doi:10.1029/2011GL047735.

Richter-Menge, J., and S. L. Farrell, 2013: Arctic sea ice conditions in spring 2009-2013 prior to melt. *Geophys. Res. Lett.*, 40, doi:10.1002/2013GL058011, in press.

Tschudi, M. A., C. Fowler, J. A. Maslanik, and J. A. Stroeve, 2010: Tracking the movement and changing surface characteristics of Arctic sea ice. *IEEE J. Selected Topics in Earth Obs. and Rem. Sens.*, 3, doi: 10.1109/JSTARS.2010.2048305.

Ocean Temperature and Salinity

M.-L. Timmermans[1], I. Ashik[2], Y. Cao[3], I. Frolov[2], H.K. Ha[4], R. Ingvaldsen[5], T. Kikuchi[6], T.W. Kim[4], R. Krishfield[7], H. Loeng[5], S. Nishino[6], R. Pickart[7], I. Polyakov[8], B. Rabe[9], I. Semiletov[8], U. Schauer[9], P. Schlosser[10], N. Shakhova[8], W.M. Smethie[10], V. Sokolov[2], M. Steele[11], J. Su[3], J. Toole[7], W. Williams[12], R. Woodgate[11], J. Zhao[3], W. Zhong[3], S. Zimmermann[12]

[1]Yale University, New Haven, CT, USA
[2]Arctic and Antarctic Research Institute, St. Petersburg, Russia
[3]Ocean University of China, Qingdao, China
[4]Korea Polar Research Institute, Incheon, Republic of Korea
[5]Institute of Marine Research, Bergen, Norway
[6]Japan Agency for Marine-Earth Science and Technology, Tokyo, Japan
[7]Woods Hole Oceanographic Institution, Woods Hole, MA, USA
[8]International Arctic Research Center, University of Alaska Fairbanks, Fairbanks, AK, USA
[9]Alfred Wegener Institute, Bremerhaven, Germany
[10]Lamont-Doherty Earth Observatory of Columbia University, Palisades, NY, USA
[11]Applied Physics Laboratory, University of Washington, Seattle, WA, USA
[12]Institute of Ocean Sciences, Sidney, BC, Canada

November 27, 2013

Highlights

- Summer sea surface temperatures in 2013 were higher than previous years in the Barents and Kara seas and can be attributed to increased solar heating associated with the early retreat of the sea ice cover.
- A reduction in freshwater content by about 7% was observed in the Beaufort Gyre region in 2013 relative to 2012.
- Pacific Water transport through Bering Strait into the Arctic Ocean was reduced in 2012 by more than 25% relative to 2011, with consequent reductions in heat and freshwater fluxes.

Summer Sea Surface Temperature

Arctic Ocean mean sea surface temperatures (SST) in August 2013 ranged between ~0°C and 4°C, with even higher SSTs in some marginal seas (**Fig. 23a**). While most Arctic boundary regions displayed anomalously warm SSTs in August 2013, relative to the 1982 - 2006 August mean (**Fig. 23b**), cold anomalies were evident in the Chukchi and East Siberian seas; cooler SSTs are linked to later and less-extensive sea-ice retreat in these regions relative to recent years. Anomalously warm August SSTs in the Barents and Kara seas are related to earlier ice retreat in these regions and possibly also the advection of anomalously warm water from the North Atlantic. Wind stresses derived from NCEP/NCAR reanalysis sea level pressure fields suggest sea ice in summer 2013 was driven away from the Barents and Kara seas, opposite to August conditions of the preceding six years (see Fig. 2.8, Timmermans et al. 2012). See the essay on *Sea Ice* for information on ice extent, age and thickness.

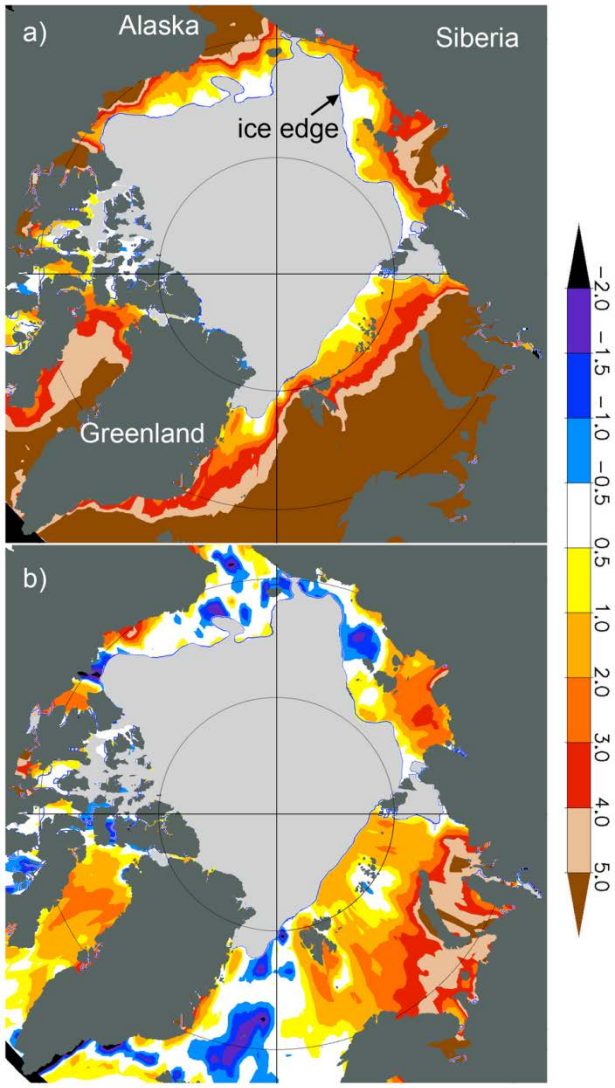

Fig. 23. (a) Mean sea surface temperature (SST, °C) in August 2013, and (b) SST anomalies in August 2013 relative to the August mean of 1982-2006. The anomalies are derived from satellite data according to Reynolds et al. (2007). The blue line shows the August 2013 mean ice edge according to the National Snow and Ice Data Center (NSIDC).

Hydrographic data show surface waters in the vicinity of the Barents Sea Opening (BSO) in September 2013 were about 3°C warmer than in September 2012. SSTs in the southern Barents Sea in September 2013 were as high as 11°C; these anomalously high temperatures, up to 5°C above the 1977-2006 mean, were likely caused by increased heating during summer (Trofimov and Ingvaldsen 2013).

Upper Ocean Salinity

No appreciable differences in upper-ocean (at 20 m depth) salinity were observed between 2012 and 2013, although definitive statements are precluded by the spatial and temporal limitations of the available data. The central Canada Basin remains the freshest region of the Arctic Ocean, and the saltiest upper ocean is observed at the boundaries of the Eurasian Basin and the Barents Sea (**Fig. 24a**). Relative to the 1970s Environmental Working Group (EWG)

climatology (Timokhov and Tanis 1997, 1998), the major upper-ocean salinity differences in 2012-2013 (**Fig. 24b**) were saltier waters in the central Eurasian Basin and fresher waters in the Beaufort Gyre region of the Canada Basin. The upper waters of the Barents and Kara seas were predominantly anomalously salty relative to climatology, although the magnitude of the salinity difference was smaller than in the central Arctic Basin.

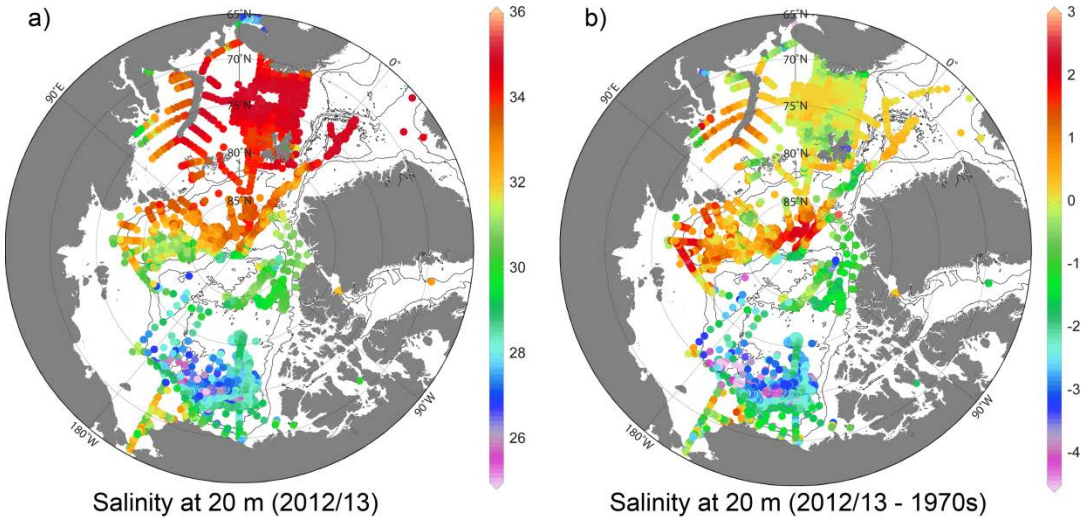

Fig. 24. (a) Salinity at 20 m depth in 2012-2013, and (b) salinity anomalies at 20 m depth in 2012-2013 relative to the 1970s climatology of Timokhov and Tanis (1997, 1998). Contour lines show the 500 m and 2500 m isobaths. Salinities are reported using the Practical Salinity Scale, which has no units.

Freshwater Content

The maximum liquid freshwater content anomaly is centered in the Beaufort Gyre (**Fig. 25**). The Beaufort Gyre accumulated more than 5000 km^3 of freshwater, measured relative to a salinity of 34.8, during 2003-2012; this is a gain of approximately 25% (update to Proshutinsky et al. 2009) relative to climatology of the 1970s (see Fig. 5.24b, Timmermans et al. 2013). Most of this increase occurred between 2004 and 2008, with freshwater content remaining relatively stable between 2008 and 2012, although with a 2012 shift in the freshwater center to the northwest relative to previous years.

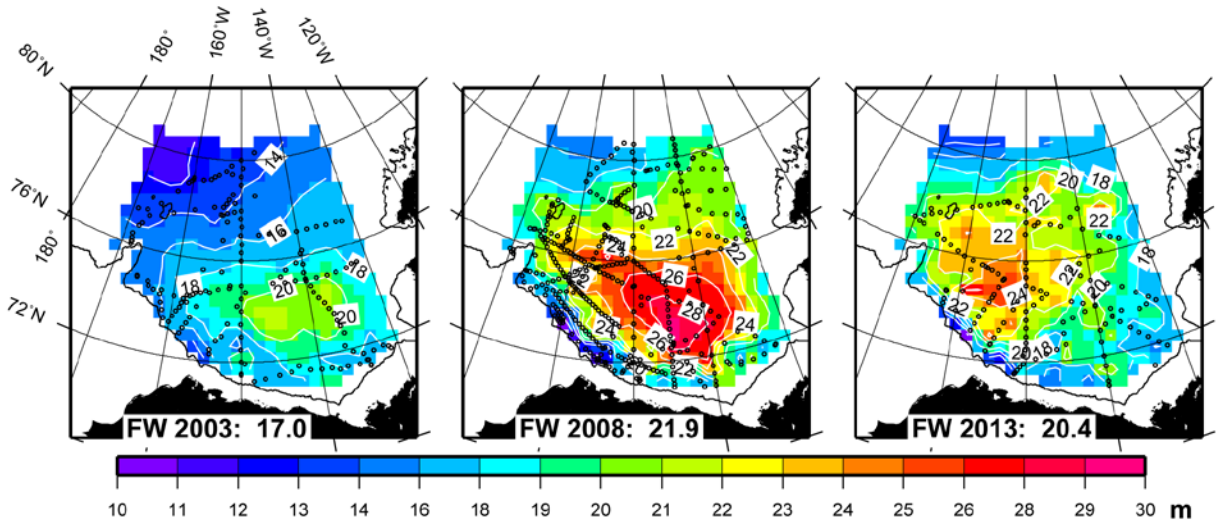

Fig. 25. Freshwater content (in meters and calculated relative to a reference salinity of 34.8) in the Beaufort Gyre of the Canada Basin based on hydrographic surveys in the year shown. Inset numbers at the bottom of each panel give total freshwater volume (1000 km^3) in the region. Black dots depict hydrographic station locations. 2013 data are from the Beaufort Gyre Observing System (BGOS)/Joint Ocean Ice Studies (JOIS) expedition (http://www.whoi.edu/beaufortgyre); 2013 data and calculations are preliminary.

In 2013, a reduction in freshwater content by about 7% was observed relative to 2012 (**Fig. 25**). This reduction may be attributed in part to weaker wind-stress gradients in 2013 resulting in reduced wind-forced accumulation of surface-waters (and relaxation of downwelling) in the region. Aside from this change, wind stresses indicate the average circulation pattern for the September 2012-August 2013 period was generally similar to the average over the preceding 12 months (see Fig. 2.7, Timmermans et al. 2012). Strong anticyclonic (clockwise) wind forcing in winter 2013 was followed by anomalously weak forcing (in nearly the opposite sense) in summer 2013. It is of note that trends in Beaufort Gyre heat content generally follow freshwater trends; there is ~25% more heat on average in the summer now compared to the 1970s.

Pacific Water Layer

The Pacific Water Layer in the Arctic Ocean originates from the Bering Strait inflow and resides in the Canada Basin at depths between about 50 and 150 meters. As reported in Woodgate et al. (2012), 2011 was a high transport year for Pacific Water inflow through the Bering Strait, with transports being ~1.1 Sv, much higher than the accepted climatology (1991-2003) of ~0.8 Sv (Woodgate et al. 2005). This high transport resulted in heat fluxes comparable to 2007 (the previous record high since 1991), and record maximum freshwater fluxes since 1991. In contrast, preliminary data suggest that the 2012 annual means were much lower than in 2011; annual mean 2012 transport was close to the climatological mean of 0.8 Sv. The annual mean temperature of the Pacific Water Layer in 2012 was colder than the last decade, and comparable to the annual means of the 1991-2001 period. These two factors yield a heat flux in 2012 comparable to the record low in 2001. Freshwater transport was also reduced in 2012 compared to 2011; in general freshwater flux through the Bering Strait shows interannual variability that is larger than the interannual variability in the other major freshwater sources to the Arctic (i.e., rivers and net precipitation).

Pacific Water enters the Canada Basin via different mechanisms and pathways. Moored measurements of the Pacific water boundary current in the Beaufort Sea north of Alaska (the Beaufort shelfbreak jet) show an 80% decrease in volume transport in the current between 2002 and 2011 (Brugler et al. 2013), where this decrease is predominantly in the summer months. Brugler et al. (2013) attribute the decrease in transport to an increase in easterly winds associated with a stronger Beaufort High and deeper Aleutian Low. These authors propose that in recent years Pacific heat and freshwater is being advected directly north into the Canada Basin interior instead of progressing eastward in the Beaufort shelfbreak jet.

In the central Canada Basin, observations show heat and freshwater content in the Pacific Water Layer increased by about 40% during 2003-2013, with the largest increases in the southern Canada Basin before 2010. Freshwater content has been relatively stable since 2010. In 2013 maximum Pacific Water Layer temperatures over the abyssal plain of the Canada Basin were ~0.5°C.

Atlantic Water Layer

Warm water of North Atlantic origin, lying below the halocline at depths between about 200 m and 900 m (but nearer the surface in the vicinity of the Barents Sea Opening and Fram Strait), is characterized by temperatures >0°C and salinities >34.5. Maximum Atlantic Water temperatures are generally around 1-2°C cooler in the Canadian Basin than in the Eurasian Basin (see Fig. 5.22b in Proshutinsky et al. 2012). In 2012 and 2013, the warmest Atlantic Water temperatures (~5°C) were observed in the Barents Sea. The coolest temperatures (~0°C) were observed off the north coast of Greenland. No significant changes were observed in 2013 in the Atlantic Water Layer compared to 2012 conditions.

Relative to 1970s climatology, maximum Atlantic Water temperature anomalies were <0.5°C warmer in the Canadian Basin and ~0.5-1°C warmer in the Eurasian Basin. Maximum temperatures of the Atlantic Water flowing into the southern Barents Sea in 2013 were about 0.5°C higher than the 1977-2006 mean (Trofimov and Ingvaldsen 2013). There was little to no temperature anomaly (<0.1°C) at the southeast boundary of the Canada Basin nor in the basin boundary regions adjacent to Greenland and the Canadian Archipelago.

References

Brugler, E. T., R. S. Pickart, G. W. K. Moore, S. Roberts, T. J. Weingartner, and H. Statscewich, 2013: Seasonal to Interannual Variability of the Pacific Water Boundary Current in the Beaufort Sea. Submitted to *Progress in Oceanography*.

Proshutinsky, A. and 27 others, 2012: [The Arctic] Ocean [in "State of the Climate in 2011"]. *Bulletin of the American Meteorological Society*, 93 (7), S57-92.

Proshutinsky, A., and 9 others, 2009: Beaufort Gyre freshwater reservoir: State and variability from observations. *J. Geophys. Res.*, 114(C1), doi:10.1029/2008JC005104.

Reynolds, R. W., T. M. Smith, C. Liu, D. B. Chelton, K. S. Casey, and M. G. Schlax, 2007: Daily high-resolution-blended analyses for sea surface temperature. *J. Climate*, 20, 5473-5496.

Timmermans, M.-L., and 29 others. 2012a: Ocean, in *Arctic Report Card, Update for 2012*, http://www.arctic.noaa.gov/report12/ocean.html.

Timmermans, M.-L., and 24 others, 2013: [The Arctic] Ocean Temperature and Salinity [in "State of the Climate in 2012"]. *Bulletin of the American Meteorological Society*, 94(8), S128 - S130.

Timokhov, L., and F. Tanis, Eds., 1997, 1998: Environmental Working Group Joint U.S.-Russian Atlas of the Arctic Ocean-Winter Period. Environmental Research Institute of Michigan in association with the National Snow and Ice Data Center, Arctic Climatology Project, CD-ROM, http://nsidc.org/data/g01961.html.

Trofimov, A., and R. Ingvaldsen, 2012: Hydrography. In: E. Eriksen (Ed.) Survey report from the joint Norwegian/Russian ecosystem survey in the Barents Sea August-October 2012. IMR/PINRO Joint Report Series, No. 2/2012, pp. 7-15, ISSN 1502-8828, 118 pp.

Trofimov, A., and R. Ingvaldsen, 2013: Hydrography. In: E. Eriksen (Ed.) Survey report from the joint Norwegian/Russian ecosystem survey in the Barents Sea August-October 2013. IMR/PINRO Joint Report Series, in press.

Woodgate R. A., K. Aagaard, and T. J. Weingartner, 2005: Monthly temperature, salinity, and transport variability of the Bering Strait through flow. *Geophys. Res. Lett.*, 32, L04601, doi:10.1029/2004GL021880.

Woodgate, R. A., T. J. Weingartner, and R. Lindsay, 2012: Observed increases in Bering Strait oceanic fluxes from the Pacific to the Arctic from 2001 to 2011 and their impacts on the Arctic Ocean water column. *Geophys. Res. Lett.*, 39, L24603, doi:10.1029/2012GL054092.

Marine Ecosystems Summary

Section Coordinators: Mike Gill[1], Sue Moore[2]

[1]Canadian Wildlife Service, Environment Canada, Whitehorse, YT, Canada & CAFF/CBMP
[2]NOAA/Fisheries Office of Science and Technology, Seattle, WA, USA

November 8, 2013

The Marine Ecosystems section provides some insights into how the marine ecosystem is responding to changes in environmental conditions, especially the rapid and dramatic loss of sea ice (see the essay on *Sea Ice*). The central role of sea ice in structuring various components of the marine ecosystem is highlighted in essays on Sea Ice Biota, Marine Benthic Communities and Marine Fish of the Arctic.

Sea ice-derived organic matter continues to be an important early food source for sympagic (ice-associated), benthic (lowermost water column and seafloor) and pelagic (offshore water column) biota in the Arctic. However, sea ice habitats appear to be changing - for example, there is less multiyear ice (see the essay on *Sea Ice*), but melt ponds are becoming more frequent - in ways that are relevant for ice-associated biota, as indicated by regional decreases in their abundance and biomass. Arctic benthic communities are particularly good biological indicators of the impact of longer-term climate changes on the marine ecosystem, versus seasonal oscillations, because contributing species typically have long life spans (see the essay on *Benthos* in Report Card 2012). Responses of Arctic benthic communities to climate and anthropogenic factors can be observed from shifts in species distribution patterns and in the appearance of new species. The detection of changes and trends in Arctic benthic communities depends on sustained long-term observing programs, such as the HAUSGARTEN observatory in the Atlantic sector and the Distributed Biological Observatory (DBO) in the Pacific sector of the Arctic (see the essay on *Ecosystem Observations in Barrow Canyon* in Report Card 2012).

Observed and expected continuing reductions in sea ice and associated changes in productivity (see the essay on *Arctic Ocean Primary Productivity* in Report Card 2011) will likely affect marine and anadromous fish fauna in the Arctic and the adjacent sub-Arctic seas. There are strong gradients in species richness from warmer, sub-Arctic waters to colder, Arctic waters, implying a strong potential for species to expand their ranges into Arctic waters as temperatures increase. New (to the Arctic) fish species have been reported from several areas, especially the Canadian Beaufort Sea, which likely represent both altered distributions resulting from climate change and previously occurring but undetected species. Here again, comprehensive research surveys are required, extending to more northerly and deeper ocean regions, to establish baselines critical for assessing fish responses to Arctic change.

Arctic Sea Ice Biota

H. Hop[1], B.A. Bluhm[2], M. Daase[1], R. Gradinger[2], M. Poulin[3]

[1]Norwegian Polar Institute, Fram Centre, Tromsø, Norway
[2]School of Fisheries and Ocean Sciences, University of Alaska Fairbanks, Fairbanks, AK, USA
[3]Research and Collections Division, Canadian Museum of Nature, Ottawa, ON, Canada

November 20, 2013

Highlights

- Sea ice-derived organic matter continues to be an important early food source for sympagic (ice-associated), pelagic and benthic biota in the Arctic.
- Sea ice habitats appear to be undergoing change with regard to availability and suitability for associated biota during their entire life cycles, as indicated by regional declines in their abundance and biomass.
- As multiyear ice habitat declines, pressure ridges in first-year ice may become increasingly important as refugia for sympagic organisms.

The sympagic (ice-associated) realm, with its associated food web, is unique and intricately connected to both the pelagic (offshore water column) and benthic (hyperbenthic, i.e., above seafloor, and seafloor) systems. Sympagic biota range from microbes to the charismatic megafauna, including seals, walrus and polar bears. It is challenging to sample small organisms quantitatively inside this highly seasonal ecosystem, in its boundary layer with the underlying sea water and in three-dimensional pressure ridge systems. Consequently, small sea ice biota are not monitored regularly in the Arctic and little information exists on its status and trends. Here we report on: (1) the state of knowledge of sympagic biodiversity and its role in the Arctic marine food web, and (2) the types of sea ice biotic communities that appear to be prominent in today's Arctic cryosphere, which is dominated by first-year ice at the end of winter (see the essay on *Sea Ice*).

A new paradigm has become apparent in the past few years: sympagic diversity contributes considerably to total Arctic biodiversity, and biotic inventories and density patterns are unique to sea ice compared to the underlying water column (Collins et al. 2010, Niemi et al. 2011). This discovery mainly reflects the use of newer taxonomic tools, such as molecular and genetic techniques, in studies of sea ice biota. Consequently, we now appreciate the presence of over a thousand morphological taxa of single-celled eukaryotes (Poulin et al. 2011) and over 1500 unique operational taxonomic units (OTUs, equating molecular species) of microbes (Collins and Deming 2011, Bowman et al. 2012). The multicellular ice fauna is relatively well described (e.g., Melnikov 1997, Hop and Pavlova 2008, Gradinger et al. 2010), but also subject to taxonomic revision based on molecular relationships (e.g., Ki et al. 2011).

The sympagic contribution to the Arctic marine food web and the importance of ice-derived particulate organic matter (I-POM) to vertical flux and the pelagic-benthic coupling have been described regionally (e.g., Søreide et al. 2006, Tamelander et al. 2006, 2009), but with no overall trends for the Arctic. Recent studies have strengthened the notion that I-POM continues to be an important food source in Arctic systems, particularly during early spring (April), when few other carbon sources are available (Søreide et al. 2010, 2013, Matrai et al. 2013). On the

Canadian Arctic shelf and in the Canada Basin, sympagic primary production may contribute 8-50% to total shelf and 20-90% to total basin net community production, with values ranging from low in the western and central Canadian Arctic to high around Ellesmere Island (Matrai and Appolonio 2013). Reduced ice cover extent (Maslanik et al. 2011, Comiso 2012) tends to diminish the ice algal contribution to total primary production, whereas thinner ice may enhance it regionally. A thick layer of snow on the ice may block out >90% of the irradiation and limit ice algal production, whereas little or no snow on the ice increase light transmission and tend to enhance production of shade-adapted ice algae, with varying degrees of photo-protection (Juhl and Krembs 2010, Alou-Font et al. 2013). Thus, the central Arctic, with thin snow cover, may harbor higher biomass of ice algae than the marginal areas of the pack ice (Legendre et al. 1992). The marginal seas are also influenced by advected heat from the Atlantic current, for example, which varies in relation to marine climate (Walczowski et al. 2012). This results in rapid melting of sea ice from below and seasonal loss of the sympagic flora and fauna.

Consumers of I-POM include representatives from all three marine realms: ice-associated fauna and early ascending zooplankton, including grazers like the Arctic-endemic copepod *Calanus glacialis*, as well as benthic fauna (Søreide et al. 2010, 2013, Brown and Belt 2012, Boetius et al. 2013, Cooper et al. 2013, and see the essay on *Arctic Benthic Communities*). The high nutritional value of I-POM has been tied to the abundance of high proportions of polyunsaturated fatty acids in ice algae during early spring (March-April) (Leu et al. 2011). One might speculate that the nutritional value may be increasingly compromised in today's Arctic dominated by thinner, first-year sea ice (see the essay on *Sea Ice*), because the abundance of the highly nutritional components in ice algae decreases with increasing irradiance (Leu et al. 2010).

Projections for future distribution patterns of sympagic fauna are unclear for the Arctic as a whole. The only available time-series of sympagic biota is based on composite data of ice amphipod abundance and biomass estimates from the 1980s to present in the Svalbard and Fram Strait region (**Fig. 26**). Ice amphipod biomass, particularly that of the gammarid amphipod *Gammarus wilkitzkii* (**Figs. 27**), has been low in the last decade and abundances as high as those reported in the 1980s have not been observed recently. These observations are likely tied to the reduced presence of multiyear sea ice in the region (Polyakov et al. 2012), the preferred habitat of long-lived *G. wilkitzkii* (Lønne and Gulliksen 1991b).

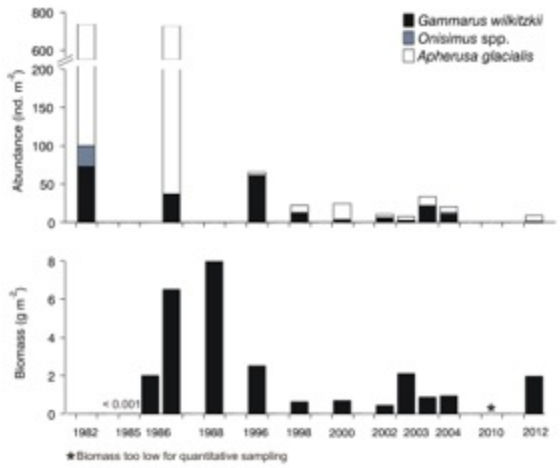

Fig. 26. (a, top) Abundance (ind.$^{-2}$) estimates of the most common ice amphipod species, and (b, bottom) estimates of biomass (wet weight, g m^{-2}, for all three species combined) between July and September in sea ice north of Svalbard (>79°N). Abundance and biomass data are not always available for the same years. Data are from Hop and Pavlova (2008), Lønne and Gulliksen (1991a, b) and also include unpublished data from the Norwegian Polar Institute (H. Hop), the UiT- The Arctic University of Norway (B. Gulliksen) and the University Centre in Svalbard (O. J. Lønne, J. Berge).

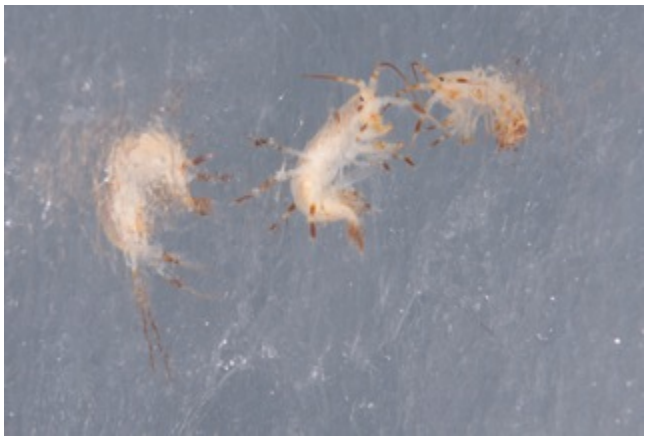

Fig. 27. (a) The ice amphipod *Gammarus wilkitzkii* is a characteristic species of Arctic sea ice, and particularly abundant in multiyear ice or in ridges (Hop et al. 2000). (b) Adults are up to 5 cm long and live inside brine channels or pockets in the ice. Photograph: Peter Leopold.

In contrast to such observations and the common belief that reduced ice cover will generally be detrimental to sympagic fauna, several mechanisms have recently been suggested that may counteract the direct consequences of loss of habitat to some extent. First, in the Svalbard/Jan Mayen region, the amphipod *Apherusa glacialis* appears to descend to deep water where it likely encounters Atlantic currents that transport it back to the north, thereby avoiding export from the Arctic (Berge et al. 2012). Second, the vertical extent of first-year sea ice pressure ridges, a habitat that often survives the summer melt season, may be crucial for summer survival of sea ice meio- and macrofauna (Hop and Pavlova 2008, Gradinger et al. 2010).

Besides the reduction of the multiyear ice, there is some evidence that other sea ice habitats are also changing. Melt ponds appear to have increased in frequency, now being abundant

during early summer (Nicolaus et al. 2012, Polashenski et al. 2012). Small flagellated taxa with limited primary productivity dominate the algal communities in such melt ponds (Lee et al. 2012), while meio- and macrofaunal communities are similar to those found in the bottom layers of sea ice (Kramer and Kiko 2011). Unusually abundant and large (1-15 cm diameter) ice-algal aggregates were observed floating below melting Arctic sea ice north of Svalbard during the 2012 record ice minimum year (Assmy et al. 2013, **Fig. 28**). These algal lumps constituted a food source for the ice-associated fauna, as revealed by pigments indicative of zooplankton grazing (i.e., degraded chlorophyll products inside the lumps), high abundance of naked ciliates, and ice amphipods associated with them. During the summer melt season, these floating aggregates likely play an important ecological role in an otherwise impoverished near-surface sea ice environment. They may be more prominent in areas or years of enhanced melting. Such observations match those of rapidly sinking large ice algal aggregates recorded at the Arctic deep-sea sea floor in August-September 2012, where they were exploited by epibenthic organisms (Morata et al. 2011, Boetius et al. 2013). See the essay on *Arctic Benthic Communities* for additional discussion of sea ice algal production and export to the deep benthos.

Fig. 28. Ice algal lumps under melting sea ice were a food source for sympagic organisms in late July, 2012. Photograph: Peter Leopold.

References

Alou-Font, E., C. J. Mundy, S. Roy, M. Gosselin, and S. Agusti, 2013: Snow cover affects ice algal pigment composition in the coastal Arctic Ocean during spring. *Mar. Ecol. Prog. Ser.*, 474, 89-104.

Assmy, P., J. K. Ehn, M. Fernández-Méndez, H. Hop, C. Katlein, A. Sundfjord, K. Bluhm, M. Daase, A. Engel, A. Fransson, M. A. Granskog, S. A. Hudson, S. Kristiansen, M. Nicolaus, I. Peeken, A. H. H. Renner, G. Spreen, A. Tatarek, and J. Wiktor, 2013: Floating ice-algal aggregates below melting Arctic sea ice. *PLoS ONE*, 8 (10), e76599.

Berge, J., Ø. Varpe, M. A. Moline, A. Wold, P. E. Renaud, M. Daase, and, S. Falk-Petersen, 2012: Retention of ice-associated amphipods: possible consequences for an ice-free Arctic Ocean. *Biol. Lett.*, 8, 1012-1015.

Boetius, A., S. Albrecht, K. Bakker, C. Bienhold, J. Felden, M. Fernández-Méndez, S. Hendricks, C. Katlein, C. Lalande, T. Krumpen, M. Nicolaus, I. Peeken, B. Rabe, A. Rogacheva, E. Rybakova, R. Somavilla, F. Wenzhöfer, and RV Polarstern ARK27-3-Shipboard Science Party, 2013: Export of algal biomass from the melting Arctic sea ice. *Science*, 339, 1430-1432.

Bowman, J. S., S. Rasmussen, N. Blom, J. W. Deming, S. Rysgaard, and T. Sicheritz-Ponten, 2012: Microbial community structure of Arctic multiyear sea ice and surface seawater by 454 sequencing of the 16S RNA gene. *ISME J.*, 6, 11-20.

Brown, T., and S. T. Belt, 2012: Identification of the sea ice diatom biomarker IP_{25} in Arctic macrofauna: direct evidence for a sea ice diatom diet in Arctic heterotrophs. *Polar Biol.*, 35, 131-137.

Collins, E., and J. W. Deming, 2011: Abundant dissolved genetic material in Arctic sea ice Part I: extracellular DNA. *Polar Biol.*, 34, 1819-1830.

Collins, R. E., G. Rocap, and J. W. Deming, 2010: Persistence of bacterial and archaeal communities in sea ice through an Arctic winter. *Environ. Microbiol.*, 12, 1828-1841.

Comiso, J. C., 2012: Large decadal decline of the Arctic multiyear ice cover. *J. Clim.*, 25, 1176-1193.

Cooper, L.W., M. G. Sexson, J. M. Grebmeier, R. Gradinger, C. W. Mordy, and J. R. Lovvorn, 2013: Linkages between sea-ice coverage, pelagic-benthic coupling, and the distribution of spectacled eiders: Observations in March 2008, 2009 and 2010, northern Bering Sea. *Deep-Sea Res. Part II*, 94, 31-43.

Gradinger, R., B. Bluhm, and K. Iken, 2010: Arctic sea-ice ridges-Safe heavens for sea-ice fauna during periods of extreme ice melt? *Deep-Sea Res. Part II*, 57, 86-95.

Hop, H., and O. Pavlova, 2008: Distribution and biomass transport of ice amphipods in drifting sea ice around Svalbard. *Deep-Sea Res. Part II*, 55, 2292-2307.

Juhl, A. R., and C. Krembs, 2010: Effects of snow removal and algal photoacclimation on growth and export of ice algae. *Polar Biol.*, 33, 1057-1065.

Ki, J. -S., H. -U. Dahms, I. -C. Kim, H. G. Park, H. Hop, and J. -S. Lee, 2011: Molecular relationships of gammaridean amphipods from Arctic sea ice. *Polar Biol.*, 34, 1559-1569.

Kramer, M. and R. Kiko, 2011: Brackish meltponds on Arctic sea ice - a new habitat for marine metazoans. *Polar Biol.*, 34, 603-608.

Lee, S. H., D. A. Stockwell, H. -M. Joo, Y. B. Son, C. -K. Kang, and T. E. Whitledge, 2012: Phytoplankton production from melting ponds on Arctic sea ice. *J. Geophys. Res.*, 117, C04030, doi:10.1029/2011JC007717.

Legendre, L., S. F. Ackley, G. S. Dieckmann, B. Gulliksen, R. Horner, T. Hoshiai, I. A. Melnikov, W. S. Reeburgh, M. Spindler, and C. W. Sullivan, 1992: Ecology of sea ice biota. 2. Global significance. *Polar Biol.*, 12, 429-444.

Leu, E., J. E. Søreide, D. O. Hessen, S. Falk-Petersen, and J. Berge, 2011: Consequences of changing sea-ice cover for primary and secondary producers in the European Arctic shelf seas: Timing, quantity, and quality. *Prog. Oceanogr.*, 90, 18-32.

Leu, E., J. Wiktor, J. E. Søreide, J. Berge, and S. Falk-Petersen, 2010: Increased irradiance reduces food quality of sea ice algae. *Mar. Ecol. Prog. Ser.*, 411, 49-60.

Lønne, O. J., and B. Gulliksen, 1991a: On the distribution of sympagic macro-fauna in the seasonally ice covered Barents Sea. *Polar Biol.*, 11, 457-469.

Lønne, O. J., and B. Gulliksen, 1991b: Sympagic macro-fauna from multiyear sea-ice near Svalbard. *Polar Biol.*, 11, 471-477.

Maslanik, J., J. Stroeve, C. Fowler, and W. Emry, 2011: Distribution and trends in Arctic sea ice ave through spring 2011: *Geophys. Res. Lett.*, 38, L13502, doi:10.1029/211GL047735.

Matrai, P., and S. Apollonio, 2013: New estimates of microalgae production based upon nitrate reductions under sea ice in Canadian shelf seas and the Canada Basin of the Arctic Ocean. *Mar. Biol.*, 160, 1297-1309.

Matrai, P.A., E. Olson, S. Suttles, V. Hill, L. A. Codispoti, B. Light, and M. Steele, 2013: Synthesis of primary production in the Arctic Ocean: I. Surface waters, 1954-2007. *Prog. Oceanogr.*, 110, 93-106.

Melnikov, I., 1997: *The Arctic Sea Ice Ecosystem*. Gordon and Breach Science Publishers, Amsterdam, 204 pp.

Morata, N., M. Poulin, and P. E. Renaud, 2011: A multiple biomarker approach to tracking the fate of an ice algal bloom to the sea floor. *Polar Biol.*, 34, 101-112.

Nicolaus, M., S. Arndt, C. Katlein, J. Maslanik, and S. Hendricks, 2012: Changes in Arctic sea ice result in increasing light transmission and absorption. *Geophys. Res. Lett.*, 40, 2699-2700.

Niemi, A., C. Michel, K. Hille, and M. Poulin, 2011: Protist assemblages in winter sea ice: setting the stage for the spring ice algal bloom. *Polar Biol.*, 34, 1803-1817.

Polashenski, C., D. Perovic, and Z. Courville, 2012: The mechanisms of sea ice pond formation and evolution. *J. Geophys. Res.*, 117, C01001, doi:10.1029/2011JC007231.

Polyakov, I. V., J. E. Walch, and R. Kwok, 2012: Recent changes of Arctic multiyear sea ice coverage and likely causes. *Am. Meterol. Soc.*, 93, 125-151.

Poulin, M., N. Daugbjerg, R. Gradinger, L. Ilyash, T. Ratkova, and C. von Quillfeldt, 2011: The pan-Arctic biodiversity of marine pelagic and sea-ice unicellular eukaryotes: a first-attempt assessment. *Mar. Biodivers.*, 41, 13-28.

Søreide, J.E., M. L. Carroll, H. Hop, W. G. Ambrose Jr., E. N. Hegseth, and S. Falk-Petersen, 2013: Sympagic-pelagic-benthic coupling in Arctic and Atlantic waters around Svalbard revealed by stable isotopic and fatty acid tracers. *Mar. Biol. Res.*, 9, 892-911.

Søreide, J. E., H. Hop, M. L. Carroll, S. Falk-Petersen, and E. N. Hegseth, 2006: Seasonal food web structures and sympagic-pelagic coupling in the European Arctic revealed by stable isotopes and a two-source food web model. *Prog. Oceanogr.*, 71, 59-87.

Søreide et al. 2007, Corrigendum. *Prog. Oceanogr.*, 73, 96-98.

Søreide, J. E., E. Leu, J. Berge, M. Graeve, and S. Falk-Petersen, 2010: Timing in blooms, algal food quality and *Calanus glacialis* reproduction and growth in a changing Arctic. *Global Change Biol.*, 16, 3154-3163.

Tamelander, T., M. Reigstad, H. Hop, and T. Ratkova, 2009: Ice algal assemblages and vertical export of organic matter from sea ice in the Barents Sea and Nansen Basin (Arctic Ocean). *Polar Biol.*, 32, 1261-1273.

Tamelander, T., P.E. Renaud, H. Hop, M. L. Carroll, W. G. Ambrose Jr., and K. A. Hobson, 2006: Trophic relationships and pelagic-benthic coupling during summer in the Barents Sea Marginal Ice Zone, revealed by stable carbon and nitrogen isotope measurements. *Mar. Ecol. Prog. Ser.*, 310, 33-46.

Walczowski, W., J. Piechura, I. Goszczko, and P. Wieczorek, 2012: Changes in Atlantic water properties: an important factor in the European Arctic marine climate. *ICES J. Mar. Sci.*, 69, 864-869.

Marine Fishes of the Arctic

F.J. Mueter[1], J.D. Reist[2], A.R. Majewski[2], C.D. Sawatzky[2], J.S. Christiansen[3], K.J. Hedges[3], B.W. Coad[4], O.V. Karamushko[5], R.R. Lauth[6], A. Lynghammar[3], S.A. MacPhee[2], C.W. Mecklenburg[7]

[1]University of Alaska Fairbanks, School of Fisheries and Ocean Sciences, Fairbanks, AK, USA
[2]Fisheries and Oceans Canada, 501 University Crescent, Winnipeg, MB, Canada
[3]Department of Arctic and Marine Biology, UiT The Arctic University of Norway, Tromsø, Norway
[4]Canadian Museum of Nature, P.O. Box 3443, Station D, Ottawa, ON, Canada
[5]Murmansk Marine Biological Institute, Kola Science Centre, Russian Academy of Sciences, Murmansk, Russia
[6]Alaska Fisheries Science Center, National Marine Fisheries Service, NOAA, 7600 Sand Point Way NE, Seattle, WA, U.S.A.
[7]California Academy of Sciences, San Francisco, CA & Point Stephens Research, Auke Bay, AK, USA

December 6, 2013

Highlights

- New Arctic and sub-Arctic species have been reported from several areas, particularly the Canadian Beaufort Sea; they likely represent both altered distributions resulting from climate change and previously occurring but unsampled species.
- There are strong gradients in species richness from warmer, sub-Arctic waters to colder, Arctic waters, implying a high potential for species expanding into Arctic waters as temperatures increase.
- As accessibility increases, comprehensive research surveys are required for more northerly and deeper areas to establish baselines critical to assessing fish response to Arctic change.

Introduction

Observed and expected future reductions in sea ice (Jeffries & Richter-Menge 2013) and associated changes in productivity (Wassmann 2011) will likely affect the fish fauna in the Arctic and its adjacent sub-Arctic seas. Anticipated changes include movement of fishes from the sub-Arctic to the Arctic as well as changes in local productivity and abundance. The specific nature and magnitude of such effects will depend on the sensitivity and adaptive capacity of the affected species (Hollowed et al. 2013) and will differ among species and habitats. These changes are of interest primarily because Arctic marine fishes play a fundamental role in the transfer of bioenergy from lower trophic levels to seabirds and marine mammals (Bluhm and Gradinger 2008), which provide the livelihood for many Arctic residents. Moreover, some species could support future fisheries in areas that have historically been of little commercial interest. However, credible assessments of Arctic fisheries resources are not yet possible due to a lack of basic data. Concerns over potential impacts of unregulated fishing on Arctic marine ecosystems prompted the US Secretary of Commerce to approve a Fishery Management Plan that closes Arctic waters north of Bering Strait and within the US EEZ (Exclusive Economic Zone) to fishing (Wilson and Ormseth 2009). However, international agreements governing fishing in the Arctic are currently limited to a few regional agreements in the Atlantic sector.

Surveys of the Arctic have been limited by sea ice conditions, remoteness and related costs, compounded by perception of low economic potential for fisheries. These factors have

historically limited sampling to areas where sea ice melted during summer (more southerly regions, coastal zones and shallower locations), upper layers within the summer pack ice, and locations where fisheries potential was thought to be high. The ice has also limited the types of gear that can be deployed in Arctic waters; e.g., deepwater fishing using active gear such as trawls has been very limited. Instead, sampling of fish eggs and larvae in ice-covered waters has provided what basic information is available for much of the area. This has restricted our knowledge about fishes occupying Arctic waters, particularly those under perennial sea ice and in deeper locations. Interest in oil and gas potential and increased shipping, combined with recent progressive degradation in the extent, duration, and thickness of summer sea ice, have stimulated efforts to effectively survey more extensive areas.

Here we summarize some recent observations on the status and trends of fishes within several regional seas (**Fig. 29**). The focus is on marine species, but an overview of Arctic marine fishes is incomplete without considering anadromous fishes, which occur in nearshore areas freshened by summer runoff but may extend into offshore pelagic waters. In addition, some freshwater species occur in highly freshened estuaries or nearshore marine locations. So far as is known, all anadromous and freshwater species leave Arctic marine waters in winter when sea ice formation results in hypersalinities, temperatures below 0°C and physical disruption of shallow habitats due to grounding of sea ice. Most Arctic marine species are associated with benthic habitats (Christiansen et al. 2013b). In contrast, the polar (or Arctic) cod (*Boreogadus saida*) is both cryopelagic and demersal, living under the sea ice in waters as deep as 700-1400 m or more and in ice-free waters in the water column down to about 400 m, where it tends to become more associated with the bottom (Mecklenburg et al. 2011, 2013a, Karamushko 2012). Arctic species inhabiting deeper waters are rarely seen unless such habitats are specifically sampled or they are caught as bycatch in fisheries targeting deep-water species.

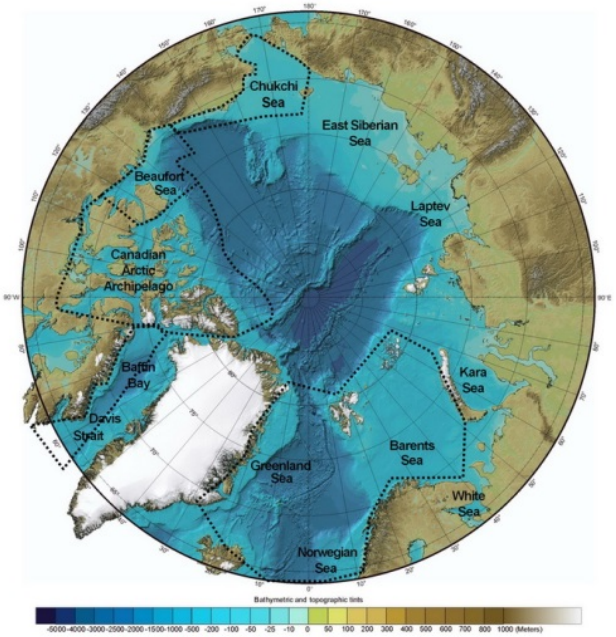

Fig. 29. Map of the Arctic showing approximate extent of marine regions discussed in the text. Main regions for which recent data are available and discussed in the text are delineated.

Note that common names for fishes can differ regionally and sometimes different vernaculars refer to the same species. This can cause considerable confusion, as it has among names for cods. Arctic cod in North America refers to *Boreogadus saida*, but in Eurasia this common name can refer to either *Arctogadus glacialis* or Atlantic cod, *Gadus morhua*, Also, *A. glacialis* has been referred to as both polar cod and ice cod. Here we refer to *B. saida* as **polar cod** and *A. glacialis* as **ice cod**. A recent list of marine fishes in the Arctic gives the most commonly used English, French Canadian, Norwegian and Russian names (Mecklenburg et al. 2013b).

Pacific Arctic: Chukchi Sea and Alaskan Beaufort Sea (Mueter, Lauth, Mecklenburg)

The Chukchi Sea is a shallow (< 100 m) continental Arctic shelf connected to the Bering Sea by northward transport of Pacific waters through Bering Strait (Weingartner 1997). These waters mix and are modified as they flow north, but maintain a gradient from warmer, fresher, coastal water to saltier, colder waters offshore. These north-south and onshore-offshore gradients are reflected in the distribution of benthic (bottom dwelling), demersal (near bottom) and pelagic fishes, which form assemblages associated with specific temperature and salinity conditions (Norcross et al. 2010, Eisner et al 2012). The relatively shallow water of the Chukchi Sea transitions to deeper slope waters near and beyond the 200-mile EEZ, whereas the Alaskan Beaufort Sea has a narrow shelf and is mostly over the continental slope and Canada Basin.

Historical collections on the US portions of the Chukchi Sea shelf from 1959 through 2008 showed low abundances of generally small fishes and recorded a total of at least 59 benthic and demersal species in 17 families (Norcross et al. 2013). This compares to >280 species on the eastern Bering Sea shelf (Mecklenburg et al. 2002, Maslenikov et al. 2012). Over 90% of the fish collected were composed of eight species in three families (Cottidae: *Artediellus scaber*, *Gymnocanthus tricuspis*, *Myoxocephalus scorpius*; Gadidae: *Boreogadus saida*, *Eleginus gracilis*; Pleuronectidae: *Hippoglossoides robustus*, *Limanda aspera*, *Pleuronectes quadritubercula*tus) (Norcross et al. 2013). About 60% of the species in the Chukchi Sea are boreal-subarctic species, compared with, for instance, 30% in the East Siberian Sea (Karamushko 2012) and 11% in northeast Greenland fjords (Christiansen 2012). For the high proportion of boreal species, the Chukchi Sea has been called the Pacific Arctic Gateway.

The continental slope from the Chukchi Borderland, a relatively unexplored region jutting north from the Chukchi Sea into the Canada Basin, to the Beaufort Sea is home to a different assemblage of fishes than on the shelf. It includes, for example, the Arctic skate (*Amblyraja hyperborea*), polar sculpin (*Cottunculus microps*), and threadfin seasnail (*Rhodichthys regina*). Sampling in 2009-2012 along the slope of the Chukchi and Beaufort seas revealed that several benthic species previously known only from rare records or not at all in the Pacific Arctic are actually common in the region. These species include the eelpouts *Lycodes adolfi*, *L. sagittarius*, *L. squamiventer*, and *L. seminudus*. All 32 species documented from mid-depths (200-1200 m) on the slopes of the Chukchi and Alaskan Beaufort seas are also present in the Atlantic sector of the Arctic (Mecklenburg et al. 2013a). The presence of Atlantic Water at mid-depths around the Arctic suggests that most of those species maintain genetic continuity through exchange along the intervening Eurasian or Canadian Arctic slopes, although at present there is no documentation for some species' presence in those regions. Future sampling in data-poor regions will determine whether species have a continuous or circumpolar distribution, or some are truly amphiboreal, like *Reinhardtius hippoglossoides* and *Gadus chalcogrammus*, or absent from large regions, like *Leptoclinus maculatus* appears to be from Siberian seas and slopes (Mecklenburg et al. 2013a).

Comprehensive oceanographic and fisheries surveys in the US portion of the Chukchi Sea during 2012-2013 found that the biomass of demersal fishes in 2012 was similar to or lower than during a similar survey in 1990 (Barber et al. 1997), while the relative species composition remained remarkably stable over this 30-year period (**Fig. 30**). Compared to the southeastern Bering Sea, where the large commercial fisheries are located, the total biomass per unit area of demersal fishes in the Chukchi Sea is at least two orders of magnitude lower (Stevenson and Lauth 2012, Mueter unpublished data).

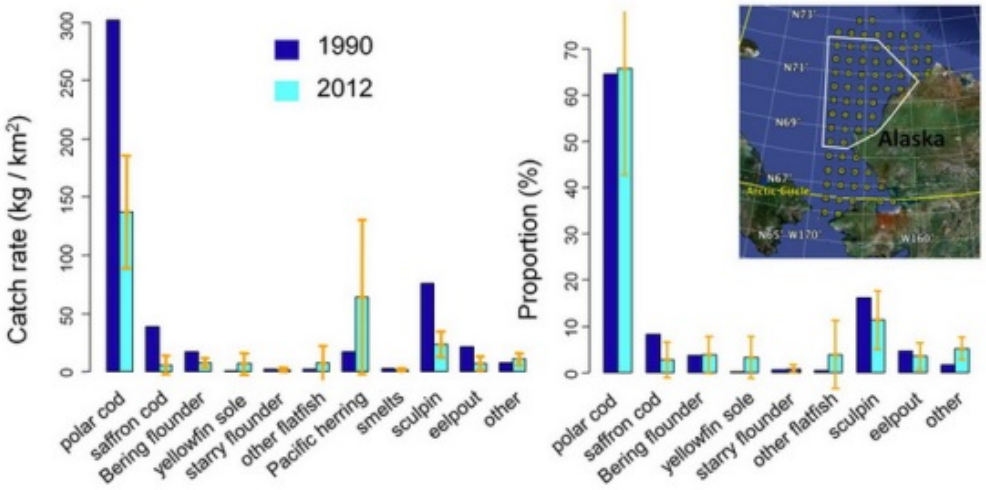

Fig. 30. Average catch rates (left) and relative proportions (right) of major species groups captured in the central and northern Chukchi Sea (stations within white polygon, map inset) during bottom trawl surveys in 1990 and 2012. Pelagic species (Pacific herring and smelts) are not included in the proportional composition plot. Orange bars represent 95% confidence intervals for catches in 2012. Only mean estimates are available for 1990.

Based on surface trawl and mid-water acoustic surveys in 2012-13, the pelagic fish fauna has fewer species than the demersal fauna and is dominated by Pacific herring (*Clupea pallasii*) and juvenile chum salmon (*Oncorhynchus keta*) in the southern Chukchi Sea and by juvenile polar cod and capelin (*Mallotus villosus*) in the north. While juvenile polar cod were abundant and ubiquitous in both 2012 and 2013, other pelagic species were much more variable, both spatially and temporally, based on surveys in 2007 (Eisner et al. 2012), 2012 and 2013. In contrast to studies in the Beaufort Sea (Parker-Stetter 2011, personal communication from Maxime Geoffroy, Laval University, Quebec), an exploratory acoustic survey extending from the Chukchi Sea shelf onto the slope and into the basin near Barrow found no evidence of older cod in deeper waters in September 2013, except for a narrow band in the deep Atlantic water layer at 220-250 m depth in the center of Barrow Canyon, just below the colder (-1.5°C) Pacific water layer.

Subsistence fisheries in the Chukchi Sea focus on nearshore anadromous fishes (salmon, whitefish and char) with few marine species being caught (primarily saffron cod, herring and smelt) (Magdanz et al. 2010). There are no commercial fisheries in the Chukchi Sea. Observations covering a recent warm (2001-2005) and cold (2007-2013) period, combined with life history considerations (Hollowed et al. 2013), suggest little potential for large-scale marine fisheries in the Chukchi Sea now or in the foreseeable future. Moreover, no obvious trends in the abundance or distribution of Chukchi Sea fishes are evident in the available data, although water masses and their associated fish fauna have been highly variable in recent decades (Norcross et al. 2013).

Canadian Arctic Waters (Reist, Majewski, Sawatzky, Hedges, MacPhee, Coad)

Canadian Arctic marine waters are spatially extensive with a very long coastline (~173,000 km, **Fig. 29**). This geographically large area, with extensive physiographic and climatic variation, and wide range of habitats, all contribute to variability of regional seas and their fishes. Accordingly, three distinct regions are discussed: Canadian Beaufort Sea, Canadian Arctic Archipelago waters, and Baffin Bay/Davis Strait waters.

Overall, Coad and Reist (2004) listed 189 marine fish species comprised of 115 genera in 48 families of marine and anadromous fishes in Canadian Arctic marine waters (including Hudson Bay, which is not included here). Coad and Reist (2004) reported 41 species new to the Canadian Arctic marine fish fauna since previous synopses (McAllister 1990, Coad et al. 1995), including 13 species not previously reported from Canadian waters. The most species-rich family in the Canadian Arctic is the Zoarcidae with 31 species, followed by the Salmonidae with 17 and Cottidae with 14 (Coad and Reist 2004).

Species diversity of both anadromous and freshwater fishes in the Canadian Arctic declines northwards and eastwards (**Table 1**). These patterns reflect the pattern of recolonization following deglaciation. In contrast, diversity of marine species increases in more easterly locations. This reflects the high association of fishes in eastern Archipelago, Baffin Bay and Davis Strait waters with the North Atlantic fauna. It is suspected, but not definitively known, that marine diversity decreases northwards in the Archipelago and perhaps the Beaufort Sea. Diversity also appears to decrease with latitude in the Arctic Ocean generally (Christiansen et al. 2013b); however, this may simply be due to increasing depth in the Arctic Ocean with latitude and/or limited sampling.

Table 1. Overview of the number of fish species in Canadian Arctic waters.

Region	**Species prior to 2012**[2]			**Species newly added**	**Totals as of 2012**[4]
	Marine species	Anadromous & freshwater species[1]	Total		
Beaufort Sea (Canadian sector)	52	20	72	12[3]	84
Archipelago	68	13	81	0	81
Baffin Bay & Davis Strait	104	5	109	No data	109

Notes: 1. Anadromous fishes enter coastal marine waters and may extend offshore into pelagic marine waters; some freshwater species enter freshened estuaries and waters in marine locations. 2. Total of marine and anadromous/freshwater counts. 3. Species added in 2012 surveys (see text). 4. Counts for Hudson and James bays are not included (see Coad and Reist 2004).

It is very likely that the number of species found in Canadian waters will increase with additional sampling effort. This contribution thus provides a synopsis of baseline information for the Beaufort Sea and Canadian Arctic Archipelago (henceforth the Archipelago) regions to the mid-2000s, supplemented by additional knowledge accrued through recent surveys conducted in some areas.

Canadian Beaufort Sea (Majewski, MacPhee, Reist): Research in the 1970s and 1980s established the first comprehensive baselines for the diversity of anadromous and estuarine-adapted marine fishes that inhabit the coastal region in summer (e.g., Galbraith and Hunter 1975, Percy 1975, Lawrence et al. 1984, Baker 1985, Chiperzak et al. 2003). In the 2000s, in response to potential nearshore oil and gas development, work focused on the shelf area (to 150 m depths) near the Mackenzie River estuary (e.g., Northern Coastal Marine Studies (NCMS) 2003-2009, Majewski et al. 2013), increasing the Beaufort Sea species count of Coad and Reist (2004) by four species. Thus, prior to 2012, 52 marine fish species, representing 31 genera and 14 families, were confirmed to occur in the Canadian Beaufort Sea (Coad and Reist 2004, Majewski et al. 2009a,b, 2011, Lowdon et al. 2011) (**Fig. 31**). Nearshore work indicated that benthic fishes comprised the majority of diversity (46 species from 11 families), in contrast to pelagic fishes (6 species, 3 families). Polar cod numerically dominated catches during benthic trawl surveys on both the Canadian Beaufort Shelf and continental slope in Alaska (Majewski et al. 2009b, 2011, Lowdon et al. 2011, Rand and Logerwell 2011). While polar cod are ubiquitous across the Beaufort Shelf, there appear to be distinct assemblages of benthic fishes between nearshore and outer shelf areas (Majewski et al. 2013). Species within the marine pelagic waters of the outer shelf have not been comprehensively sampled; however, work in adjacent Alaskan waters indicated that polar cod accounted for much of the fish biomass in the marine pelagic zone (Logerwell et al. 2010).

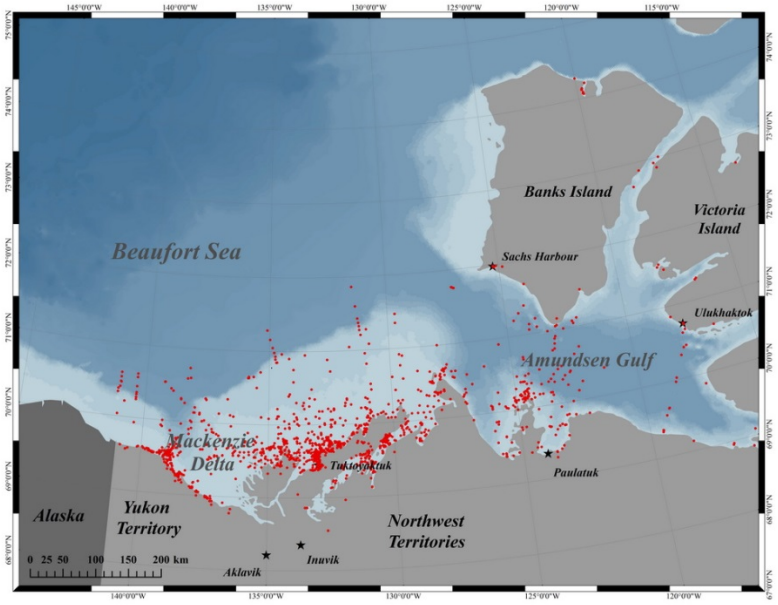

Fig. 31. The Canadian Beaufort Sea and Amundsen Gulf. Points indicate the location of captures of marine fishes through surveys, specimens in museum collections, and verified literature records. Research surveys in 2012 and 2013 extended knowledge to 1000-1500 m depths in some areas. Inland occurrences represent marine fish isolated in freshwater locations.

Declines in summer sea-ice extent and potential offshore oil development prompted a comprehensive survey of the deeper waters of the southern Canadian Beaufort Sea (Marine Fishes Project of the Beaufort Regional Environmental Assessment program, 2011-2015). Work to depths of 1000 m in 2012 added 12 primarily benthic species from five families to the Canadian Arctic marine fauna in this area (Reist et al. unpublished data). Eleven of these are associated with Bering, Chukchi or Alaskan Beaufort Sea areas, and one is of eastern Arctic association. These records may represent either distributional changes due to recent environmental shifts driven by climate change or may be the result of sampling in previously unsurveyed areas and habitats. The vertical distribution of water masses in this area is complex, with Pacific (surface layers), Atlantic (mid-slope layer) and Arctic basin (deep layer) influences. Species associations differ among the layers. Future colonizations, should they occur, could therefore include species from all of these sources. The new records, some of which require further confirmation of specific identities, thus bring the Canadian Arctic faunal total of Coad and Reist (2004) to ~221 species (**Table 1**). Early results from 2013 in the Amundsen Gulf (**Fig. 31**) and eastern Beaufort Sea suggest the occurrence of additional 'new' species.

Virtually all occurrences of anadromous species in the Canadian Beaufort Sea are shoreward of the 20m isobath or in freshened surface waters. Occurrences of freshwater species are limited to coastal areas. For marine species, preliminary results (Majewski et al. 2013; Reist et al. unpublished data) indicate that diversity is relatively high on the extensive shelves, particularly near the Mackenzie River estuary. Diversity declines beyond 200m depths and becomes very low (1-2 species) at depths greater than 1200 m. Survey effort has been concentrated in the southern Beaufort Sea due to the presence of perennial pack ice further north (**Fig. 31**).

Marine fisheries in the Canadian Beaufort Sea focus on coastal species during the summer open-water season; in decreasing order of importance they are anadromous species (e.g., whitefishes and chars), freshwater species (e.g., Burbot, *Lota lota*) and some nearshore marine species (e.g., polar cod, Greenland cod, *Gadus ogac*). Most fisheries are subsistence food fisheries conducted by indigenous peoples of the area; some local-sale commercial fisheries for anadromous species may also occur. No large-scale commercial fisheries presently exist in the Canadian Beaufort Sea.

Canadian Arctic Archipelago (Sawatzky, Reist): The Archipelago includes the Arctic islands north of mainland Canada and their surrounding waters out to the 200 nautical mile EEZ boundary (**Figs. 26** and **29**). Based on surveys of the literature and museum records, 123 species of marine and anadromous fishes representing 31 families have been identified to date within this region (Coad and Reist 2004). Thus, fish found in marine waters of the Canadian Arctic Archipelago include approximately 51% of all Arctic marine species and 69% of all Arctic marine families. Four families account for half (50%) of the species present, namely, Zoarcidae (24 species), Salmonidae (16), Cottidae (12) and Gadidae (10). No recent surveys have been conducted in this area, thus the species richness enumerated here is almost certainly incomplete. Moreover, the vast majority of sampling to date has taken place in southern coastal regions (**Fig. 32**). The harsh climate, remoteness and ice conditions have limited historical sampling to areas where open water existed and was often opportunistic in nature. Recent sea-ice decline (Jeffries & Richter-Menge 2013) and increased industrial interest in the region will likely stimulate scientific sampling in previously unsampled locations and further increase the number of species identified in the Archipelago.

Fig. 32. Fish occurrence records within the Canadian Arctic Archipelago. Inland points represent occurrences of anadromous species adjacent to marine locations. Point locations in deeper areas north of the Archipelago represent pelagic species (e.g., polar cod) captured through or in sea ice.

Similar to the Beaufort Sea, fisheries in the Archipelago are primarily subsistence in nature, target locally available species, and occur in traditional use areas near communities. Local-sale commercial fisheries occur in some areas and two larger-scale commercial fisheries occur for Arctic Char (*Salvelinus alpinus*). Inshore commercial fisheries for Greenland Halibut (*Reinhardtius hipposglossoides*) occur in fjords on the eastern margin of the Archipelago, particularly Baffin Island.

Baffin Bay/Davis Strait (Hedges): Baffin Bay (**Fig. 32**) is a large semi-enclosed basin that extends southward into Davis Strait (separating southeastern Baffin Island from west Greenland). It contains a large abyssal plain that descends below 2300 m. Both Pacific and Atlantic origin water masses occur in Baffin Bay (Jones et al. 2003) and water circulation is dominated by counter-clockwise flowing currents. Northward flowing water on the east side of Baffin Bay and Davis Strait is comprised of North Atlantic water in the West Greenland Slope Current and arctic origin water in the West Greenland Current (Tang et al. 2004, Myers et al. 2009). Southward flowing water on the west side, in the Baffin Island Current, originates from the Arctic Ocean via the Canadian Arctic Archipelago; Pacific Water is present in the upper 50-60 m of the water column (Tang et al. 2004, Stein 2004, Cuny et al. 2005).

Surveys have been conducted with a variety of gear, collecting environmental data including water temperature, salinity and depth at each sampling station. Multi-species bottom trawl surveys are conducted in Baffin Bay and Davis Strait/Hudson Strait at depths from 100 to 1500 m in alternate years to support stock assessments for Greenland halibut (*Reinhardtius hippoglossoides*) and shrimp fisheries and to monitor biodiversity. The survey started in 1999 in Baffin Bay and Davis Strait, with a focus on Greenland halibut, and expanded to include Hudson Strait in 2006. Baffin Bay was surveyed in fall 2012. Davis Strait and Hudson Strait were surveyed in fall 2013.

A benthic longline survey for Greenland halibut has been conducted annually in Cumberland Sound (southeastern Baffin Island) at depths from 200 m to 1200 m since 2011. The survey generates population indices for Greenland halibut as well as Greenland shark (*Somniosus microcephalus*) and Arctic skate (*Amblyraja hyperborea*), the two primary bycatch species. Fish surveys using benthic longlines, gillnets and bottom trawls have also been conducted annually along the east coast of Baffin Island since 2011 to support the development of community-based commercial fisheries and to assess biodiversity.

Greenland halibut is the dominant fish species in most survey trawls or longline sets, particularly at depths below 400 m. Bottom trawls collect a variety of benthic fishes (e.g., skates, eelpouts, grenadiers, redfishes) at relatively low abundances and sporadically encounter polar cod. Longlines primarily catch Greenland halibut, followed by Arctic skate and Greenland shark.

Using data from bottom trawl surveys conducted in the waters of both Canada and Greenland, Jørgensen et al. (2005, 2011) identified five demersal fish assemblages in northern Baffin Bay and seven in southern Baffin Bay and Davis Strait. Assemblages changed from north to south and from shallower to deeper waters. In addition, there were marked differences in the assemblages off western Greenland and off eastern Baffin Island.

No new species were encountered during offshore bottom trawling in Baffin Bay in 2012 and species abundances were similar to previous years. During bottom trawling near the shore outside Scott Inlet (eastern Baffin Island) in September 2013, a high concentration of polar cod was encountered while trawling at 200 m.

Northeast Atlantic and Russian Arctic shelves (Christiansen, Mecklenburg, Karamushko, Lynghammar)

The Northeast Atlantic is dominated by the Arctic Greenland Sea to the west and the sub-Arctic/boreal Norwegian and Barents seas to the east. Increasingly referred to as the 'Atlantic Arctic Gateway' (AAG), the latter two seas connect the Atlantic Ocean with the Arctic Ocean proper. The Greenland and Norwegian seas are characterized by shelves and deep waters (> 2000 m), whereas the Barents Sea is entirely a shelf sea with a mean depth of ~200 m. The Norwegian Sea is the most diverse with 204 fish species, followed by the Barents Sea (153) and the Greenland Sea (57) (**Table 2**). More than 85% of the species are ray-finned fishes, while sharks and their allies (chondrichthyans) constitute 9-14 % of the fish fauna. These proportions are similar to those reported for oceans worldwide, and suggest that ray-finned fishes and chondrichthyans are equally successful in exploiting these cold marine waters (Lynghammar et al. 2013).

Table 2. Numbers (N) and proportions (%) of marine fishes and fish-like species in the northeast Atlantic Ocean and Arctic seas of Russia. Currently, only ray-finned fishes are targeted by industrial fisheries, although sharks and their allies constitute a significant, but largely unreported, bycatch.

Class	Greenland		Norwegian		Barents		White		Kara		Laptev		East Siberian	
	N	%	N	%	N	%	N	%	N	%	N	%	N	%
Hagfishes (Myxini)	-	-	1	0.5	1	0.7	-	-	-	-	-	-	-	-
Sharks and their allies (Chondrichthyes)	5	8.8	28	13.7	19	12.4	4	8.0	2	3.3	1	2.0	1	3.8
Ray-finned fishes (Actinopterygii)	52	91.2	175	85.8	133	86.9	46	92.0	58	96.7	49	98.0	25	96.2
Total number of fish species	57	100	204	100	153	100	50	100	60	100	50	100	26	100
Fishes targeted by industrial fisheries	7	12.3	24	11.8	21	13.7	8	16.0	1	1.7	-	-	-	-

One of the most important industrial fisheries in the world occurs in the AAG, where presently 21-24 fish stocks are harvested (**Table 2**). Hence, the AAG fishes are well surveyed and their fisheries are subjected to strict management regimes within the respective EEZs of the Arctic coastal states. This is in marked contrast to the understudied Russian Arctic shelves (e.g., Kara, Laptev and East Siberian seas), which are characterized by low fish diversity (26-60 species). These seas support small-scale subsistence catches by indigenous peoples (Zeller et al. 2011).

In light of ocean warming and loss of Arctic sea ice, however, harvested marine fishes such as Atlantic mackerel (*Scomber scombrus*), capelin and Atlantic cod (*Gadus morhua*) have moved poleward into Arctic seas (Christiansen et al. 2013a and references therein). The Atlantic cod in the Barents Sea is presently at a historical high with a spawning stock of 2.1 million tonnes and a record quota shared between Norway and Russia of 1 million tonnes in 2013. Industrial fisheries, already in place on several Arctic shelves, will strongly affect the local fish fauna as it turns up as bycatch, and precautionary management practices are needed to mitigate the impacts of industrial fisheries in Arctic waters.

Conclusion

Arctic fish communities remain poorly understood because of the challenges of sampling in remote and mostly ice-covered waters. Recent interest in resource development has spurred research in a number of shallow, nearshore regions that has provided important baselines for understanding future changes. These activities have inevitably increased estimates of species richness and distributions while also highlighting the limitations of present knowledge. However, deeper waters in the Arctic Basin, as well as many parts of the outer shelf regions, remain poorly sampled. Consequently, additional baseline information will be needed before changes in the fish community of these regions can be reliably detected.

The potential for new species expanding into Arctic waters is strong because of a pronounced gradient in species diversity from warmer, sub-Arctic waters to colder Arctic waters. This gradient is evident in a decrease in species richness from south to north in the Pacific sector and in the differences in species richness between the Norwegian, Barents and Greenland seas in the Atlantic sector. New species have been reported in some areas, but most of these

species were likely present but had not been detected due to lack of sampling before. Currently under-sampled regions will likely yield more new species in the future.

While large-scale fisheries currently exist in both the Pacific and Atlantic sectors of the Arctic defined by the 10°C July isotherm, there are no commercial fisheries in the Pacific sector north of the Arctic Circle. Fisheries in the high Arctic on the Russian, US and Canadian shelves are limited to small-scale subsistence fisheries, mostly for anadromous species. However, the most abundant and most widely distributed fish species in the Arctic, polar cod, has been the target of commercial fisheries in the past (Zeller et al 2011). Given its ecological role as a major prey species for seabirds and mammals, its circumpolar distribution, its unknown stock structure, and its high sensitivity to temperature variability, a better understanding of polar cod biology will be critical to the management of Arctic fishery resources.

References

Baker, R. F., 1985: A Fisheries Survey of Herschel Island, Yukon Territory from 9 July to 12 August, 1985. North/South Consultants Inc., 25 pp.

Barber, W. E., R. L. Smith, M. Vallarino, and R. M. Meyer, 1997: Demersal fish assemblages of the northeastern Chukchi Sea, Alaska. *Fish. Bull.*, 95, 195-209.

Bluhm, B. A., and R. Gradinger, 2008: Regional variability in food availability for arctic marine mammals. *Ecol. Appl.*, 18, S77-S96.

Chiperzak, D. B., G. F. Hopky, M. J. Lawrence, D. F. Schmid, and J. D. Reist, 2003: Larval and post-larval fish data from the Canadian Beaufort Sea shelf, July to September, 1987. *Can. Data Rep. Fish. Aquat. Sci.*, 1121, (iv + 84 pp.).

Christiansen, J. S., 2012: The TUNU-Programme: Euro-Arctic marine fishes-diversity and adaptation. *Adaptation and Evolution in Marine Environments 1: The impacts of global change on biodiversity*. G. di Prisco and C. Verdi, Eds., Springer Verlag, 35-50.

Christiansen, J. S, C. W. Mecklenburg, and O. V. Karamushko, 2013a: Arctic marine fishes and their fisheries in light of global change. *Global Change Biol.*, doi:10.1111/gcb.12395.

Christiansen, J. S., and 33 others, 2013b: Fishes, *Arctic Biodiversity Assessment*, Conservation of Arctic Flora and Fauna (CAFF), in press.

Coad, B. W., H. Waszczuk, and I. Labignan, 1995: *Encyclopedia of Canadian Fishes*. Canadian Museum of Nature, Ottawa and Canadian Sportfishing Productions, (viii + 928 pp., 128 colour plates).

Coad, B. W., and J. D. Reist, 2004: Annotated list of the arctic marine fishes of Canada. *Can. MS. Rep. Fish. Aquat. Sci.*, 2674, (iv + 112 pp.).

Cuny, J., P. B. Rhines, and R. Kwok, 2005: Davis Strait volume, freshwater and heat fluxes. *Deep Sea Res.*, 52, 519-542.

Eisner, L., N. Hillgruber, E. Martinson, and J. Maselko, 2012: Pelagic fish and zooplankton species assemblages in relation to water mass characteristics in the northern Bering and southeast Chukchi seas. *Polar Biol.*, 36, 87-113.

Galbraith, D. F., and J. G. Hunter, 1975: Fishes of offshore waters and Tuktoyaktuk vicinity. *Beaufort Sea Project Tech. Rep.*, 7, 47.

Hollowed, A. B., B. Planque, and H. Loeng, 2013: Potential movement of fish and shellfish stocks from the sub-Arctic to the Arctic Ocean. *Fish. Oceanogr.*, 22(5), 355-370.

Jeffries, M. O., and J. Richter-Menge, Eds., 2013: Arctic [in "State of the Climate in 2012"]. *Bull. Amer. Meteor. Soc.*, 94, S111-S146.

Jørgensen, O. A., C. Hvingel, P. R. Møller, and M. A. Treble, 2005: Identification and mapping of bottom fish assemblages in Davis Strait and southern Baffin Bay. *Can. J. Fish. Aquat. Sci.*, 62, 1833-1852.

Jørgensen, O. A., C. Hvingel, and M. A. Treble, 2011: Identification and mapping of bottom fish assemblages in northern Baffin Bay. *J. Northw. Atl. Fish. Sci.*, 43, 65-79.

Jones, E. P., J. H. Swift, L. G. Anderson, G. Civitarese, K. K. Falkner, G. Kattner, M. Lipizer, F. McLaughlin, and J. Olafsson, 2003: Tracing Pacific water in the North Atlantic Ocean. *J. Geophys. Res.*, 108, 3116.

Karamushko, O. V., 2012: Structure of ichthyofauna in the Arctic seas off Russia. *Berichte zur Polar- und Meeresforschung*. Reports on Polar and Marine Research. *Arctic Mar. Biol.*, 129-136.

Lawrence, M. J., G. Lacho, and S. Davies, 1984: A survey of the coastal fishes of the southeastern Beaufort Sea. *Can. Tech. Rep. Fish. Aquat. Sci.*, 1220, (x + 178 pp.).

Logerwell, E., K. Rand, S. Parker-Stetter, J. Horne, T. Weingartner, and B. Bluhm. 2010: Beaufort Sea Marine Fish Monitoring 2008: Pilot Survey and Test of Hypotheses. Final Report. Minerals Management Service, U.S. Department of the Interior, BOEMRE 2010-048, 263 pp.

Lowdon, M. K., A. R. Majewski, and J. D. Reist, 2011: Fish catch data from Herschel Island, Yukon Territory, and other offshore sites in the Canadian Beaufort Sea, July and August 2008, aboard the *CCGS Nahidik*. *Can. Data Rep. Fish. Aquat. Sci.*, 1237, (vi + 99 pp.).

Lynghammar, A., J. S. Christiansen, C. W. Mecklenburg, O. V. Karamushko, P. R. Møller, and V. F. Gallucci, 2013: Species richness and distribution of chrondrichthyan fishes in the Arctic Ocean and adjacent seas. *Biodiv.*, 14, 57-66.

Magdanz, J. S., N. S. Braem, B. S. Robbins, and D. S. Koster, 2010: Subsistence harvests in Northwest Alaska, Kivalina, and Noatak, 2007. Alaska Department of Fish and Game Division of Subsistence Technical Paper, Kotzebue, No. 354.

Majewski, A. R., J. D. Reist, B. J. Park, J. E. Sareault, and M. K. Lowdon, 2009a: Fish catch data from offshore sites in the Mackenzie River estuary and Beaufort Sea during the open water season, July and August, 2005, aboard the *CCGS Nahidik. Can. Data Rep. Fish. Aquat. Sci.*, 1204, (vii + 53 pp.).

Majewski, A. R., J. D. Reist, B. J. Park, and M. K. Lowdon, 2009b: Fish catch data from offshore sites in the Mackenzie River estuary and Beaufort Sea during the open water season, July and August, 2006, aboard the *CCGS Nahidik. Can. Data Rep. Fish. Aquat. Sci.*, 1218, (vii + 37 pp.).

Majewski, A. R., M. K. Lowdon, J. D. Reist, and B. J. Park, 2011: Fish catch data from Herschel Island, Yukon Territory, and other offshore sites in the Canadian Beaufort Sea, July and August 2007, aboard the *CCGS Nahidik. Can. Data Rep. Fish. Aquat. Sci.*, 1231, (vi + 50 pp.).

Majewski, A. R., B. R. Lynn, M. K. Lowdon, W. J. Williams, and J. D. Reist, 2013: Community composition of demersal marine fishes on the Canadian Beaufort Shelf and at Herschel Island, Yukon Territory. *J. Mar. Syst.*, in press.

Maslenikov, K. P., J. W. Orr, and D. E. Stevenson, 2013: Range extensions and significant distributional records for eighty-two species of fishes in Alaskan marine waters. *Northwestern Nat.*, 94, 1-21.

McAllister, D. E., 1990: A List of the Fishes of Canada / Liste des poissons du Canada. *Syllogeus*, 64, 1-310.

Mecklenburg, C. W., T. A. Mecklenburg, and L. K. Thorsteinson, 2002: *Fishes of Alaska*. American Fisheries Society. 1037 pp.

Mecklenburg, C. W., P. R. Møller, and D. Steinke, 2011: Biodiversity of arctic marine fishes: taxonomy and zoogeography. *Mar. Biodiv.*, 41, 109-140.

Mecklenburg, C. W., I. Byrkjedal, O. V. Karamushko, and P. R. Møller, 2013a: Atlantic fishes in the Chukchi Borderland. *Mar. Biodiv.*, in press.

Mecklenburg C. W., I. Byrkjedal, J. S. Christiansen, O. V. Karamushko, A. Lynghammar, and P. R. Møller, 2013b: List of marine fishes of the arctic region annotated with common names and

zoogeographic characterizations. CAFF, Akureyri, Iceland. http://www.caff.is/publications/view_document/257.

Myers, P. G., D. Chris, and M. H. Ribergaard, 2009: Structure and variability of the West Greenland Current in summer derived from 6 repeat standard sections. *Prog. Oceanogr.*, 80, 93-112.

Norcross, B. L., B. A. Holladay, M. S. Busby, and K. L. Mier, 2010: Demersal and larval fish assemblages in the Chukchi Sea. *Deep Sea Res. II*, 57, 57-70.

Norcross, B. L., B. A. Holladay, and C. W. Mecklenburg, 2013: Recent and historical distribution and ecology of demersal fishes in the Chukchi Sea Planning Area. Final Report to the Bureau of Ocean Energy Management, Alaska OCS Region, Anchorage, Alaska, 200 pp.

Parker-Stetter, S. L., J. K. Horne, and T. J. Weingartner, 2011: Distribution of polar cod and age-0 fish in the U.S. Beaufort Sea. *Polar Biol.*, 34, 1543-1557.

Percy, R., 1975: Fishes of the outer Mackenzie Delta. *Beaufort Sea Project Tech. Rep.*, 8, (vi + 114 pp.).

Rand, K. M., and E. A. Logerwell, 2011: The first demersal trawl survey of benthic fish and invertebrates in the Beaufort Sea since the late 1970's. *Polar Biol.*, 34, 475-488.

Stein, M., 2004: Climatic overview of NAFO Subarea 1, 1991-2000. *J. Northw. Atl. Fish. Sci.*, 34, 29-41.

Stevenson, D. E., and R. R. Lauth, 2012: Latitudinal trends and temporal shifts in the catch composition of bottom trawls conducted on the eastern Bering Sea shelf. *Deep Sea Res., Part II*: 65-70, 251-259.

Tang, C. L., C. K. Ross, T. Yao, B. Petrie, B. D. Detracey, and E. Dunlap, 2004: The circulation, water masses and sea ice of Baffin Bay. *Prog. Oceanogr.*, 63, 183-228.

Wassmann, P., 2011: Arctic marine ecosystems in an era of rapid climate change. *Prog. Oceanogr.,* 90, 1-17.

Weingartner, T. J., 1997: A review of the physical oceanography of the northeastern Chukchi Sea. Proceedings, *Fish Ecology in Arctic North America*, J. B. Reynolds, Ed., American Fisheries Society Symposium, 19, 40-59.

Wilson, W. J., and O. A. Ormseth, 2009: A new management plan for Arctic waters of the United States. *Fisheries*, 34, 555-558.

Zeller, D., S. Booth, E. Pakhomov, W. Swartz, and D. Pauly, 2011: Arctic fisheries catches in Russia, USA, and Canada: baselines for neglected ecosystems. *Polar Biol.*, 34, 955-973.

Arctic Benthic Communities

K. Iken[1], B.A. Bluhm[1], J.E. Søreide[2]

[1]School of Fisheries and Ocean Sciences, University of Alaska Fairbanks, Fairbanks, AK, USA
[2]The University Centre in Svalbard, Norway

November 15, 2013

Highlights

- Responses of Arctic benthic communities to climate and anthropogenic factors can be observed from shifts in species distribution patterns and in the appearance of new species.
- Recent changes in Arctic primary production, especially those related to changes in sea ice cover, have the potential to influence Arctic benthic biomass and community structure, which respond to changes in food supply.
- The detection of changes and trends in Arctic benthic communities depends on sustained long-term observing programs, such as the HAUSGARTEN observatory in the Atlantic sector and the Distributed Biological Observatory (DBO) in the Pacific sector of the Arctic.

Arctic benthic communities are good biological indicators of long-term, directional ecosystem change because contributing species typically have long life spans, which result in slow community changes. Therefore, benthic communities do not respond as much to minor (such as seasonal) oscillations as they do to longer-term changes in climate. With continued strong climate change effects and increasing human impacts in the marine Arctic, an understanding of the spatial and temporal scales in environmental controls of Arctic benthic communities is essential. Observed latitudinal and depth-related shifts in benthic taxa have been found to strongly correlate with pronounced rates of environmental shifts, especially in temperature (Pinsky et al. 2013). As climate shifts in the Arctic are particularly strong, benthic communities may soon start to mirror these shifts in their distribution patterns (e.g., Grebmeier 2012).

The largest impediment to understanding benthic community shifts in the Arctic is the dearth of adequate time series. Existing patterns in species distributions and community composition are shaped by multiple processes over geological and recent time scales. As a result, today's Arctic benthos is a composite of Atlantic boreal, Pacific boreal, Arctic, and cosmopolitan origins (Krylova et al. 2013). Recently observed and predicted species expansions and constrictions have mostly been attributed to, or at least discussed in the context of, climate warming (Kortsch et al. 2012, Michel et al. 2012). For example, in a 30-year time series (1980-2010) of hard bottom fjord communities in Svalbard, macroalgal cover increased substantially and the invertebrate community reorganized as seawater temperatures gradually increased and ice cover decreased (Kortsch et al. 2012). As another example, productivity, as measured by growth rates in several benthic clams (**Fig. 33a**) in the Barents Sea, was found to change significantly depending on climate variations such as temperature (Carroll et al. 2011a, 2011b). In 2004, a population of blue mussels was detected in Svalbard, a species that had been extinct in the region for a millennium and was able to re-enter the Arctic region after sea surface

temperatures increased (Berge et al. 2005). These examples suggest that future climate variations could significantly affect benthic community production and competitive interactions.

Fig. 33. (a) The Greenland cockle, *Serripes groenlandicus*, is one of the species with higher growth rates related to climate forcing, especially temperature. (b) The snow crab, *Chionoecetes opilio*, is a common member of Pacific Arctic benthic communities, but is a recent invader in the Atlantic Arctic, with potentially destructive effects on benthic communities. (c) The brown coloration on the bottom of sea ice in a high-Arctic fjord in Svalbard indicates strong ice algal growth that is important food for benthic communities. Picture credits: (a) and (b): K. Iken and B. A. Bluhm; (c) J. E. Søreide.

Not all species or community distributions or functional changes can easily be related directly to climate changes. Other possible causes for large-scale distribution changes include indirect consequences of climate change such as invasion of new species through ballast water, as suspected for an Atlantic-origin ascidian (sea squirt) recently found in the North Pacific Ocean (Lambert et al. 2010). Invasive predatory species such as red king and snow crab (**Fig. 33b**) in the Barents Sea can have ecosystem-wide adverse effects on the biodiversity and biomass of the invaded areas (Falk-Petersen et al. 2011). The invasion of king crab, a clawed predator that is able to crush calcified prey, caused an impoverishment of soft-bottom fauna, mainly through reductions in bivalves, echinoderms and tube-dwelling polychaetes (Oug et al. 2011). On a local scale, species distributions and community patterns can change over time in response to industrial activity in the oil and gas arena. For example, macrofaunal diversity was reduced near historic drilling-sites in the Alaskan Beaufort Sea compared to reference sites, while trophic relationships and bulk abundance and biomass did not change (Trefry et al. 2013). Another impact of human activities is the increase in marine debris deposited on the sea floor as observed at the HAUSGARTEN observatory in the Fram Strait, where litter affected food particle uptake in benthic macrofauna and, with time, also their growth and reproduction (Bergmann and Klages 2012).

Most of the species shifts, or changes described above and in the literature, are related to the physiological tolerances and vulnerabilities of taxa to external stressors such as changing temperatures or pollution. Other changes in Arctic benthic communities may be driven by changes in their resources, such as food. Among the most important ultimate sources of benthic food webs in the Arctic benthos are phytoplankton and ice algae, although in coastal regions, terrestrial organic matter and other sources can also be important (Dunton et al. 2012, Kędra et al. 2012, McTigue and Dunton 2013, Søreide et al. 2013). To identify candidate regions for long-term observing efforts, recent work has focused on mapping benthic biomass 'hot spots', i.e., areas in which the coupling between water column primary production and the benthic system is particularly strong (Grebmeier et al. 2010, 2012). These include areas of high primary production, such as polynyas (permanently ice-free regions), shallow seas, and upwelling regions (Darnis et al. 2012, Conlan et al. 2013, Kędra et al. 2013, Link et al. 2013).

The importance of sea ice algal primary production (**Fig. 33c**, and also see **Fig. 28** in the essay on *Sea Ice Biota*) in contributing to maintenance of benthic hot spots is still poorly known. However, emerging new analytical methods provide strong evidence for tight coupling between sea ice production and benthic consumers (Brown et al. 2013, Søreide et al. 2013, Xiao et al. 2013). In regions with permanent sea ice, the vertical flux of both ice and water column production is low, resulting in generally low benthic biomass (Bluhm et al. 2011, Søreide et al. 2013, Xiao et al. 2013). New findings from the central Arctic Ocean in the record-low ice year of 2012 (Perovich et al. 2012), however, reveal widespread deposition of ice algae on the deep-sea floor (Boetius et al. 2013). If such strong sea ice algal export were to become more frequent it might fuel higher biomass in the deep sea. Whether or not this will happen will only be confirmed by more systematic observations of sea ice algal production and export to the deep-sea benthos in the central Arctic Ocean.

Determining long-term trends in Arctic benthic communities related to climate change, and related anthropogenic influences on ecosystem changes in food supply, will only be possible with continued long-term observation efforts. The Circumpolar Biodiversity Monitoring Program, an international forum that developed a pan-Arctic biodiversity monitoring plan (Gill et al. 2011), may facilitate the coordination of long-term benthic monitoring from regional to pan-Arctic scales. One example of such integrated monitoring in the Pacific Arctic is the Distributed Biological Observatory (Grebmeier et al. 2010, http://www.arctic.noaa.gov/dbo/). In the Atlantic Arctic, the HAUSGARTEN observatory is an excellent example that provides important long-term observations of the deep benthos (Soltwedel et al. 2005).

References

Berge, J., G. Johnsen, F. Nilsen, B. Gulliksen, and D. Slagstad, 2005: Ocean temperature oscillations enforce the reappearance of *Mytilus edulis* in Svalbard after 1,000 years of absence. *Mar. Ecol. Prog. Ser.*, 303, 167-175.

Bergmann, M., and M. Klages, 2012: Increase of litter at the Arctic deep-sea observatory HAUSGARTEN. *Mar. Poll. Bull.*, 64, 2734-2741.

Bluhm, B. A., W. G. Ambrose, Jr., M. Bergmann, L. M. Clough, A. V. Gebruk, C. Haseman, K. Iken, M. Klages, I. R. MacDonald, P. E. Renaud, I. Schewe, T. Soltwedel, and M. Włodarska-Kowalczuk, 2011: Diversity of the Arctic deep-sea benthos. *Mar. Biodiv.*, 41, 87-107.

Bluhm, B. A., J. M. Grebmeier, P. Archambault, M. Blicher, G. Guðmundsson, K. Iken, L. Lindal Jørgensen, and V. Mokievsky, 2012: Benthos. Arctic Report Card: Update for 2012.

Boetius, A., 16 others, and Party RPA-SS, 2013: Export of algal biomass from the melting Arctic sea ice. *Science*, 339,1430-1432.

Brown, T. A., E. N. Hegseth, and S. T. Belt, 2013: A biomarker-based investigation of the mid-winter ecosystem in Rijpfjorden, Svalbard. *Polar Biol.*, doi.org/10.1007/s00300-013-1352-2.

Carroll, M. L., W. G. Ambrose, Jr., B. S. Levin, S. K. Ryan, A. R. Ratner, G. A. Henkes, and M. J. Greenacre, 2011a: Climate regulation of *Clinocardium ciliatum* (Bivalvia) growth in the northwestern Barents Sea. *Paleoclim. Paleogeogr. Paleoecol.*, 302, 10-20.

Carroll, M. L., W. G. Ambrose, Jr, B. S. Levin, W. L. Locke v, G. A. Henkes, H. Hop, and P. E. Renaud, 2011b: Pan-Svalbard growth rate variability and environmental regulation in the Arctic bivalve *Serripes groenlandicus*. *J. Mar. Sys.*, 88, 239-251.

Conlan, K., E. Hendrycks, A. Aitken, B. Williams, S. Blasco, and E. Crawford, 2013: Macrofaunal biomass distribution on the Canadian Beaufort Shelf. *J. Mar. Sys.*, doi.org/10.1016/j.jmarsys.2013.07.013.

Darnis, G., and 11 others, 2012: Current state and trends in Canadian Arctic marine ecosystems: II. Heterotrophic food web, pelagic-benthic coupling, and biodiversity. *Clim. Change*, 115, 179-205.

Dunton, K., S. Schonberg, and L. Cooper, 2012: Food web structure of the Alaskan nearshore shelf and estuarine lagoons of the Beaufort Sea. *Estuar. Coasts*, 35, 416-435.

Falk-Petersen, J., P. Renaud, and N. Anisimova, 2011: Establishment and ecosystem effects of the alien invasive red king crab (*Paralithodes camtschaticus*) in the Barents Sea - a review. *ICES J. Mar. Sci.*, 68, 479-488.

Gill, M. J., and 20 others, 2011: Arctic marine biodiversity monitoring plan. CAFF Monitoring Series Report No. 3.

Grebmeier, J. M., S. E. Moore, J. E. Overland, K. E. Frey, and R. Gradinger, 2010: Biological response to recent Pacific Arctic Sea ice retreat. *EOS Trans. Am. Geophys. Union*, 91, 161-162.

Grebmeier, J. M., 2012: Shifting patterns of life in the Pacific Arctic and Sub-Arctic seas. *Ann. Rev. Mar. Sci.*, 4, 63-78.

Grebmeier, J. M., and 11 others, 2011: Ecosystem observations in Barrow Canyon: A focus for the international Distributed Biological Observatory. In *Arctic Report Card 2012*, http://www.arctic.noaa.gov/report12.

Kędra, M., K. Kuliński, W. Walkusz, and J. Legeżyńska, 2012: The shallow benthic food web structure in the high Arctic does not follow seasonal changes in the surrounding environment. *Estuar. Coast. Shelf Sci.*, 114, 183-191.

Kędra, M., P. E. Renaud, H. Andrade, I. Goszczko, and W. G. Ambrose, Jr., 2013: Benthic community structure, diversity, and productivity in the shallow Barents Sea bank (Svalbard Bank). *Mar. Biol.*, 160, 805-819.

Kortsch, S., R. Primicerio, F. Beuchel, P. Renaud, J. Rodrigues, O. J. Lønne, and B. Gulliksen, 2012: Climate-driven regime shifts in Arctic marine benthos. *Proc. Nat. Acad. Sci.*, 109, 14052-14057.

Krylova, E. M., D. L. Ivanov, and A. N. Mironov, 2013: The ratio of species of Atlantic and Pacific origin in modern Arctic fauna of bivalve molluscs. *Invert. Zool.*, 10, 89-126.

Lambert, G., N. Shenkar, and B. J. Swalla. 2010. First Pacific record of the north Atlantic ascidian *Molgula citrina* - bioinvasion or circumpolar distribution? *Aquat. Inv.*, 5, 369-378.

Link, H., D. Piepenburg, and P. Archambault, 2013: Are hotspots always hotspots? The relationship between diversity, resource and ecosystem functions in the Arctic. *PLoS ONE*, 8(9), e74077.

McTigue, N. D., and K. H. Dunton, 2013: Trophodynamics and organic matter assimilation pathways in the northeast Chukchi Sea, Alaska. *Deep-Sea Res. II*, doi.org/10.1016/j.dsr2.2013.07.016.

Michel, C., and 10 others, 2012: Biodiversity of Arctic marine ecosystems and responses to climate change. *Biodiversity*, 13, 200-214.

Oug, E., S. K. J. Cochrane, J. H. Sundet, K. Norling, and H. C. Nilsson, 2011: Effects of the invasive red king crab (*Paralithodes camtschaticus*) on soft-bottom fauna in Varangerfjorden, northern Norway. *Mar. Biodiv.*, 41, 467-479.

Perovich, D., W. Meier, M. Tschudi, S. Gerland, and J. Richter-Menge, 2012: Sea ice. In *Arctic Report Card 2012*, http://www.arctic.noaa.gov/report12.

Pinsky, M. L., B. Worm, M. J. Fogarty, J. L. Sarmiento, and S. A. Levin, 2013: Marine taxa track local climate velocities. *Science*, 341, 1239-1242.

Soltwedel, T., and 17 others, 2005: HAUSGARTEN: Multidisciplinary investigations at a deep-sea, long-term observatory in the Arctic Ocean. *Oceanography*, 18, 46-61.

Søreide, J. E., M. L. Carroll, H. Hop, W. G. Ambrose, Jr., E. N. Hegseth, and S. Falk-Petersen, 2013: Sympagic-pelagic-benthic coupling in Arctic and Atlantic waters around Svalbard revealed by stable isotopic and fatty acid tracers. *Mar. Biol. Res.*, 9, 831-850.

Trefy, J. H., K. H. Dunton, R. P. Trocine, S. V. Schonberg, N. D. McTigue, E. S. Hersh, and T. J. McDonald, 2013: Chemical and biological assessment of two offshore drilling sites in the Alaskan Arctic. *Mar. Environ. Res.*, 86, 35-45.

Xiao, X., K. Fahl, and R. Stein, 2013: Biomarker distributions in surface sediments from the Kara and Laptev seas (Arctic Ocean): indicators for organic-carbon sources and sea-ice coverage. *Quat. Sci. Rev.*, 79, 40-52.

Terrestrial Ecosystems Summary

Section Coordinator: Michael Svoboda

Canadian Wildlife Service, Environment Canada, Whitehorse, YT, Canada & CAFF/CBMP

November 8, 2013

The Terrestrial Ecosystems Section of Arctic Report Card 2013 updates previous accounts of vegetation and migratory tundra caribou and reindeer (*Rangifer*), and introduces the inaugural Muskox (*Ovibos moschatus*) essay, which demonstrates the immense impact of conservation efforts on arctic wildlife.

It is not surprising that changes in vegetation and habitat quality are closely scrutinized, as many key wildlife species depend on the short summer growing seasons for access to food. Information from long-term, ground-based observations shows that, in addition to increasing air temperatures and loss of summer sea ice, widespread increased 'greening' (a measure of vegetative productivity), is continuing in response to other factors. These include increases in the length of the growing season, large-scale atmospheric circulation patterns, and regional summer cloud cover (see the essay on *Vegetation*). Substantial tall shrub and tree expansion at the forest-tundra ecotone in Siberia has also been linked to active cryospheric disturbances.

The impacts of increased biomass production in Arctic tundra ecosystems on arctic wildlife are unclear. As is often the case with arctic wildlife (e.g., migratory birds - see the essay on *Seabirds* in Report Card 2012), many factors such as disease, hunting rates, and changes to management regimes have demonstrated significant influence on productivity and abundance. This complexity is reflected in both the caribou/reindeer and muskox abundance essays. Nevertheless, migratory caribou and reindeer appear to be within known ranges of natural variation, with many herds having experienced massive declines in the past decade (see the essay on *Migratory Tundra Rangifer*).

In contrast to caribou, muskoxen have spread geographically and increased in number from reduced ranges after historic declines (see the essay on *Muskoxen*). Aided by significant re-introductions and conservation efforts, muskox populations appear to be stable/increasing since the 1970s. Although muskoxen have shown sensitivity to over-harvesting and disease, their resilience to extreme weather periods/events have also been recorded. For example, in the mid-2000s on Wrangel Island, east Siberia, several years of late autumn freezing rain, effectively encased food sources in ice rather than under snow. This event caused large declines in Rangifer populations, but had little effect on muskoxen numbers.

Vegetation

H.E. Epstein[1], U.S. Bhatt[2], D.A. Walker[3], M.K. Raynolds[3], P.A. Bieniek[4], J. Comiso[5], J. Pinzon[6], C.J. Tucker[6], I.V. Polyakov[4,7], G.J. Jia[8], H. Zeng[8], B.C. Forbes[9], M. Macias-Fauria[10], L. Xu[11], R. Myneni[12], G.V. Frost[1], G.R. Shaver[13], M.S. Bret-Harte[3], M.C. Mack[14], A.V. Rocha[15]

[1]Department of Environmental Sciences, University of Virginia, Charlottesville, VA, USA
[2]Geophysical Institute, University of Alaska Fairbanks, Fairbanks, AK, USA
[3]Institute of Arctic Biology, University of Alaska Fairbanks, Fairbanks, AK, USA
[4]International Arctic Research Center, University of Alaska Fairbanks, AK, USA
[5]Cryospheric Sciences Branch, NASA Goddard Space Flight Center, Greenbelt, MD, USA
[6]Biospheric Science Branch, NASA Goddard Space Flight Center, Greenbelt, MD, USA
[7]Department of Atmospheric Sciences, University of Alaska Fairbanks, Fairbanks, AK, USA
[8]Institute of Atmospheric Physics, Chinese Academy of Sciences, Beijing, China
[9]Arctic Centre, University of Lapland, Rovaniemi, Finland
[10]Department of Zoology, University of Oxford, Oxford, UK
[11]Institute of the Environment and Sustainability, University of California Los Angeles, Los Angeles, C.A., USA
[12]Department of Earth and Environment, Boston University, Boston, MA, USA
[13]The Ecosystems Center, Marine Biological Laboratory, Woods Hole, MA, USA
[14]Department of Biology, University of Florida, Gainesville, FL, USA
[15]Department of Biological Sciences, University of Notre Dame, Notre Dame, IN, USA

December 3, 2013

Highlights

- Since observations began in 1982, Arctic tundra vegetation productivity (greenness) has increased, monotonically in Eurasia and at an accelerated rate since 2005-09 in North America.
- The length of the growing season (photosynthetically active period) has increased by 9 days per decade since 1982.
- Tall shrubs and trees have expanded their range across the forest-tundra ecotone in Siberia, with areal expansion rates of up to 25% since the mid- to late-1960s.
- The number and severity of tundra wildfires on the North Slope of Alaska has increased dramatically during the last decade. Since the 2007 Anaktuvuk River fire, above-ground net primary productivity has been greater on moderately burned sites than sites that did not burn.

Tundra Vegetation Productivity

Vegetation productivity (greenness) trends for the arctic tundra have been updated for the period 1982-2012 using the Global Inventory Modeling and Mapping Studies (GIMMS) Maximum Normalized Difference Vegetation Index (MaxNDVI, no units) from the Advanced Very High Resolution Radiometer (AVHRR). MaxNDVI (NDVI at the peak of the growing season) trends from 1982 to 2012 are broadly positive, with exceptions in northwestern Siberia, eastern Russia and western Alaska (**Fig. 34**). To better understand the trends, break points in the time series were quantified using the Breakfit algorithm (Mudelsee 2009). MaxNDVI has increased monotonically in Eurasia since 1984, and at accelerated rates since 2005 and 2009 in western North America and eastern North America, respectively (**Fig. 35**). Using the latest GIMMS dataset, Xu et al. (2013) reported that 39% of Arctic vegetation is now significantly greener ($p < 0.1$) than in 1982, with 4% more brown (a significant decrease) and 57% showing

no significant change. Consistent with Bhatt et al. (2013), the greatest increases were found in the North American High Arctic and adjacent to the Beaufort Sea, and in northwestern Siberia.

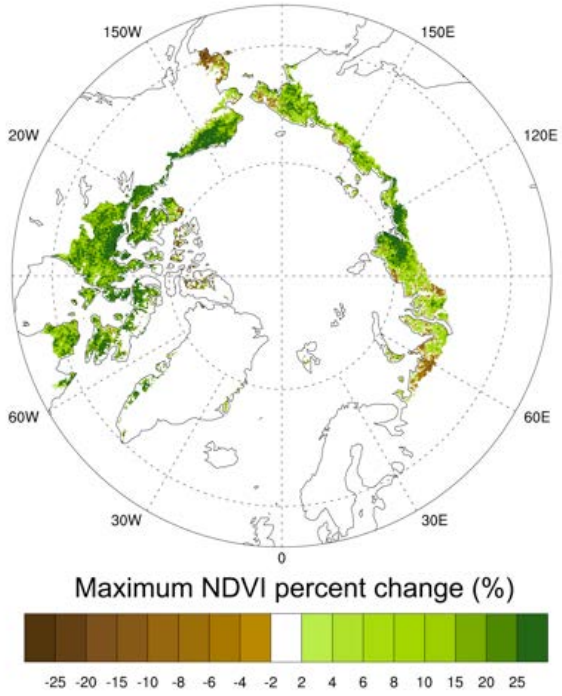

Fig. 34. Trend of change (in %) in annual MaxNDVI between 1982 and 2012 calculated using a least squares regression at each pixel (from Bhatt et al. 2013).

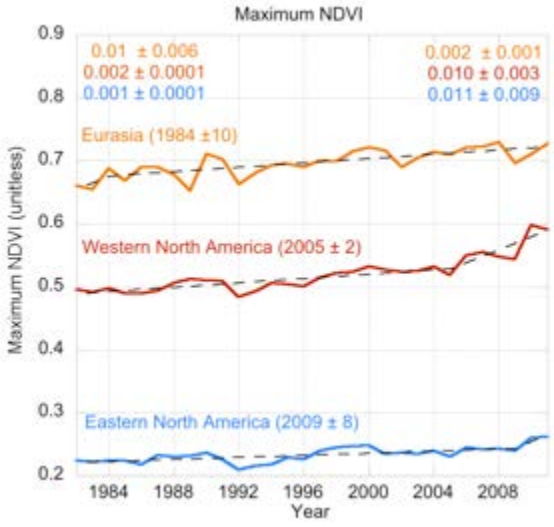

Fig. 35. MaxNDVI from 1982 to 2011 for Eurasia, western North America and eastern North America. Trend lines with break points and associated errors are show for each time series together with the slopes before (top left) and after (top right) the break points (Bhatt et al. 2013).

NDVI is often positively related to summer temperature, as indicated in a recent synthesis by Post et al. (2013). However, factors other than warming affect NDVI and plant growth (Pouliot et al. 2009, Forbes et al. 2010, Macias-Fauria et al. 2012). For example, large-scale atmospheric circulation is likely a key contributor to lower temperatures and more consistent greening over Eurasia through increased summer cloud cover, compared to the accelerated greening in North America under more cloud-free skies (Bhatt et al. 2013).

The length of the growing season (photosynthetically active period, PAP) in the Arctic has increased by 9 days per decade since 1982 (Xu et al. 2013) (**Fig. 36**). Snow cover variability is considered to be an important cause of such phenological change in Arctic tundra. For example, for the period 2000-2010 on the Yamal Peninsula (western Arctic Russia), Zeng and Jia (2013) found greening onset was related to final snowmelt date (r^2 range 0.78-0.93) and the end of the growing season was strongly related to the date of first snow cover (r^2 range 0.86-0.94), with the exception of the initiation of growth for prostrate-shrub tundra. (See the essay on *Snow* for more information about its extent, duration, depth and water equivalence). Post et al. (2013) also demonstrated that the mid-point of the plant-growing season at an inland Greenland site was positively related to June sea-ice extent, i.e., sea-ice reduction has led to an earlier growing season. (See the essay on *Sea Ice* for more information about its extent, age and thickness).

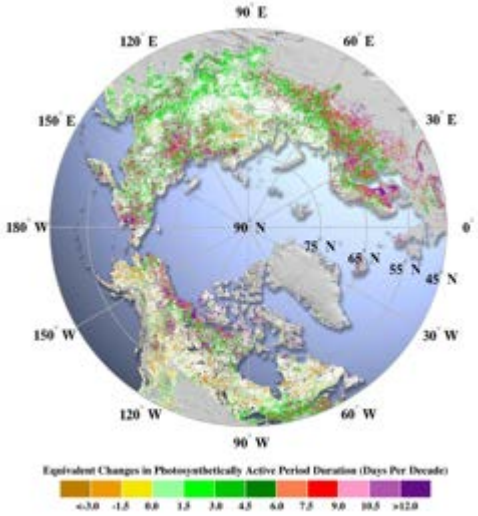

Fig. 36. Trends of change (days/decade) in the length of the growing season (photosynthetically active period, PAP) between 1982 and 2011 based on the GIMMS NDVI product (Xu et al. 2013).

Tall Shrub and Tree Expansion at the Forest-Tundra Ecotone in Siberia

Numerous studies over the past decade have indicated the expansion of shrubs throughout the Arctic (Isla Myers-Smith 2011) and experiments continue to show that warming increases vegetation productivity and the dominance of woody plants (Sistla et al. 2013). Few observations of woody plant expansion had been made in Siberia until Frost and Epstein (2013) quantified changes in tall shrub and tree canopy cover in eleven, widely-distributed Siberian forest-tundra ecotone landscapes. This study compared very-high-resolution photography from the Cold War-era "Gambit" and "Corona" satellite surveillance systems (1965-1969) with modern imagery. The total cover of tall shrubs increased by 5.3-25.9% in nine of ten ecotones (**Fig. 37a**), and tree cover increased by 3.0-18.2% in four of five ecotones (**Fig. 37b**). Shrub and

tree canopy cover expansion rates were better correlated with mean annual precipitation than with mean summer temperature.

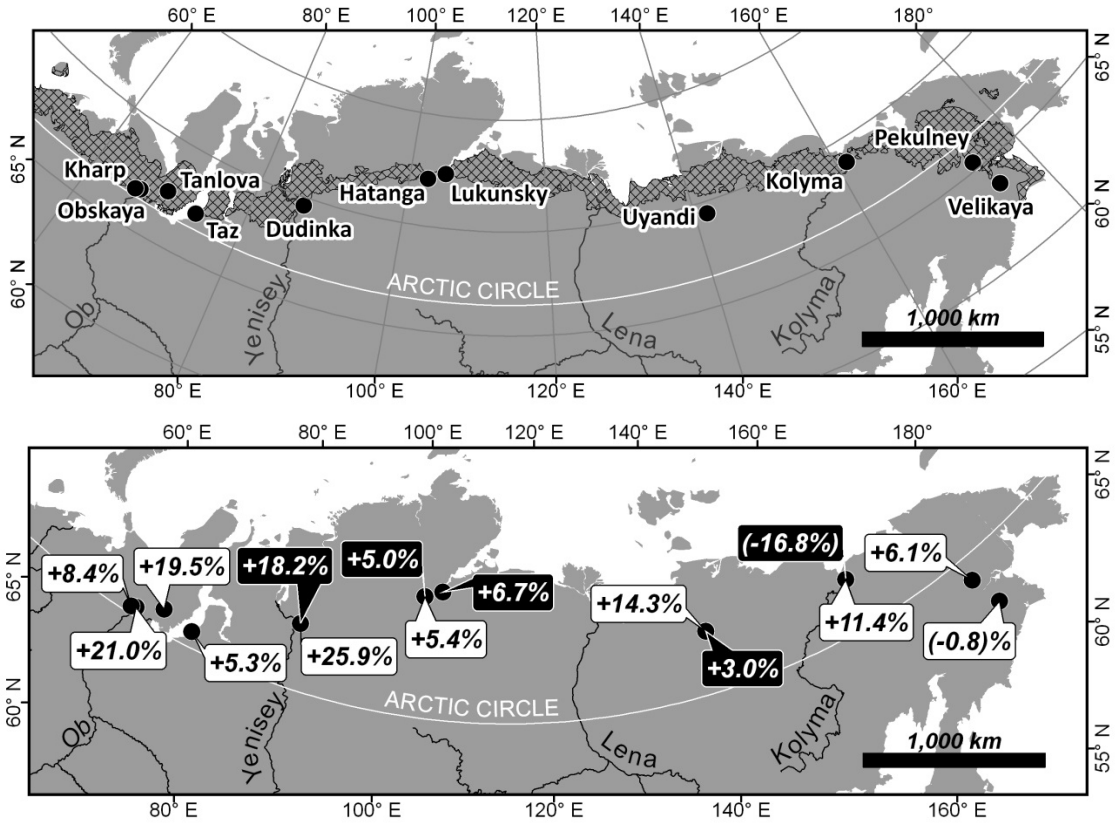

Fig. 37. Tall shrub and tree expansion at the forest-tundra ecotone in Siberia since the mid- to late-1960s (from Frost and Epstein 2013). (a) Location of study areas and Bioclimate Subzone E of the Circumpolar Arctic Vegetation Map (cross-hatched area; Walker et al. 2005), the warmest, southernmost belt of the tundra biome. The southern edge of the cross-hatched area represents the northern limit of trees. (b) Change (in %) of the cover of tall shrubs and trees, white and black boxes, respectively.

Frost et al. (2013) sampled two tall shrub ecotonal landscapes near the Polar Urals of northwestern Siberia and found that establishment of tall alder was strongly facilitated by small, widely-distributed disturbances associated with patterned-ground landscapes resulting from frost-heave (**Fig. 38**). Within expanding and newly-established shrub stands, almost all new shrubs occurred on bare, circular microsites disturbed by seasonal frost-heave, a widespread phenomenon that maintains mosaics of mineral seedbeds with warm soils and few competitors. The bare circles of mineral soil are immediately available to shrubs during favorable climatic periods. Alder abundance and extent have likely increased rapidly in the northwest Siberian Low Arctic since at least the mid-20th century, and this region has high potential for continued expansion of tall shrubs due to the broad distribution of patterned-ground landscapes.

Fig. 38. Alder expansion across a patterned-ground landscape near Kharp, Russia (photograph by G. V. Frost).

Vegetation Response Following Tundra Fire

Historically, wildfires have been rare in the Arctic, although they are a dominant feature of the boreal forests south of the Arctic tundra. In the last decade, however, the number and severity of tundra wildfires on the North Slope of Alaska has increased dramatically, including more than half of all wildfires reported since 1950, and greatly increasing the area known to have burned.

The recent, 2007, Anaktuvuk River wildfire, burned >1000 km^2 of tundra about 40 km north of Toolik Lake on the North Slope of Alaska, and alone accounts for over half of the area burned on the North Slope since 1950. One result of the fire was a huge emission of soil carbon, approximately 2.1 Tg, effectively equivalent to the present-day annual uptake (sink) of the entire global arctic tundra biome (Mack et al. 2011). All of the above-ground vegetation was burned, and there were major increases in energy inputs (radiative forcing) to the system and other changes such as large increases in depth of soil thaw.

Recovery of the vegetation canopy and concomitant surface energy exchange has been quite rapid in the region of the Anaktuvuk River fire, as indicated by a soil and plant biomass harvest conducted in 2011 at the burn site, which included areas that had not been burned, or were moderately or severely burned (Rocha et al. 2012). The results suggest that the vegetation, particularly the graminoids (dominated by the tussock-forming sedge *Eriophorum vaginatum*), was able to regrow relatively quickly from below-ground rhizomes, with above-ground net primary productivity of the moderately burned tundra being slightly greater than in tundra that had not been burned (**Fig. 39**) (Bret-Harte et al. in press). However, lichens and mosses are showing little sign of recovery, and shrub wood was lost in the fire. Therefore, the total biomass of the vegetation is substantially lower in the burned areas than those that did not burn.

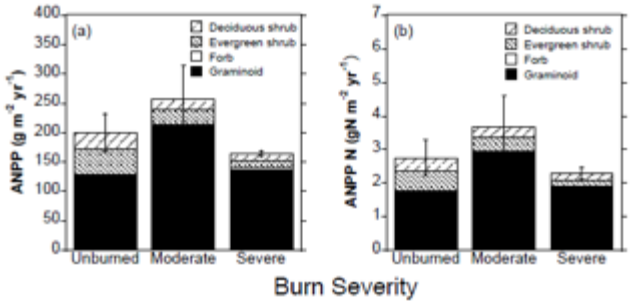

Fig. 39. (a) Above-ground net primary productivity (ANPP) and (b) ANPP Nitrogen for four plant functional types in unburned, moderately burned and severely burned tundra following the Anaktuvuk River fire of 2007 on the North Slope of Alaska (Bret-Harte et al. 2013).

References

Bhatt, U. S., D. A. Walker, M. K. Raynolds, P. A. Bieniek, H. E. Epstein, J. C. Comiso, J. E. Pinzon, C. J. Tucker, and I. V. Polyakov, 2013: Recent declines in warming and arctic vegetation greening trends over pan-Arctic tundra. *Remote Sens.* (Special NDVI3g Issue), 5, 4229-4254.

Bret-Harte, M. S., M. C. Mack, G. R. Shaver, D. C. Huebner, M. Johnston, C. A. Mojica, M. C. Pizano, and J. A. Reiskind, 2013: The response of arctic vegetation and soils following the Anaktuvuk River fire of 2007. *Proc. Roy. Soc. B*, 368, 20120490.

Forbes, B. C., M. Macias Fauria, and P. Zetterberg, 2010: Russian Arctic warming and 'greening' are closely tracked by tundra shrub willows. *Global Change Biol.*, 16, 1542-1554.

Frost, G. V., and H. E. Epstein, 2013: Tall shrub and tree expansion in Siberian tundra ecotones since the 1960s. *Global Change Biol.*, doi:10.1111/gcb.12406.

Frost, G. V., H. E. Epstein, D. A. Walker, G. Matyshak, and K. Ermokhina, 2013: Patterned-ground facilitates shrub expansion in Low Arctic tundra. *Environ. Res. Lett.*, 8, 015035.

Macias Fauria, M., B. C. Forbes, P. Zetterberg, and T. Kumpula, 2012: Eurasian Arctic greening reveals teleconnections and the potential for structurally novel ecosystems. *Nat. Climate Change*, 2, 613-618.

Mack, M. C., M. S. Bret-Harte, T. N. Hollingsworth, R. R. Jandt, E. A. Schuur, G. R. Shaver, and D. L. Verbyla, 2011: Carbon loss from an unprecedented Arctic tundra wildfire. *Nature*, 475, 489-492.

Mudelsee, M., 2009: Break function regression. *Eur. Phys. J. Spec. Top.*, 174, 49-63.

Myers-Smith, I., B. C. Forbes, M. Wilmking, M. Hallinger, K. D. Tape, D. Blok, U. S. Klaassen, T. Lantz, E. Lévesque, S. Boudreau, P. Ropars, L. Hermanutz, A. Trant, L. S. Collier, S. Weijers, J.

Rozema, S. A. Rayback, N. M. Schmidt, G. Schaepman-Strub, L. Andreu, S. Venn, C. Ménard, S. Goetz, H. E. Epstein, J. Welker, and D. Hik., 2011: Causes and implications of the increasing dominance of shrubs in tundra ecosystems. *Environ. Res. Lett.*, 6, 045509.

Pouliot, D., R. Latifovic, and I. Olthof, 2009: Trends in vegetation NDVI from 1 km AVHRR data over Canada for the period 1985-2006. *Int. J. Remote Sens.*, 30, 149-168.

Post, E. U. S. Bhatt, C. M. Bitz, J. F. Brodie, T. L. Fulton, M. Hebblewhite, J. Kerby, S. J. Kutz, I. Stirling, and D. A. Walker, 2013: Ecological consequences of sea-ice decline. *Science*, 341, 519-524.

Rocha, A. V., M. M. Loranty, P. E. Higuera, M. C. Mack, F. S. Hu, B. M. Jones, A. L. Breen, E. B. Rastetter, S. J. Goetz, and G. R. Shaver, 2012: The footprint of Alaskan tundra fires during the past half-century: implications for surface properties and radiative forcing. *Environ. Res. Lett.*, 7, 044039.

Sistla, S. A., J. C. Moore, R. T. Simpson, L. Gough, G. R. Shaver, and J. P. Schimel, 2013: Long-term warming restructures Arctic tundra without changing net soil carbon storage. *Nature*, 497, 615:619.

Walker, D. A., 12 others, and the other members of the CAVM team, 2005: The circumpolar Arctic vegetation map. *J. Vegetation Sci.*, 16, 267-282, DOI: 10.1111/j.1654-1103.2005.tb02365.x.

Xu, L., R. B. Myneni, F. S. Chapin III, T. V. Callaghan, J. E. Pinzon, C. J. Tucker, Z. Zhu, J. Bi, P. Ciais, H. Tømmervik, E. S. Euskirchen, B. C. Forbes, S. L. Piao, B. T. Anderson, S. Ganguly, R. R. Nemani, S. . Goetz, P. S. A. Beck, A. G. Bunn, C. Cao, and J. C. Stroeve, 2013: Temperature and vegetation seasonality diminishment over northern lands. *Nat. Climate Change*, doi:10.1038/NCLIMATE1836.

Zeng, H., and G. Jia, 2013: Impacts of snow cover on vegetation phenology in the Arctic from satellite view. *Adv. in Atmos. Sci.*, 30, 1421-1432.

Muskoxen

A. Gunn[1], J. Eamer[2], P. Reynolds[3], T.P. Sipko[4], A.R. Gruzdev[5]

[1]Roland Road, Salt Spring Island, BC, Canada
[2]Eamer Science Services, Jackpine Street, Gabriola Island, BC, Canada
[3]Fairbanks, AK, USA
[4]Institute of Ecology and Evolution, Russian Academy of Sciences, Moscow, Russia
[5]Wrangel Island State Nature Reserve, Pevek, Chukchi Autonomous Region, Russia

November 20, 2013

Highlights

- Muskoxen have spread geographically and increased in number from contracted ranges (smaller area) after historic declines, and since introduction and/or re-introduction to other locations.
- Alaska muskox numbers have stabilized and in 2010 numbered about 4,200.
- In Russia, re-introductions since 1974-1975 have increased to a total of 10,000 at eight different locations.
- Canada has about 113,300 muskoxen and, after increasing in abundance for about 30 years, numbers appear to have peaked and in some areas are declining.

Introduction

Muskoxen are distributed through northern Canada and Greenland and have been introduced or re-introduced to Alaska, western Greenland, Scandinavia and Russia (**Fig. 40**). Not all introduction sites represent current populations; for example, 17 muskoxen were introduced to Svalbard in 1929 and the small population that initially became established was extinct by 1982 (Klein and Stalaand 1984).

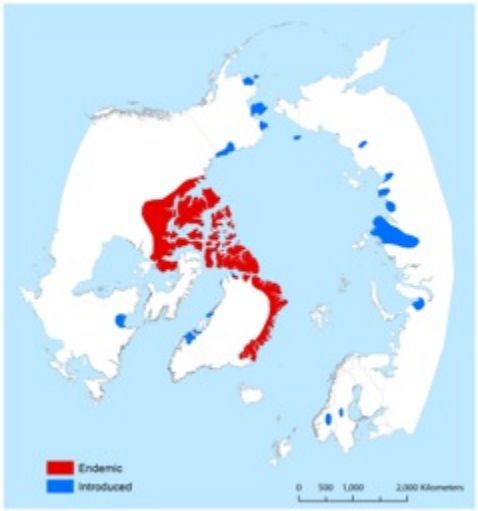

Fig. 40. Map of the historical distribution of muskoxen and where they have been introduced.

Muskoxen in Canada

In 2012, Canada had about 113,300 muskoxen, ~75% of the the World population. Muskox numbers reached an estimated 135,000 in 1998, but the total has decreased, partly because the largest population, on Banks Island, declined. Trends in abundance and distribution between 1998 and 2012 vary regionally and this variation is compounded by changes in survey areas as well as changes in muskox distribution.

European exploration and settlement had a defining role, reducing muskoxen on the mainland to isolated remnants of a few hundred muskoxen by the early 1900s, as traders encouraged commercial hunting for sales of hides in European markets (Barr 1991). Harvesting of muskoxen was suspended from 1924 to 1969, then conservative quotas for harvesting became more widespread as hunters' reports and surveys revealed increasing muskox numbers (Barr 1991). Recovery appeared to be relatively slow, partly as a consequence of lack of information, and partly because the muskoxen were dispersing and recolonizing their previously occupied ranges (Gunn and Adamczewski 2003).

Muskoxen are unequally distributed across northern Canada; their abundance is highest on the large mid-Arctic islands and the tundra of the central mainland, but scarce along the western coast of Hudson Bay and northeast mainland, and absent from Baffin Island. Although the mid-Arctic Banks and Victoria islands are only 9% of the landmass of the Arctic tundra, they hold 72% of Canada's muskoxen, while only 14% of total muskoxen are on the mainland (**Fig. 41**).

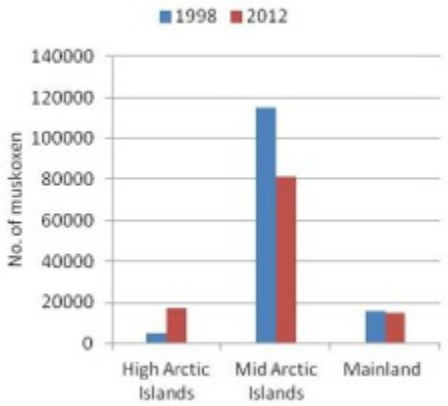

Fig. 41. Change in muskoxnumbers in Canada between 1997 and 2012 for the High Arctic Islands, the mid-Arctic islands and the mainland.

Muskox numbers on Banks Island recovered from almost complete scarcity after an icing storm in the late 1800s. Numbers peaked at 60,000-70,000 between 1994 and 2001, before declining to 36,676±4031 (standard error, S.E.) in 2010 (Davison et al. 2013). The cause of the decline is uncertain, but severe icing in fall 2003 and disease outbreaks have been factors. *Yersinia pseudotuberculosis*, a bacterial disease causing sudden death in outbreaks, has been known since 1986. More recently, in 2012, the disease erysipelas was responsible for an outbreak with at least 100 deaths on Banks Island (personal communication from M. Branigan, Government of the Northwest Territories). Erysipelas has also been reported on neighbouring Victoria Island, but Yersinia has not (Wu et al. 2010).

On southeast Victoria Island, muskoxen increased from 3,300±345 (standard error, s.e.) in 1983 to 18,290±1,100 muskoxen (s.e.) in 1999, partially through re-distribution as well as increasing numbers (Gunn and Patterson 2012). Subsequently, there have been reports of fewer muskoxen, but it is not yet clear whether this is from re-distribution or a numerical decline (personal communication from L.-M. Leclerc). On northwest Victoria Island, numbers increased in the 1980s and 1990s, reached a peak of about 18,000 muskoxen between 1998 and 2001, declined by 2005, and stabilized at about 11,000 muskoxen between 2005 and 2010 (Davison and Williams 2013).

On the High Arctic islands, muskox numbers appeared to increase between 1997 and 2012 (**Fig. 41**), but much of increase is because the eastern islands were systematically surveyed for the first time (Jenkins et al. 2011). On the western islands, muskoxen declined during 1994-97, when snow accumulation and snow density were very high, but numbers have since increased from 2,400 to 3,800 (Davison and Williams 2012).

During the early 20th Century on the Canadian Arctic mainland, muskoxen were restricted to a few scattered remnants, but by the 1990s they had re-colonized most of their historic ranges extending from the Mackenzie River east almost to the west coast of Hudson Bay (Barr 1991, Fournier and Gunn 1998). Muskoxen are also found on the west side of the Mackenzie River, a consequence of recolonization from Alaska. Along the periphery of their ranges, muskoxen are scarce and re-colonization is slow, perhaps spreading at <10 km/year (Fournier and Gunn 1998). The pattern is for muskoxen to expand into areas, while abundance declines behind the colonizing front, although it is difficult to distinguish between numerical declines and redistribution. In western Nunavut, muskox abundance first increased and peaked at 1,800 in 1987, but by 1994 had declined by about 50% and then remained stable through 2007 (Dumond 2007). The muskoxen were infected with a newly discovered lungworm *Umingmakstronylus pallikuukensis*, which may increase vulnerability to predation, especially by grizzly bear, as the lungworm forms cysts in the lungs causing breathing difficulties. Climate models predicted a range expansion of the parasite and it has now spread to southern Victoria Island (Kutz et al. 2009).

Muskoxen in the United States (Alaska)

After disappearing by the 1890s, muskoxen have been successfully restored to Alaska during the past 40 years. There are currently over 4,200 muskoxen in Alaska in 5 different regions. Of these, 66% are on the Seward Peninsula. However, only 1 of 5 populations (Nelson Island) may be increasing. The other four are declining or stable. Several factors, including predation by grizzly bears, hunting, access to winter habitats, winters with freezing rain or deep snow, nutritional deficiencies and disease may be affecting recruitment, survival and distribution. Entire groups of 30-50 animals have died during spring floods, storm surges and lake ice break-up. The effects of parasites, disease and mineral deficiencies in forage are still being evaluated.

Nunivak Island: By the mid-1800s, muskoxen were rare in northern Alaska and they had disappeared from the state by the late 1890s (Lent 1999). In 1935-1936, efforts to restore muskoxen began with the release of 31 animals, originally from Greenland, onto Nunivak Island, in the eastern Bering Sea. After several years of slow growth, the population began to rapidly increase, and reached 500 by 1965. Nunivak Island has no large predators and is located too far offshore for muskoxen to disperse to the mainland. Studies indicated that winter forage for muskoxen on the island was limited due to deep snow (Lent 1999). By the late 1960s, the population exceeded management goals and animals were available for translocation to other regions formerly occupied by muskoxen. Between 1968 and 1981, a total of 236 muskoxen

(mostly sub-adult animals) were moved from Nunivak Island to nearby Nelson Island, to the Arctic National Wildlife Refuge on the North Slope of Alaska, to the Seward Peninsula, and to Cape Thompson in northwestern Alaska. The Nunivak population is currently managed by hunting regulations to maintain a population of 500-550 animals. In 2009 and 2010, pre-calving population estimates were 469 and 433, respectively, and hunting quotas for female muskoxen were reduced (Jones and Perry 2011).

Nelson Island: In 1967 and 1968, 31 muskoxen were moved to Nelson Island, 20 miles from Nunivak Island. Because the channels between the island and the Yukon-Kuskokwim River delta freeze in winter, muskoxen move between the island and the mainland. Fluctuations in abundance are influenced by snow and ice conditions and the availability of escape terrain and forage. In 2009 and 2010, surveys counted 541 and 561 muskoxen, respectively, on the island. At least 100 animals are estimated to be on the mainland but illegal hunting has prevented the establishment of a reproductively viable population (Jones and Perry 2011). The Nelson Island population is the only Alaskan population that appears to be increasing in number.

Arctic National Wildlife Refuge: In 1969 and 1970, 51 and 13 muskoxen, respectively, from Nunivak Island were released near the Arctic National Wildlife Refuge on the North Slope of Alaska, but only about 35-40 animals survived or remained in the area (Reynolds 1998). After the first reproduction was observed in 1973, the population increased rapidly for over a decade and expanded its range westward into north-central Alaska and eastward into the northern Yukon, Canada. The population reached a peak of almost 700 animals in the late 1990s, but then declined by 50% (Reynolds et al. 2002). Several factors, including predation by grizzly bears, access to winter habitats, hunting and disease, likely caused observed declines in recruitment and adult survival and shifts in distribution. Between 2006 and 2012, numbers were relatively stable (184-190) in north-central Alaska in spite of good recruitment (Lenart 2011). Predation by grizzly bears was the major cause of adult and calf mortalities, but other factors may also be important (Arthur and Del Vecchio 2013). Currently, few muskoxen live in the Arctic National Wildlife Refuge, the region first occupied by muskoxen. The population is divided between two non-adjacent regions, with about 200 occupying north-central Alaska and 100 in the northern Yukon.

Cape Thompson: In 1970, 36 muskoxen from Nunivak Island were released near Cape Thompson in northwestern Alaska and 7 years later 34 more animals were moved to the same site (Westing 2011). This population has experienced the slowest growth of all populations re-established in Alaska. After increasing at a rate of 8% from 1970 to 1998, population growth slowed. Numbers in originally occupied areas may be declining, while numbers in other regions may be increasing (Westing 2011). Recruitment has been relatively high (10-18% of total observed). Sources of known mortality include predation by grizzly bears and illegal hunting. From 2000 to 2010, numbers of muskoxen ranged from 236 to 363 (Westing 2011).

Seward Peninsula: In 1970 and 1981, 36 and 35 muskoxen, respectively, from Nunivak Island were released on the Seward Peninsula, where muskoxen may have been absent for hundreds of years. The population grew rapidly, at an annual rate of 14% between 1970 and 2000, and expanded its range throughout the area (Gorn 2011). In 1988, numbers exceeded 500, almost 1500 were counted in 1998 and by 2007 almost 2700 muskoxen occupied the Seward Peninsula. A new distance sampling technique used in 2010 and 2012 counted 2754 and 2013 muskoxen, respectively, suggesting a decline in abundance had occurred (Schmidt and Gorn 2013). Over-harvest of adult males may be contributing to a decline in survival and reproductive success (Schmidt and Gorn 2013).

Muskoxen in Russia

Muskox have been introduced to many locations in Russia since the mid-1970s (**Fig. 42**, **Table 3**). In all cases, muskox numbers have increased, with the exception of the most recent introduction to the Chaoun District, Chukotka. In the almost 40 years since the first animals were introduced, there has been a 40-fold increase in their total number (**Table 3**). Three particular populations are described below.

Fig. 42. Annual muskox population change (%) on Wrangel Island (blue line) and the Taimyr Peninsula (red bars), Russia (Sipko et al. 2007).

Table 3. Number of muskox re-introduced to eight regions of northern Russia since the mid-1970s and estimate of current numbers.

Years of Introduction	Total Introduced	District	Current Estimate
1974, 1975	30	Taymyr Peninsula, Krasnoyarsk Krai	8700
1975	20	Wrangel Island, Čhukotka	900
1996, 2010	46	Bulunskiy District, Sakha Republic	400
1997, 2000	41	Anabarskiy District, Sakha Republic	450
2000, 2009	38	Alajhovskij region, Yakutia	110
2001, 2002	25	Begichev Island, Yakutia	98
1997, 1998, 2001, 2003	63	Polar Urals, Yamal	115
2009, 2010	8	Chaoun District, Chukotka	8
Total	271		10781

Wrangel Island: After their introduction, the number of animals increased until early 2000. Since then, the population has stabilized at around 900 individuals. Surprisingly, the sex ratio of males is substantially lower than expected, causing concern for the population's long term outlook (Sipko et al. 2007). In the mid-2000s, there were several years with late autumn freezing

rain rather than snow. This had little effect on muskox numbers, but caused a large decline in reindeer numbers (Gruzdev and Sipko 2007).

Taimyr Peninsula: After years of stable population growth since introduction, the rate of growth has slowed (**Fig. 42**) and in 2013 the number of muskox was estimated to be 8,700 individuals. Since 2001, this population has been subject to hunting. In the North there are always animals at Cape Chelyuskin, while the migration to the east via the Khatanga River has prevented heavy harvesting by local communities (Sipko, 2004). There has been a substantial increase in numbers in the Gydan region.

Yamal: Since its establishment in 1997 in the polar Urals, the Yamal population has been growing slowly, and mostly due to relatively high birth rates and recruitment. Prospects for growth are limited by the number of domesticated reindeer in the region. Individuals are bred and used to introduce/repopulate other Arctic islands.

Muskoxen in Greenland

Muskox are endemic in the north and northeastern part of Greenland (**Fig. 40**), where the population was estimated to be 9,500-12,000 animals in 1990 (Boertmann et al. 1992). In the 1960s, a total of 27 muskoxen were introduced from Rypefjord to the Scoresbysund area, east Greenland and to Angujaartorfiup Nunaa near Kangerlussuaq, west Greenland (Pedersen and Aastrup 2000). The Angujaartorfiup Nunaa population was thought to have stabilized at approximately 3,000 animals by the late 1990's (Pedersen and Aastrup 2000), well below the estimated habitat carrying capacity of 5,000 animals in the area (Olesen 1993). Surveys in the early 2000s suggested that the population actually numbered 7,000-10,000 animals (Cuyler and Witting 2004), and today the population may even be as large as 25,000 animals (Cuyler et al. 2009), as inferred from an annual harvest of 2,500 animals. Since the successful introduction of muskoxen to Kangerlussuaq, that population has supported six other introductions elsewhere in west Greenland (**Table 4**) (Boertmann et al. 1992, Born et al. 1998).

Table 4. Muskox introductions in west Greenland.

Year	Number	Location	Current estimate and year
1986	7	Kap Atoll/Kangaarsuk (76.5°N; 69,63°W)	47 (2010)
1986	6	Mac Cormic Fjord/Iterlassuaq (77.5°N; 72.40°W)	Disappeared (1986-87)
1986	14	Inglefield Land/Avannarliit (78.5°N; 69,0°W)	270 (1999)
1987	15	Ivittuut (61°N; 48,0°W)	900 (2009)
1991	31	Svartenhug/Nunavik (72°N; 55,0°W)	193 (2002)
1993	31	Lersletten/Naternaq (68.5°N; 52,0°W)	112 (2004)

References

Arthur, S. M. and P.A. Del Vecchio, 2013: Population dynamics of muskoxen in northeastern Alaska. Alaska Department of Fish and Game, Final Wildlife Research Report ADF&G/DWC/|WRR-2013-1, Project 16.10, Juneau, Alaska, USA.

Barr, W., 1991: Back from the brink: the road to muskox conservation in the Northwest Territories. The Arctic Institute of North America, University of Calgary, Calgary, AB. Komatik Series 3. 127 pp.

Born, E., M. Jørgensen, F. Merkel, C. Cuyler, P. Neve, A. Rosing-Asvid, 1998: Grønlandske fugle, havpattedyr og landpattedyr - en status over vigtige ressourcer. Pinngortitaleriffik, Grønlands Naturinstitut, Teknisk rapport, 16.

Boertmann, D., M. Forchhammer, C. R. Olesen, P. Aastrup, and H. Thing, 1992: The Greenland muskox population status 1990. *Rangifer*, 12, 5-12.

Cuyler, L. C., and L. Witting, 2004: Kangerlussuaq (Angujaartorfiup Nunaa) muskox in West Greenland: Possible harvests for 2005, 2006, 2007 and herd status 2004. Advisory document prepared for the Directorate for Environment and Nature. Greenland Institute of Natural Resources, Nuuk. M. S. Kingsley (ed.). Brev. Nr. 02250, J. Nr. 4000.01.03, 16 pp.

Cuyler, C., M. Rosing, H. Mølgaard, R. Heinrich, J. Egede, and L. Mathæussen, 2009: Incidental observations of muskox, fox, hare, ptarmigan and eagle during caribou surveys in West Greenland. Greenland Institute of Natural Resources. Technical Report No. 75. 52 pp.

Davison, T. and J. Williams, 2012: Caribou and muskoxen survey on Melville and Prince Patrick Island, 2012 summary. Community summary. Environment and Natural Resources, Government of the Northwest Territories. Inuvik, NT. 6 p. Provided with comments on SARC report (draft 3) on Peary Caribou. October, 2012.

Davison, T., J. Pongracz, and J. Williams, 2013: Population survey of Peary caribou (*Rangifer tarandus pearyi*) and muskoxen (*Ovibos moschatus*) on Banks Island, Northwest Territories, July 2010. *Rangifer*, 33, Special Issue No. 2: 135-140.

Davison, T., and J. Williams, 2013: Peary caribou (*Rangifer tarandus pearyi*) and muskoxen (*Ovibos moschatus*) on northwest Victoria Island, Northwest Territories. *Rangifer*, 33, Special Issue No. 21: 129-134.

Dumond, M., 2007: Muskox distribution and abundance in the area west of the Coppermine River, Kitikmeot Region, Nunavut. Status Report No. 33. Government of Nunavut, Department of Environment. Iqaluit. 31 p.

Fournier, B., and A. Gunn, 1998: Muskox numbers and distribution in the Northwest Territories, 1997. Department of Resources, Wildlife and Economic Development (DRWED), Yellowknife, NWT, File Report 121, 55 pp.

Gorn, T., 2011: Unit 22 muskox. Pages 16-47 *in* P. Harper, editor. Muskox management report of survey and inventory activities 1 July 2008-30 June 2010. Alaska Department of Fish and Game. Project 16.0. Juneau, Alaska, USA.

Gruzdev A. R., and T. P. Sipko, 2007: State population of musk (Ovibos moschatus Zimmermann, 1780) of Wrangel Island. Scientific. Works of the GEA "Wrangel Island" "nature of Wrangel Island: current research," sat-p., ed. Asterion, P. 103-116.

Gunn, A., and J. Adamczewski, 2003: Muskox. *in* Wild Mammals of North America, G. Feldhamer, B. A. Chapman, and J. A. Chapman (eds.). The Johns Hopkins University Press, Baltimore. 1216 pp.

Gunn, A., and Patterson, B.R., 2012: Distribution and abundance of muskoxen on southeastern Victoria Island, Nunavut, 1988-1999. Manuscript Report No. 222. Department of Environment and Natural Resources, Government of the Northwest Territories. Yellowknife, NT. 41 p.

Jenkins, D. A., M. Campbell, G. Hope, J. Goorts, and P. McLoughlin, 2011: Recent trends in abundance of Peary caribou (*Rangifer tarandus pearyi*) and muskoxen (*Ovibos moschatus*) in the Canadian Arctic Archipelago, Nunavut. Wildlife Report No. 1. Department of Environment, Government of Nunavut. Pond Inlet, NU. 184 p.

Jones, P., and P. Perry, 2011: Unit 18 Muskox, *in* Muskox management report of survey and inventory activities, 1 July 2008-30 June 2010, P. Harper (ed.), 1-11, Alaska Department of Fish and Game, Project 16.0. Juneau, Alaska, USA.

Klein, D. R., and H. Staaland, 1984: Extinction of Svalbard muskoxen through competitive exclusion: a hypothesis. University of Alaska, Special Report No. 4: 26-31.

Kutz, S. J., E. J. Jenkins, A. M. Veitch, J. Ducrocq, L. Polley, B. Elkin, and S. Lair, 2009b: The Arctic as a model for anticipating, preventing, and mitigating climate change impacts on host-parasite interactions. *Vet. Parasitol.,* 163, 217-228.

Lenart, E.A., 2011: Units 26B and 26C Muskox, *in* Muskox management report of survey and inventory activities, 1 July 2008-30 June 2010, P. Harper (ed.), 63-84, Alaska Department of Fish and Game, Project 16.0. Juneau, Alaska, USA.

Lent, P. C., 1999: *Muskoxen and Their Hunters: A History*. University of Oklahoma Press, 324 pp.

Olesen, C.R., 1993: Rapid population increase in an introduced muskox population, West Greenland. *Rangifer*, 13, 27-32.

Pedersen, C. B., and P. Aastrup, 2000. Muskoxen in Angujaartorfiup Nunaa, West Greenland: Monitoring, spatial distribution, population growth, and sustainable harvest. *Arctic*, 53, 18- 26.

Reynolds, P. E., 1998: Dynamics and range expansion of a reestablished muskox population. J. Wildlife Management, 62, 734- 744.

Reynolds, P. E., K. J. Wilson, and D. R. Klein, 2002: In *Arctic Refuge Coastal Plain Terrestrial Wildlife Research Summaries*, D. C. Douglas, P. E. Reynolds, and E. B. Rhode (eds.), U. S. Geological Survey, Biological Resources, Division, Reston VA, 2002, 54-64.

Rozenfeld, S. B., A. R. Gruzdev, T. P. Sipko, and A. N. Tikhonov, 2012: Trophic relationships of muskoxen (*Ovibos moschatus*) and reindeer (*Rangifer tarandus*) on Wrangel Island. *Biol. Bull.*, 39, 779-787.

Sipko, T. P., 2009: Status of reintroductions of three large herbivores in Russia. *Alces*, 45, 23-29.

Sipko, T. P., and A. R. Gruzdev, 2006: Re-introduction of muskoxen in Northern Russia, 2006. *Re-introduction news IUCN/SSC*, 25, 25-26.

Sipko T. P., A. R. Gruzdev, S. S. Egorov, and V. G. Tikhonov, 2007: Analysis of the process of introduction of the musk in the North Asia. *Zoological J.*, 86, 620-627.

Sipko, T. P., 2004: Muskox (*Ovibos moschatus*). Fauna of vertebrates Putorana Plateau /Moscow, 377-378.

Westing, C., 2011: Unit 48-62 Muskox. *in* Muskox management report of survey and inventory activities, 1 July 2008-30 June 2010, P. Harper (ed.), 1-11, Alaska Department of Fish and Game, Project 16.0. Juneau, Alaska, USA.

Wu, J., S. S. Checkley, M. Dumond, and S. Kutz, 2010: 2010 Muskox Health Survey: Victoria Island. Unpublished report for Kitikmeot Food Ltd., Cambridge Bay, NU, Canada.

Migratory Tundra *Rangifer*

D.E. Russell[1], A. Gunn[2]

[1]Yukon College, Whitehorse, YT, Canada
[2]Roland Road, Salt Spring Island, BC, Canada

November 20, 2013

Highlights

- There is strong regional variation in *Rangifer* herd size, but many herds currently have unusually low numbers and their winter ranges in particular are smaller than they used to be.
- There are large population differences among individual herds, and the size of individual herds has varied greatly since 1970. The largest of all herds (Taimyr, Russia) has varied between 400,000 and 1,000,000; the second largest herd (George River, Canada) has varied between 28,000 and 385,000.

Current Status of Migratory Tundra *Rangifer*

The current status of migratory tundra reindeer and caribou is summarized in **Fig. 43**. The most recent population estimates indicate that many herds remain at low numbers after severe declines (Cape Bathurst, Bluenose West, Bathurst, George River, Baffin Island) or continued to decline (Chukotka, Taimyr, Yana-Indigirka, Sundrun, Akia-Maniitsoq, Western Arctic, Teshekpuk Lake, Beverly, Ahiak, Leaf River and Southampton Island). Some herds are increasing or are stable at high numbers. These include Porcupine, Central Arctic, Bluenose East, Kangerlussuaq-Sisimiut, Lena-Olenek, Qamanirjuaq, Iceland reindeer and wild reindeer in southern Norway. While it is normal for herds to vary in size over time, it is uncertain whether the current low numbers are unusual. However, for some herds, their current ranges, especially winter ranges, are a contraction over historic ranges.

Fig. 43. Current status of 24 major migratory tundra reindeer and caribou herds. Numbers identify names of herds that are described in the text.

Trends in Migratory Tundra Rangifer

Local and traditional knowledge has indicated that caribou go through periods of abundance and scarcity every 40-60 years. However, quantitative population estimates have only been employed since the late 1960s and early 1970s. These estimates have shown a single "cycle" of increasing and decreasing numbers for all herds over the last 40 years. The cycle is somewhat synchronous across the Arctic although there is individual herd variation. As well as some differences in the timing of the cycle, there are large differences between minimum and maximum numbers (**Fig. 44**). Where comparative data are available, the recent declines have varied from a 97% decline for the George River herd to a 31% decline in the Porcupine Caribou herd.

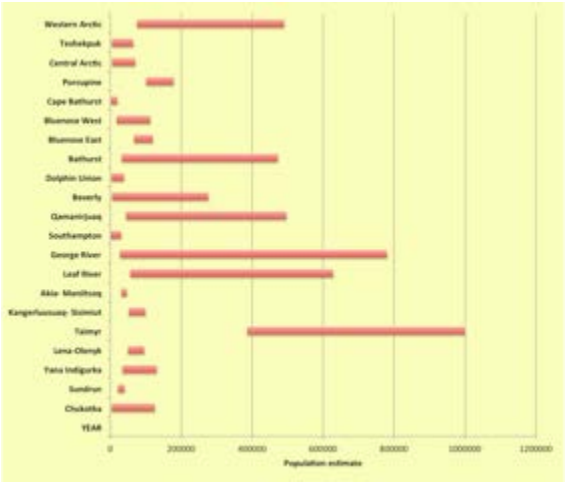

Fig. 44. Minimum and maximum population estimates for migratory tundra *Rangifer* herds, 1970-2013.

Alaska: The Western Arctic herd (**1**, see **Fig. 43** for the location of this and all other herds) was at a low (75,000) in the mid-1970s then increased during the 1980s and 1990s, and reached a peak of 490,000 in 2003. The herd then declined to 348,000 caribou in 2009 (Alaska Department of Fish and Game 2011a) and further declined to 325,000 by 2011. A photo-census in 2013 has yet to be counted. Both the Teshekpuk Lake **(2)** and Central Arctic **(3)** herds were recognized as distinct herds in the 1970s, and were estimated to number 4,000-5,000. Both herds increased, and continued to increase, during the 1990s. By 2008, the Teshekpuk Lake herd had reached 64,107 and the Central Arctic herd 67,000 (Parrett 2009, Lenart 2009). Since 2008, the Teshekpuk Lake herd has declined to 55,000 while the rate of increase of the Central Arctic herd slowed but continued to rise to 70,000 by 2012. Both herds were photographed in 2013 but estimates are not complete. The Porcupine herd **(4)** reached a peak in 1989 (178,000), declined to 123,000 by 2001, before recovering and increasing to 169,000 by 2010 (Alaska Department of Fish and Game 2011b). A photo-census in 2013 has yet to be counted.

Canada: Nine of 11 major herds have declined since peak sizes although there are uncertainties about the extent of a decline for two herds. Three herds (Cape Bathurst **(5),** Bluenose-West **(6)** and Bathurst **(8)** remain at low numbers, with no evidence for recovery despite sharply reduced harvesting. These three herds declined 84-93% from peak sizes in the mid-1980s and 1990s (personal communication from T. Davison 2010, CARMA 2011). There is uncertainty about the extent of a possible increase in the Bluenose-East **(7)** herd, but in 2010 the herd was estimated to number 122,000 (Adamczewski et al. in preparation).

A lack of monitoring has introduced uncertainty and differing interpretations into designations and population trends for some herds. The Beverly herd **(10)** was estimated at 294,000 in 1994. In 1996, to the north, the Ahiak Herd **(9)** was roughly estimated at 250,000 based on calving ground density. In the mid 2000s, agencies failed to find a concentrated calving in the traditional calving grounds of the Beverly Herd known since the 1960s. Subsequent radio-collaring revealed some caribou calving on the Beverly calving grounds, some calving in the Ahiak calving grounds, and some cows switching between calving grounds among years. One explanation is that the Ahiak herd estimated in 1996 was really the Beverly herd that had switched calving grounds in 1995, although there is no observational evidence for this. Alternatively, the Beverly herd may have declined (similar to other Northwest Territories herds), and cows switched to the neighbouring Ahiak herd to maintain the advantages of gregarious calving. In 2011, an extensive aerial survey estimated 124,000 caribou in the Beverly/Ahiak herd (Campbell et al. 2012). The estimate is either a 50% or a 75% decline from the 1994 population estimate for the Beverly Herd, depending on the explanation for the earlier herd number discrepancies.

The Qamanirjuaq **(11)** was estimated to have declined from 496,000 in 1994 to 345,000 in 2008 (Campbell et al. 2010), although the confidence limits were large, resulting in no statistical difference between the two survey estimates. However, since 1996, the trend in late winter calf-cow ratios reveal a persistent decline, which supports the likelihood of a decline in herd size (Campbell et al. 2010).

Caribou were introduced on Southampton Island **(12)** in 1967, following their earlier extirpation on the island. Ongoing studies have shown that Southampton Island caribou numbers have declined from about 30,000 caribou in 1997 to 7,800 caribou in 2011, a decline of almost 75%. Low reproductive rates and a high incidence of brucellosis (Campbell et al. unpublished) as well as a rise in the export market to other communities are contributing factors.

Baffin Island **(24)** is the largest Arctic island, where peak abundance projections of population size ranged between 60,000 and 180,000 for the early 1990s (Ferguson and Gauthier 1992). In 2012, in south Baffin Island, Jenkins et al. (2012) estimated 1,065-2,067 (95% confidence), while numbers on north Baffin Island were considered to be at a low in the cycle after a high in the 1990s.

Since the mid-1990s, the George River Herd **(14)** has declined sharply. A recent survey confirms a continuing decline of the George River migratory caribou herd population over the past few years; currently (2012), it is estimated to be about 27,600 animals, down from 385,000 in 2001 and 74,131 in 2010 (Nunatsiaq News 2013). The results of a 2011 population survey of the Leaf River caribou herd indicated it has declined to 430,000 caribou, down from 630,000 in 2001 (Nunatsiaq News 2013).

Greenland: There are 4 main populations of wild *Rangifer* in west Greenland (ca. 61°-68°N). Despite harvest management aimed at reducing caribou abundance, which began in 2000, the 2010 surveys indicated that the largest, the Kangerlussuaq-Sisimiut **(15)** remained around 98,000 animals (Cuyler et al. 2011). In contrast, the second largest, Akia-Maniitsoq **(16)**, had decreased from an estimated 46,000 in 2001 to about 17,400 in 2010 (Poole et al. 2013). One possible cause might be the topography, which prevents hunter access in the former while permitting access in the latter (personal communication from C. Cuyler).

Iceland: Reindeer were introduced to Iceland **(17)** in the late 1700s (Thórisson 1984). The Icelandic reindeer population in July 2013 was estimated at approximately 6,000. With a hunting

quota of 1,229 animals, the winter 2013-2014 population is expected to be around 4,800 reindeer (personal communication from S. Thórisson).

Norway: There are 23 different reindeer populations **(18)** in the mountain ranges of southern Norway. Population sizes vary from about 50 individuals to more than 10,000 animals in the largest herd at Hardangervidda. The total population in southern Norway typically varies between 30,000-35,000 animals, depending on harvest levels in Hardangervidda. Population numbers are managed through a tag harvest system designed to ensure stable population numbers in balance with habitat quality. Seven of the largest populations are included in a national monitoring program which surveys population age, sex structure and body condition. Habitat quality is to be included in the monitoring program in 2013 based on a combination of ground and remotely-sensed data. At present, the greatest challenges to management are loss of habitat and migration corridors to piecemeal infrastructure development and abandonment of reindeer habitat as a result of human activities and disturbance (personal communication from O. Strand).

Russia: The Taimyr Herd **(19)** is one of the largest in the world. Between the 1950s and 1970s, the herd increased from 110,000 to 450,000 in 1975. Commercial hunting increased and held the herd at about 600,000 animals. Then, subsidies to commercial hunters were removed, hunting declined and the herd grew rapidly by the year 2000 to 1 million animals. Currently the herd is assumed to have declined to about 700,000 animals, based on a 2009 survey projected to 2013 (Kolpashikov et al in press). East of the Taimyr, in the central Siberian region of Yakutia, there are currently three large herds of migratory tundra wild reindeer: the Lena-Olenek herd **(20)**, the Yana-Indigirka herd **(21)** and the Sundrun herd **(22)**. In 2009 the Lena-Olenek herd numbered over 95,000 reindeer, a slight increase from 90,000 estimated in 2001. There have been no surveys reported since 2009. The Yana-Indigirka population declined from 130,000 reindeer in 1987 to 34,000 in 2002. The Sundrun population declined from about 40,000 reindeer in 1993 to about 28,500 in 2002. The Sundrun herd was resurveyed in 2012 and estimated at 27,000, unchanged from the 2002 estimate (personal communication from L. Kolpashikov, Russian Academy of Science Norilsk). East of Yakutia, the Chukotka herd **(23)** increased following the collapse of the domestic reindeer industry. The domestic reindeer industry rapidly collapsed from 587,000 in 1971 to about 92,000 by 2001 (Klokov 2004). Subsequently, wild reindeer recovered and numbered 32,200 individuals in 1986, 120,000-130,000 in 2002, and then declined to less than 70,000 in 2009. No surveys have been reported since 2009.

References

Adamczewski, J., J. Boulanger, B. Croft, T. Davison, H. Sayine-Crawford, and B. Tracz, In preparation: A Comparison of Calving and Post-calving Photo-surveys for the Bluenose-East Herd of Barren-ground Caribou in the Northwest Territories, Canada in 2010. Department of Environment and Natural Resources, Manuscript Report No. 245, 62 pp.

Alaska Department of Fish and Game, cited 2011a: Press release—Western Arctic caribou Herd count revised, http://www.adfg.alaska.gov/index.cfm?adfg=pressreleases.pr03242011].

Alaska Department of Fish and Game, cited 2011b. Porcupine Caribou Herd shows growth. [Available online at http://www.adfg.alaska.gov/index.cfm?adfg=pressreleases.pr03022011].

Campbell, M., J. Boulanger, and D. Lee, unpublished: Demographic Effects of an Outbreak of *Brucella suis* On Island Bound Barren-Ground Caribou (*Rangifer tarandus groenlandicus*) Southampton Island Nunavut. Unpublished data presented at the 13th Arctic Ungulate Conference, 22-26 August, 2011, Yellowknife, Northwest Territories, Canada.

Campbell, M., J. Nishi, and J. Boulanger, 2010: A calving ground photo survey of the Qamanirjuaq migratory barren-ground caribou (*Rangifer tarandus groenlandicus*) population – June 2008. Technical Report Series 2010, No. 1-10, Government of Nunavut. 129 pp.

Campbell, M., J. Boulanger, D. S. Lee, M. Dumond. and J. McPherson, 2012: Calving ground abundance estimates of the Beverly and Ahiak subpopulations of barren-ground caribou (*Rangifer tarandus groenlandicus*) – June 2011. Technical summary to be replaced by Technical Report Series, No. 03-2012, Government of Nunavut. 111 pp.

CARMA, cited 2013: Circumarctic Monitoring and Assessment (CARMA) Network website [Available at www.caff.is/carma].

Cuyler, C., 2007: West Greenland caribou explosion: What happened? What about the future? Proceedings of the 11th North American Caribou Workshop, Jasper, Alberta, Canada, 23-27 April 2006. *Rangifer*, Special Issue No. 17, 219-226.

Cuyler, L. C., M. Rosing, H. Mølgaard, R. Heinrich, and K. Raundrup, 2011: revised in 2012: Status of two West Greenland caribou populations 2010; 1) Kangerlussuaq-Sisimiut, 2) Akia-Maniitsoq. - Pinngortitaleriffik, Greenland Institute of Natural Resources, Technical report No.78, Part I-II, 158 pp.

Ferguson, M. A. D., and L. Gauthier, 1992: Status and trends of Rangifer tarandus and Ovibos moschatus in Canada. *Rangifer*, 12, 127-141.

Jenkins, D. A., J. Goorts, and N. Lecomte. Cited 2012: Estimating the Abundance of South Baffin Caribou Summary Report 2012. Unpublished Report, http://env.gov.nu.ca/sites/default/files/final_summary_report_last_version.pdf].

Klokov. K., 2004: Russia. *Family-Based Reindeer Herding and Hunting Economies, and the Status and Management of Wild Reindeer/Caribou Populations*. Sustainable Development Program, Arctic Council, Centre for Saami Studies, University of Tromsø, 55-92.

Kolpashikov, L., V. Makhailov, and D. Russell, in press: The role of harvest, predators and socio-political environment in the dynamics of the Taimyr wild reindeer herd with some lessons for North America. *Ecology and Society*.

Lenart, E. A., 2009: Units 26B and 26C Caribou. Pages 299-325 *in* P. Harper. Editor. *Caribou Management report of survey and inventory activities 1 July 2006 - 30 June 2008*. Alaska Department of Fish and Game. Project 3.0 Juneau, Alaska, USA.

Nunatsiaq News, cited 2013. Inuit, Inuu, Cree in Quebec and Labrador join forces to protect Ungava caribou. [Available online at http://www.nunatsiaqonline.ca/stories/article/65674quebec_labrador_inuit_inuu_cree_join_forces_to_protect_ungava_caribou].

Parrett, L. S., 2009: Unit 26A. Teshekpuk caribou herd. Pages 271-298 *in* P. Harper. Editor. *Caribou Management report of survey and inventory activities 1 July 2006 - 30 June 2008*. Alaska Department of Fish and game. Project 3.0 Juneau, Alaska, USA.

Poole, K. G., C. Cuyler, and J. Nymand, 2013: Evaluation of caribou *Rangifer tarandus groenlandicus* survey methodology in West Greenland, *Wildlife Biology*, 19, 1-15.

Thórisson, S., 1984: The history of reindeer in Iceland and reindeer study 1979-1981. *Rangifer*, 4, 22-38.

Terrestrial Cryosphere Summary

Section Coordinator: Marco Tedesco

National Science Foundation, Division of Polar Programs,
Arctic Sciences Section, Arlington, VA, USA
&
Department of Earth and Atmospheric Science,
The City College of New York, New York, NY, USA

November 13, 2013

The Terrestrial Cryosphere section includes reports on Snow, Glaciers and Ice Caps outside Greenland, the Greenland Ice Sheet, Lake Ice and Permafrost. Each essay draws on field and satellite observations made through the end of summer 2013, with the exception of Glaciers and Ice Caps outside Greenland, for which 2013 data were not available at the time of writing. The Glaciers and Ice Caps essay is further affected by the absence of data from Russia. These limitations in the timeliness and availability of data illustrate the continued challenges that scientists and society face in the effort to observe and understand what is happening throughout the rapidly changing Arctic.

The observing year for the Terrestrial Cryosphere section began in autumn 2012, when lake ice freeze-up occurred earlier than the average for 2004-2012 in all regions of the Arctic. Then, in spring 2013, lake ice break-up occurred earlier than the average throughout the Arctic. The early lake ice break-up was consistent with observations of snow cover extent, which reached a new record low for May in Eurasia, and was below the spring (April, May, June) average for the entire Northern Hemisphere. In 2013, as in 2012, the long-term rate of reduction of June snow cover extent (-19.9% per decade relative to the 1981-2010 average) was greater than the long-term reduction of September sea ice extent (-13.7% per decade relative to the 1981-2010 average).

Once the terrestrial snow cover has melted, warming of the frozen ground begins in earnest as a seasonal active layer with temperatures >0°C develops above the permafrost. In summer 2013, the strongest trends for increasing active layer thickness since the mid-1990s occurred in Interior Alaska, the Russian European North, East Siberia and the Russian Far East. On the North Slope of Alaska, where the long-term active layer thickness change signal is weaker, there were new record high permafrost temperatures at 20 m below the surface in the two northernmost boreholes. New record high permafrost temperatures also occurred at sites in the Brooks Range, Alaska, and in the High Canadian Arctic.

Active layer thickness has also increased since the late 1990s at some Greenland locations. However, from an Arctic terrestrial cryosphere, and indeed global environmental, perspective it is the Greenland Ice Sheet that attracts most attention. After the record surface melt extent and duration of summer 2012, melt extent and duration in summer 2013 were below the average for 1981-2010, and the surface albedo (reflectivity) was above the average for 2000-2011. These observations are consistent with summer surface air temperatures that were normal with respect to the period 1981-2010, particularly along the west coast, where the equilibrium line altitude (the highest altitude at which the previous winter's snow survives) was close to the long-term (1990-2010) average and river discharge was below average.

Snow

C. Derksen[1], R. Brown[2], K. Luojus[3]

[1]Climate Research Division, Environment Canada, Toronto, ON, Canada
[2]Climate Research Division, Environment Canada, Montreal, PQ, Canada
[3]Arctic Research Centre, Finnish Meteorological Institute, 99600 Sodankylä, Finland

November 15, 2013

Highlights

- Northern Hemisphere spring snow cover extent (SCE) was lower than the historical mean (1967-2013) during 2013, with a new record low May SCE established for Eurasia. North American June SCE was the fourth lowest on record.
- The record-setting loss of Eurasian spring snow cover in May 2013, and the below normal June SCE in North America was driven by rapid snow melt, rather than anomalously low snow accumulation prior to melt onset.
- The rate of loss of June SCE between 1979 and 2013 (-19.9% per decade relative to the 1981-2010 mean) is greater than the loss of September sea ice extent (-13.7% per decade) over the same period.

Snow covers the Arctic land surface for up to 9 months of the year. Unlike other elements of the cryosphere (e.g., sea ice, glaciers) most terrestrial snow cover is seasonal, i.e., it melts and disappears completely each spring and summer. The timing of this melt has important implications for the energy budget through changes to surface albedo, for the water cycle through the release of stored water, and for geochemical cycles by influencing the ground thermal regime and the length of the growing season (Callaghan et al. 2011).

Because Arctic land areas are completely snow covered prior to the melt season, variability in spring snow cover extent (SCE) is controlled largely by surface temperatures (warmer temperatures induce earlier snowmelt onset). Arctic terrestrial snow cover is an important contributor to the cooling effect of the cryosphere, so recent reductions in Arctic spring snow cover have direct effects on the global climate system (Flanner et al. 2011). From a hydrological perspective, snow water equivalent (SWE) prior to melt onset is the key variable, as this represents the available store of freshwater. Variability in SWE is driven by the length of the accumulation season and the cumulative amount of cold season precipitation (modified by surface processes such as wind redistribution and sublimation), until the initiation of melt. Then, the rate of depletion is strongly influenced by air temperature (which is controlled largely by large scale atmospheric circulation and incoming solar radiation), and secondary influences such as incoming solar radiation and cloud feedbacks. Monitoring and understanding the interplay between SCE and SWE is vital to addressing the impacts of variability and change in Arctic terrestrial snow cover.

In spring 2013, Northern Hemisphere spring SCE anomalies computed from the weekly NOAA snow chart Climate Data Record (CDR) for months when snow cover is confined largely to the Arctic showed a continued reduction from the historical mean in May and June (**Fig. 45**). For Eurasia, a new record low May SCE was established, with June SCE tied for the second lowest since 1967. Across North America, April SCE was well above average (standardized anomaly of

+2.0), May SCE near average (standardized anomaly of -0.4), and June SCE well below average (standardized anomaly of -1.8). The SCE changes are consistent with differences in continental air temperature anomalies (Overland et al. 2013), who illustrate positive anomalies over Eurasia and negative anomalies over North America (see **Fig. 3c** in the essay on *Air Temperature*). The shift to increasingly negative SCE anomalies as the melt season progresses is consistent with observations over the past decade (**Fig. 45**) and reflected in the monthly SCE trends, computed for 1967 through 2013 (**Table 5**. The rate of snow cover loss over Northern Hemisphere land areas in June between 1979 and 2013 is -19.9% per decade (relative to the 1981-2010 mean; updated from Derksen and Brown 2012). Interestingly, this exceeds the rate of September sea ice loss over the same time period (-13.7% per decade, **Fig. 46**; also see the essay on *Sea Ice*), which is widely used as evidence of the observed response of the cryosphere to rising Arctic temperatures.

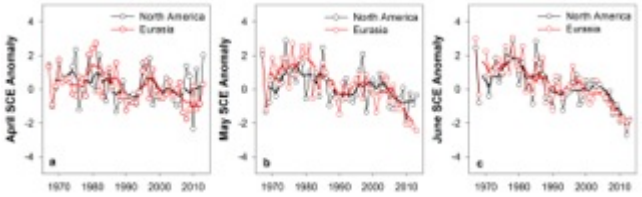

Fig. 45. Monthly Northern Hemisphere snow cover extent (SCE) standardized (and thus unitless) anomaly time series (with respect to 1981-2010) from the NOAA snow chart CDR for (a, left) April, (b, centre) May and (c, right) June. Solid black and red lines depict 5-yr running averages for North America and Eurasia, respectively. Updated from Derksen and Brown (2012). The CDR is maintained at Rutgers University and described in Brown and Robinson (2011).

Table 5. Linear trends (1967-2013) in SCE ($km^2 \times 10^6 \times decade^{-1}$) derived from the NOAA snow chart CDR using the Mann-Kendall (MK) statistic following the removal of serial correlation. **Bold**: significant at 95%; **bold italics**: significant at 99%. Updated from Derksen and Brown (2012).

	Snow Cover Extent ($km^2 \times 10^6 \times decade^{-1}$)	
	North America	Eurasia
April	-0.16	-0.33
May	**-0.21**	***-0.78***
June	***-0.43***	***-0.86***

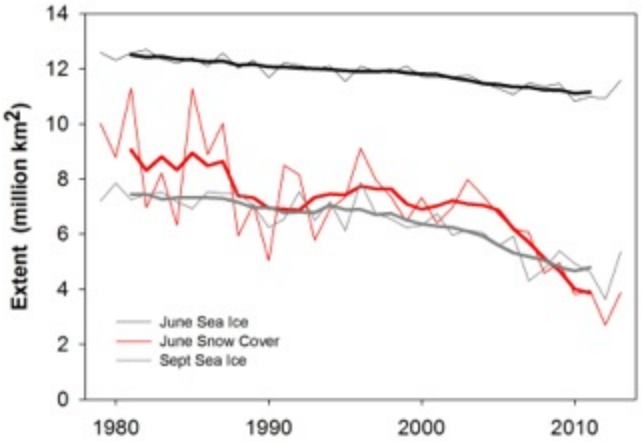

Fig. 46. Northern Hemisphere June SCE, and June and September Arctic sea ice extent, 1979-2013. The bold lines are 5-year running averages. Updated from Derksen and Brown (2012).

The timing of snow cover onset in autumn is influenced by both temperature and precipitation. Snow cover duration (SCD) departures derived from the NOAA daily IMS snow cover product (Helfrich et al. 2007) show earlier than normal snow cover onset over Scandinavia (**Fig. 47a**), with no notable departures over other Arctic regions (earlier than normal snow onset was observed for a mid-latitude region of North America, and southeastern Eurasia). The negative SCE anomalies for May and June (**Fig. 45**) are reflected in earlier than normal snow melt across the Canadian tundra and eastern Siberia (**Fig. 47b**). Snow cover persisted longer than normal across northwestern Europe, which drove the positive Eurasian SCE anomalies for April (**Fig. 45a**). This region was climatologically snow free by May, so the positive spring SCD departures in this region had no impact on the record setting low SCE across Eurasia in May.

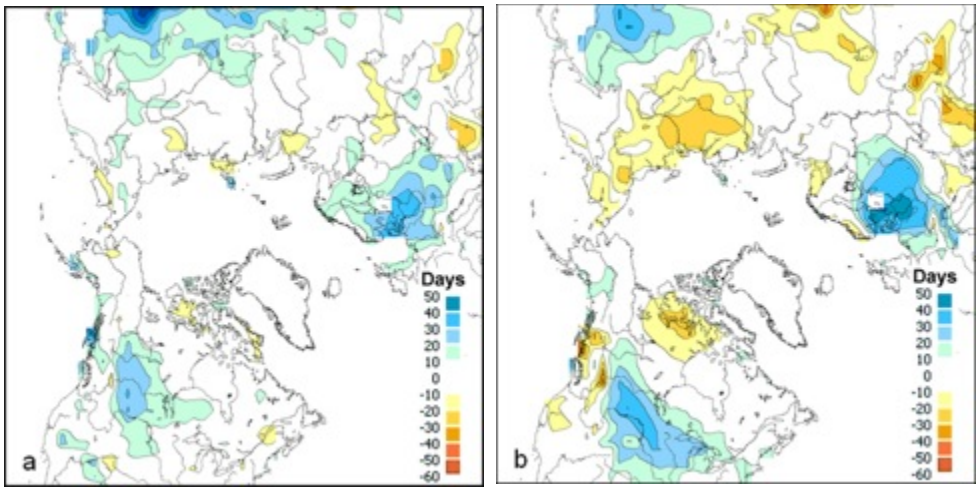

Fig. 47. Snow cover duration (SCD) departures (days; with respect to 1998-2010) from the NOAA IMS data record for the 2012-2013 snow year: (a, left) fall; and (b, right) spring.

Mean monthly snow depth anomalies from the Canadian Meteorological Centre (CMC) daily gridded global snow depth analysis (Brasnett, 1999) for April, May, and June 2013 are shown in **Fig. 48**. In April (**Fig. 48a**), snow depth anomalies were positive over most of sub-Arctic Eurasia (mean anomaly of +16.9% relative to 1999-2010 average) and North America (mean anomaly of +29.4%). This is consistent with the negative winter season Arctic Oscillation (DJF mean

of -1.12; weaker Arctic jet favourable to cold air outbreaks) which produced below average winter season temperatures over sub-Arctic Eurasia and North America (see **Fig. 3b** in the essay on *Air Temperature*). By May, however, the Eurasian snow depth anomalies were strongly negative (**Fig. 48b**; mean anomaly of -52.1%), illustrating the rapid response of snow conditions to positive surface temperature anomalies over most of Eurasia (see **Fig. 3c** in the essay on *Air Temperature*) concurrent with below normal cloud cover (as estimated by the ERA interim reanalysis; not shown).

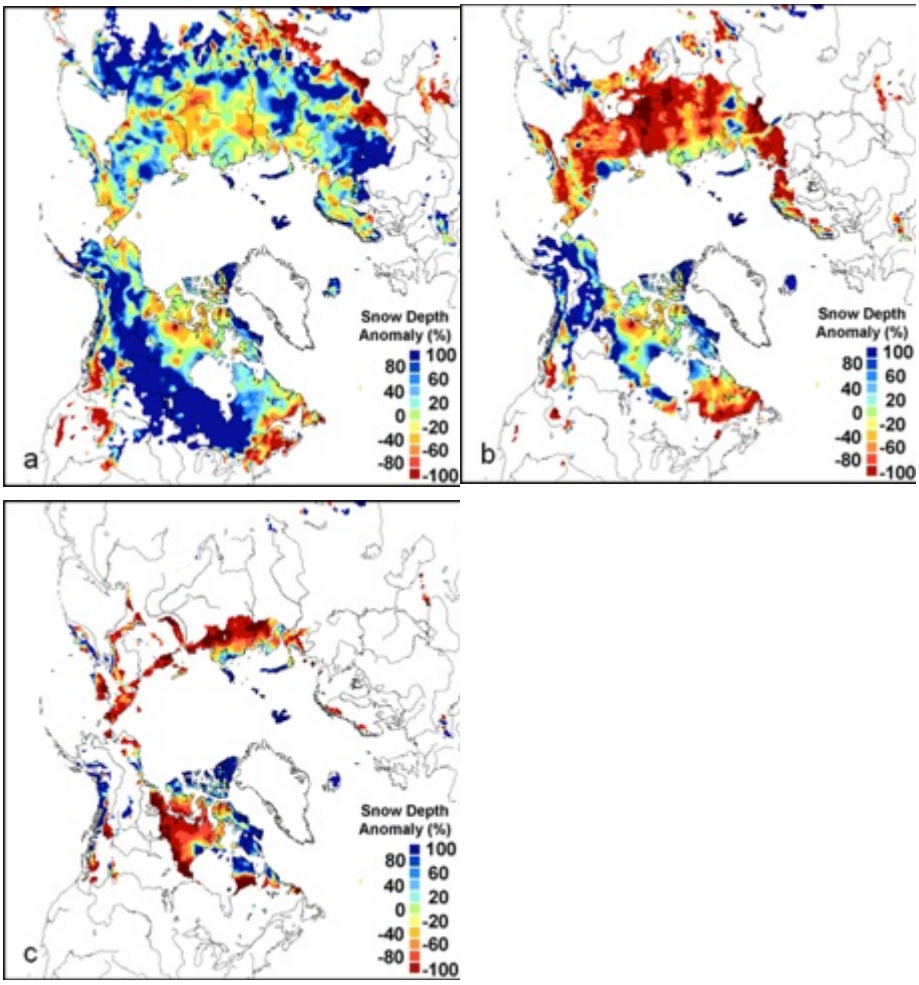

Fig. 48. 2013 snow depth anomaly (% of the 1999-2010 average) from the CMC snow depth analysis for (a, top left) April, (b, top right) May, and (c, lower left) June.

The quick transition from above normal to below normal snow depth was also captured by the daily time series of Arctic SWE (land areas north of 60°N) derived from the CMC analysis (**Fig. 49**). Before melt onset, the total SWE was above the average for the data record (since 1998) over both Eurasia and North America. During a two week period in mid-May, the record high SWE over Eurasia plummeted to well below the dataset average (**Fig. 49b**). The decline in SWE was less dramatic for North America because regionally extensive positive temperature anomalies (also concurrent with below average cloud cover) did not set in until June (see **Fig. 3** in the essay on *Air Temperature*). As was noted for 2012, this means the record setting loss of Eurasian spring snow cover in May 2013, and the below normal June 2013 SCE in North

America, was driven by rapid snow melt, rather than anomalously low cold season snow accumulation.

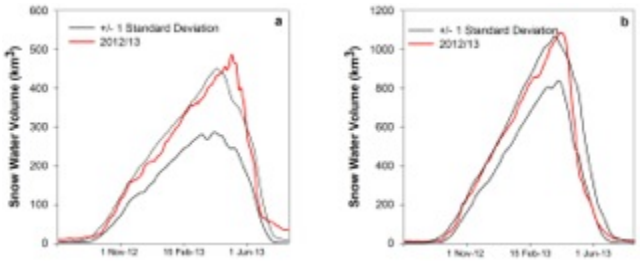

Fig. 49. Daily 2012-13 time series (red) of Arctic snow water volume for (a, left) North America and (b, right) Eurasia derived from the CMC snow depth analysis. The solid black lines show the +/- 1 standard deviation range about the mean SWE over 1998-99 to 2011-12 snow seasons. Note the different y-axis range of each graph.

References

Brasnett, B., 1999: A global analysis of snow depth for numerical weather prediction. *J. Appl. Meteorol.*, 38, 726-740.

Brown, R., and D. Robinson, 2011: Northern Hemisphere spring snow cover variability and change over 1922-2010 including an assessment of uncertainty. *Cryosphere*, 5, 219-229.

Callaghan, T., and 20 others, 2011. The changing face of Arctic snow cover: A synthesis of observed and projected changes. *Ambio*, 40, 17-31.

Derksen, C., and R. Brown, 2012, Spring snow cover extent reductions in the 2008-2012 period exceeding climate model projections. *Geophys. Res. Lett.*, 39, doi:10.1029/2012GL053387.

Helfrich, S., D. McNamara, B. Ramsay, T. Baldwin, and T. Kasheta, 2007, Enhancements to, and forthcoming developments in the Interactive Multisensor Snow and Ice Mapping System (IMS). *Hydrolog. Process.*, 21, 1576-1586.

Flanner, M., K. Shell, M. Barlage, D. Perovich, and M. Tschudi, 2011: Radiative forcing and albedo feedback from the Northern Hemisphere cryosphere between 1979 and 2008. *Nature Geosci.*, 4, 151-155, doi:10.1038/ngeo1062.

Mountain Glaciers and Ice Caps (Outside Greenland)

M. Sharp[1], G. Wolken[2], M.-L. Geai[1], D. Burgess[3], J.G. Cogley[4], A. Arendt[5], B. Wouters[6]

[1]Department of Earth and Atmospheric Science, University of Alberta, Edmonton, AB, Canada
[2]Alaska Division of Geological and Geophysical Surveys, Fairbanks, AK, USA
[3]Geological Survey of Canada, Ottawa, ON, Canada
[4]Department of Geography, Trent University, Peterborough, ON, Canada
[5]Geophysical Institute, University of Alaska Fairbanks, Fairbanks, AK, USA
[6]School of Geographical Sciences, University of Bristol, Bristol, UK

November 27, 2013

Highlights

- Annual climatic mass balance (B_{clim}) was negative at 21 of 24 glaciers monitored in 2010-2011.
- Regional mean B_{clim} (for all available glaciers in 2010-11) was the second most negative value, after 2009-10, in the period 1989-2011. The last time the regional mean B_{clim} was positive was in 1992-1993.

The area of mountain glaciers and ice caps in the Arctic exceeds 420,000 km^2, representing about 54% of the total global and ice cover other than the ice sheets of Greenland and Antarctica. Between 2003 and 2009, wastage of these glaciers accounted for a net annual input of ~174 Gt a^{-1} of water to the oceans. This is about 67% of the total global glacial input of water to the oceans from non-ice sheet sources (Gardner et al. 2013). Transfer of water from glaciers to the oceans occurs by a combination of surface melt and runoff, iceberg calving, and submarine melting of the termini of glaciers that end in the ocean.

The *climatic mass balance* (B_{clim}, Cogley et al. 2011) of a glacier, defined as the difference between annual mass gain (from precipitation on the glacier) and annual mass loss (from meltwater runoff, sublimation and evaporation), is a widely used index of how glaciers respond to climate change and variability. It is measured annually at as many as 27 glaciers in the Arctic (**Fig. 50**): three in Alaska, four in the Canadian Arctic islands, nine in Iceland, four in Svalbard and seven in northern Scandinavia. Unfortunately, there are no current measurements of B_{clim} in the Russian Arctic. Measurements of B_{clim} refer to a *mass balance year*, a one-year period between the ends of two successive melt seasons. In the Arctic, measurements are typically made in spring, when both the winter balance for the current mass balance year and the summer balance for the previous mass balance year are determined. For this reason, the most recent measurements available relate to the 2010-2011 mass balance year, except for Arctic Canada, for which data for 2011-2012 are available.

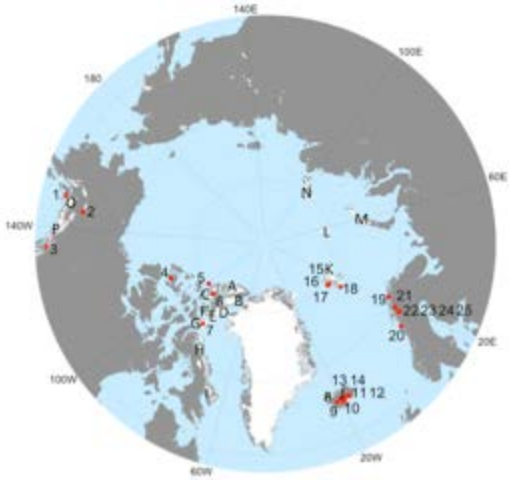

Fig. 50. Locations of Arctic glaciers for which long-term records of climatic mass balance (B_{clim}) are available, and for which recent data are reported here. See **Table 6** for glacier names and numbering. Letters represent regions for which MODIS land surface temperature data are presented in **Fig. 53** (A: Northern Ellesmere; B: Agassiz; C: Axel Heiberg; D: Prince of Wales; E: Manson; F: Sydkap; G: Devon; H: North Baffin; I: South Baffin; J: Iceland; K: Svalbard; L: Franz Josef Land; M: Novaya Zemlya; N: Severnaya Zemlya; O: South-West Alaska; P: South-East Alaska).

Measurements of B_{clim} of these glaciers for the mass balance years 2009-2010, 2010-2011 (World Glacier Monitoring Service 2012, 2013), and 2011-2012 (for Arctic Canada only) are presented in **Table 6**. In 2010-2011 B_{clim} was negative (mass loss) for 21 of the 24 glaciers, and positive (mass gain) for only three (all outlets of the northern margin of Iceland's Vatnajökull ice cap). Relative to 2009-2010, B_{clim} was more negative in 2010-2011 in coastal southern Alaska, Arctic Canada, Svalbard, and northern Scandinavia, and less negative in interior Alaska and Iceland. For the 2011-2012 mass balance year, measurements of B_{clim} for three of the glaciers in Arctic Canada were less negative than in the previous year, while in one case (Melville South ice cap) they were slightly more negative.

Table 6. Measured annual net surface mass balances of glaciers in Alaska, the Canadian Arctic, Iceland, Svalbard and northern Scandinavia for 2009-2010, 2010-2011, and (where available) 2011-12 (numbers in brackets indicate rank of year, where 1 is the most negative balance year in the record). Mass balance data for glaciers in Alaska, Svalbard, Norway, Sweden and Iceland are from the World Glacier Monitoring Service (2013); D. Burgess and J.G. Cogley supplied those for Arctic Canada).

Region	Glacier (Record length, years)	Net Balance 2009-10 (kg m^{-2} yr^{-1})	Net Balance 2010-11 (kg m^{-2} yr^{-1})	Net Balance 2011-12 (kg m^{-2} yr^{-1})	Glacier number in Fig. 50
Alaska	Wolverine (46)	-85 (30)	-1070 (11)		1
	Lemon Creek (59)	-580 (26)	-720 (16)		3
	Gulkana (46)	-1832 (3)	-1290 (7)		2
Arctic Canada	Devon Ice Cap (52)	-417 (5)	-683 (1)	-503 (4)	7
	Meighen Ice Cap (53)	-387 (12)	-1310 (1)	-1118 (2)	5
	Melville S. Ice Cap (50)	-939 (4)	-1339 (2)	-1556 (1)	4
	White (50)	-188 (20)	-983 (1)	-951 (2)	6
Iceland	Langjökull S. Dome (16)	-3800 (1)	-1279 (9)		8
	Hofsjökull E	-2830 (1)			9
	Hofsjökull N	-2400 (1)			9
	Hofsjökull SW	-3490 (1)			9
	Köldukvislarjökull (19)	-2870 (1)	-754 (5)		14
	Tungnaarjökull (21)	-3551 (1)	-1380 (8)		10
	Dyngjujökull (14)	-1540 (1)	+377 (12)		13
	Brúarjökull (19)	-1570 (1)	+515 (17)		12
	Eyjabakkajökull (19)	-1750 (3)	+525 (19)		11
Svalbard	Midre Lovenbreen (44)	-200 (31)	-920 (2)		17
	Austre Broggerbreen (45)	-440 (28)	-1004 (3)		16
	Kongsvegen (25)	+130 (18)	-434 (5)		15
	Hansbreen (23)	-14 (17)	-280 (14)		18
Norway	Engabreen (42)	-520 (9)	-910 (5)		20
	Langfjordjøkulen (21)	-760 (12)	-1257 (8)		19
Sweden	Marmaglaciaren (22)	-500 (9)	-1450 (2)		21
	Rabots Glaciar (30)	-1080 (7)	-2110 (1)		22
	Riukojietna (25)	-960 (8)	-1080 (6)		23
	Storglaciaren (67)	-690 (20)	-1060 (9)		24
	Tarfalaglaciaren (17)	-1060 (5)	-1820 (2)		25

Taking annual mean values for all available Arctic B_{clim} records over the period 1989-2011 (for which there are at least 20 records in each year), 2010-2011 had the second most negative mean B_{clim} after 2009-2010 (**Fig. 51**) (Wolken et al. 2013). The last year when the regional mean B_{clim} was positive was 1992-1993. On a regional basis, 2010-2011 was the most negative balance year in the 50-52 year-long records from three of the four measured glaciers in Arctic Canada, and the second most negative for the other one (Melville South Ice Cap). Balance year 2011-2012 was the most negative at Melville South Ice Cap, the second most negative at Meighen Ice Cap and White Glacier, and the fourth most negative at Devon Ice Cap. Four or five of the seven most negative balance years on record for this region have occurred since 2006-2007. This is a result of strong summer warming that began around 1987 and accelerated after 2005 (Gardner and Sharp 2007, Sharp et al. 2011). For the three Icelandic glaciers with positive mass balance, 2010-2011 was among the three most positive balance years in the 19-20 year long records. For all three glaciers in northern Svalbard, 2010-2011 was among the five most negative balance years in the 25 to 45 year long records. In northern Scandinavia, where record lengths range from 21-67 years, 2010-2011 was among the nine most negative balance years at all seven sites.

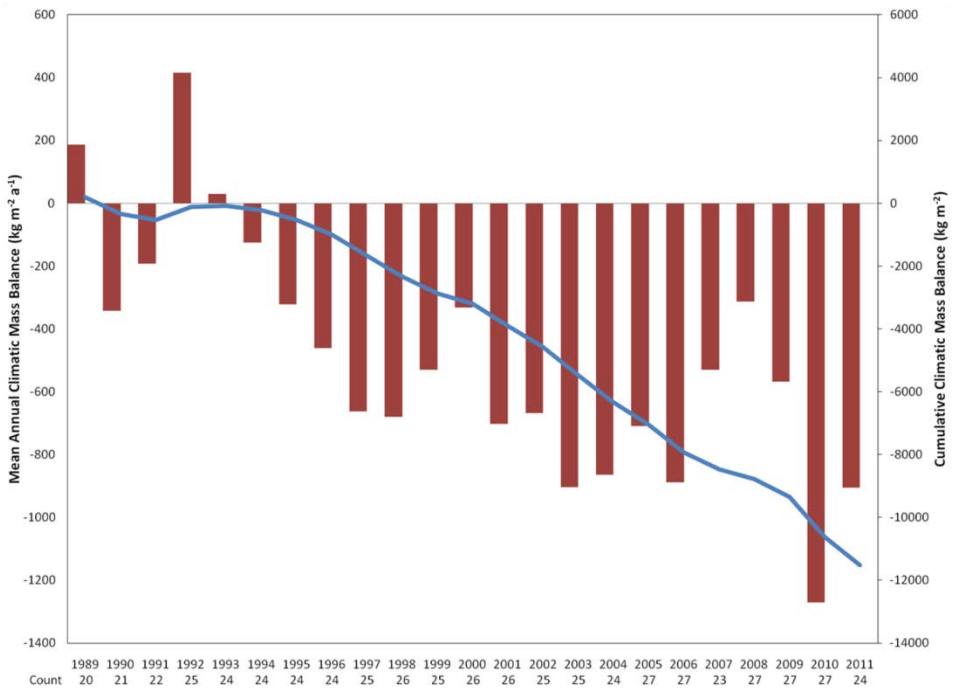

Fig. 51. Mean annual (red) and cumulative (blue) climatic mass balance (B_{clim}) from 1989-2011 based on all available annual measurements (count) from Arctic glaciers reported to the World Glacier Monitoring Service by January 2013. Each year during this period has at least 20 reported measurements.

The total mass balance (B_{clim} plus mass losses by iceberg calving and marine melting) of all glaciers in the Gulf of Alaska region and Arctic Canada can be estimated using GRACE satellite gravimetry (**Fig. 52**, Wolken et al. 2013). For the 2011-2012 mass balance year the estimate for the Gulf of Alaska is +51.9 ± 16.3 Gt, while for Arctic Canada it is -106 ± 27 Gt. The latter value is very similar to the record low value of 2010-2011, a result that is consistent with field measurements of B_{clim} (**Table 6**), and provides further evidence of the growing importance of this region as a contributor to global sea level rise (Gardner et al. 2011). Unfortunately, field

measurements from Alaska are not yet available to compare with the GRACE estimate, which was the most positive annual value for the region for any year since the launch of GRACE in 2003.

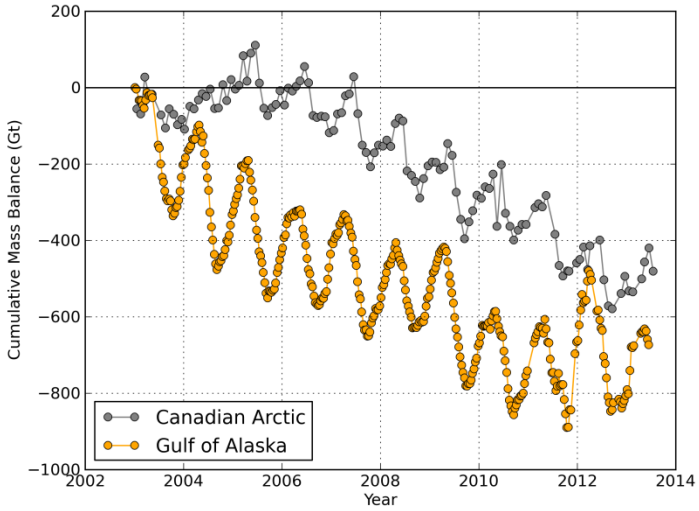

Fig. 52. Cumulative total mass balances of Canadian Arctic and Gulf of Alaska region glaciers, determined by GRACE satellite gravimetry. Canadian data are estimates from monthly Stokes coefficients from the Center for Space Research fifth release (CSR RL5) and processed following methods in Gardner et al. (2011) and Wouters and Schrama (2007). The Gulf of Alaska data are processed according to Luthcke et al. (2013) and subsetted to the region defined in Arendt et al. (2013).

Variability in mean summer temperature accounts for much of the inter-annual variability in B_{clim} in cold, dry regions like the Canadian high Arctic (Braithwaite 2005). As a result B_{clim} in these regions is likely closely related to land surface temperature (LST) over ice in summer (Hall et al. 2006). **Figure 53** shows moderate to large LST anomalies over glaciers and ice caps throughout the Arctic, particularly in summers 2011 and 2012 in the Canadian high Arctic (northern Ellesmere, Agassiz, Axel Heiberg, Prince of Wales), where B_{clim} was especially negative (**Table 6**) and GRACE data showed large mass losses (**Fig. 52**). In more maritime regions like Iceland and southern Alaska, variability in winter precipitation is also a factor.

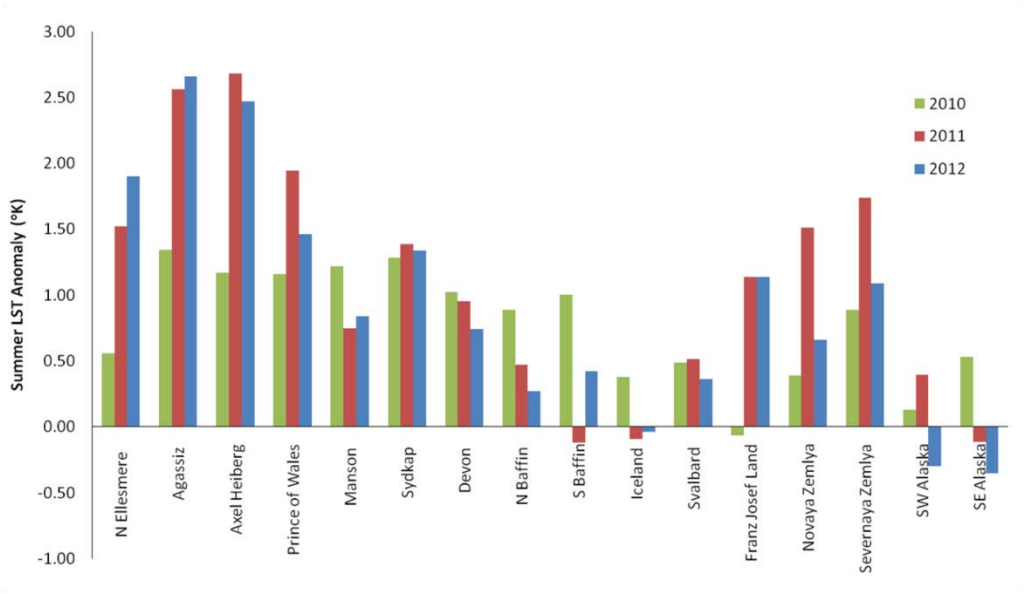

Fig. 53. Comparison of summer mean land-surface temperature (LST) anomalies (relative to 2000-2010 means) in 2010, 2011 and 2012 for 16 glaciated regions of the Arctic based on the MODIS MOD11A2 LST product (ORNL DAAC 2010). Locations of these regions (A, B, C, ….. P) are identified in **Fig. 50**.

References

Arendt, A., S. Luthcke, A. Gardner, S. O'Neel, D. Hill, G. Moholdt, and W. Abdalati, 2013: Analysis of a GRACE global mascon solution for Gulf of Alaska glaciers. *J. Glaciol.*, 59, 913-924.

Braithwaite, R. J., 2005: Mass balance characteristics of Arctic glaciers, *Ann. Glaciol.*, 42, 225-229.

Cogley, J. G., R. Hock, L. A. Rasmussen, A. A. Arendt, A. Bauder, R. J. Braithwaite, P. Jansson, G. Kaser, M. Möller, L. Nicholson, and M. Zemp, 2011: Glossary of Mass Balance and Related Terms, *IHP-VII Tech. Doc. Hydrol.* 86, *IACS Contr.* No 2, UNESCO-IHP, Paris.

Gardner, A. S., and M. Sharp, 2007: Influence of the Arctic Circumpolar Vortex on the Mass Balance of Canadian high Arctic Glaciers. *J. Climate*, 20, 4586-4598.

Gardner, A. S., G. Moholdt, B. Wouters, G. J. Wolken, D. O. Burgess, M. J. Sharp, J. G. Cogley, C. Braun, and C. Labine, 2011: Sharp acceleration of mass loss from Canadian Arctic Archipelago Glaciers and Ice Caps. *Nature* 473, 357-360.

Gardner, A. S., and 15 others, 2013: A reconciled estimate of glacier contributions to sea level rise: 2003-2009. *Science*, 340, 852-857.

Hall, D. K., R. S. Williams, Jr., K. A. Casey, N. E. DiGirolamo, and Z. Wan, 2006: Satellite-derived, melt-season surface temperature of the Greenland Ice Sheet (2000-2005) and its relationship to mass balance. *Geophys. Res. Lett.*, 33, L11501, doi:10.1029/2006GL026444.

Luthcke, S. B., T. J. Sabaka, B. D. Loomis, A. A. Arendt, J. J. McCarthy, and J. Camp, 2013: Antarctica, Greenland and Gulf of Alaska land-ice evolution from an iterated GRACE global mascon solution. *J. Glaciol.*, 59, 613-631.

Sharp, M., D. O. Burgess, J. G. Cogley, M. Ecclestone, C. Labine, and G. J. Wolken, 2011: Extreme melt on Canada's Arctic ice caps in the 21st century. *Geophys. Res. Lett.,* 38, L11501, doi:10.1029/2011GL047381.

Sasgen, I., V. Klemann, and Z. Martinec, 2012: Towards the inversion of GRACE gravity fields for present-day ice-mass changes and glacial-isostatic adjustment in North America and Greenland. *J. Geodyn.* 59-60, 49-63.

Wolken. G., M. Sharp, M.-L. Geai, D. Burgess, A. Arendt, and B. Wouters, 2013: [Arctic]. Glaciers and ice caps (outside Greenland). [in "State of the Climate in 2012"]. *Bull. Amer. Met. Soc.* 94, S119-S121.

World Glacier Monitoring Service, 2012: Preliminary glacier mass balance data for 2009/2010. http://www.wgms.ch/mbb/sum10.html.

World Glacier Monitoring Service, 2013: Preliminary glacier mass balance data for 2010/2011. http://www.wgms.ch/mbb/sum11.html.

Wouters, B., and W. J. O. Schrama, 2007: Improved-accuracy-of-grace-gravity-solutions-through-empirical-orthogonal-function-filtering-of-spherical-harmonics. *Geophys. Res. Lett.* 34, L23711, doi: 10.1029/2007GL032098.

Greenland Ice Sheet

M. Tedesco[1,2], J.E. Box[3], J. Cappelen[4], X. Fettweis[5], T. Jensen[3], T. Mote[6], A.K. Rennermalm[7], L.C. Smith[8], R.S.W. van de Wal[9], J. Wahr[10]

[1]The City College of New York, New York, NY, USA
[2]National Science Foundation, Arlington, VA, USA
[3]Geological Survey of Denmark and Greenland, Copenhagen, Denmark
[4]Danish Meteorological Institute, Copenhagen, Denmark
[5]Department of Geography, University of Liege, Liege, Belgium
[6]Department of Geography, University of Georgia, Athens, GA, USA
[7]Department of Geography, Rutgers, The State University of New Jersey, New Brunswick, NJ, USA
[8]Department of Geography, University of California Los Angeles, CA, USA
[9]Institute for Marine and Atmospheric Research Utrecht, Utrecht University, The Netherlands
[10]Department of Physics and CIRES, University of Colorado, Boulder, CO, USA

December 5, 2013

Highlights

- Surface air temperatures in summer 2013 in Greenland were near the long-term average of 1980-2010.
- Melting occurred over as much as 44% of the surface of the ice sheet in summer 2013, 14th in the 33-year record (1981-2013) and much lower than the record 97% in 2012.
- Melting occurred on >100 days, consistent with the long-term (1981-2010) average at some locations along the southwestern margin of the ice sheet, where the surface mass balance along a transect (the K-transect) was close to the 1990-2010 average.
- The average albedo of the ice sheet surface during summer 2013 was the highest since 2008, curtailing a period of increasingly lower albedo values since 2007, but close to the average for the period of record (2000-2013).

Surface Melting

Melt estimates across the Greenland ice sheet obtained from passive microwave data (Mote and Anderson 1995, Mote 2007) indicate that the June-July-August (JJA) 2013 melt period was near the long-term average for the period 1981-2010. Melt extent during summer 2013 did not deviate significantly from the 1981-2010 long-term average, and sporadic melt spikes were much smaller in magnitude than those of the extreme 2012 melt season (**Fig. 54a**). The maximum area of the Greenland ice sheet subjected to melting during summer 2013 was 44% on July 26th, a much smaller area than the record 97% of 2012 (Nghiem et al. 2013, Tedesco et al. 2013a), ranking 14th in the 33-year period of record (1981-2013). The average melt extent for summer 2013 was ~17%, ranking 16th in the period of record, was the lowest annual value since 2000. For comparison, the average melt extent during extreme summer of 2012 was ~34%.

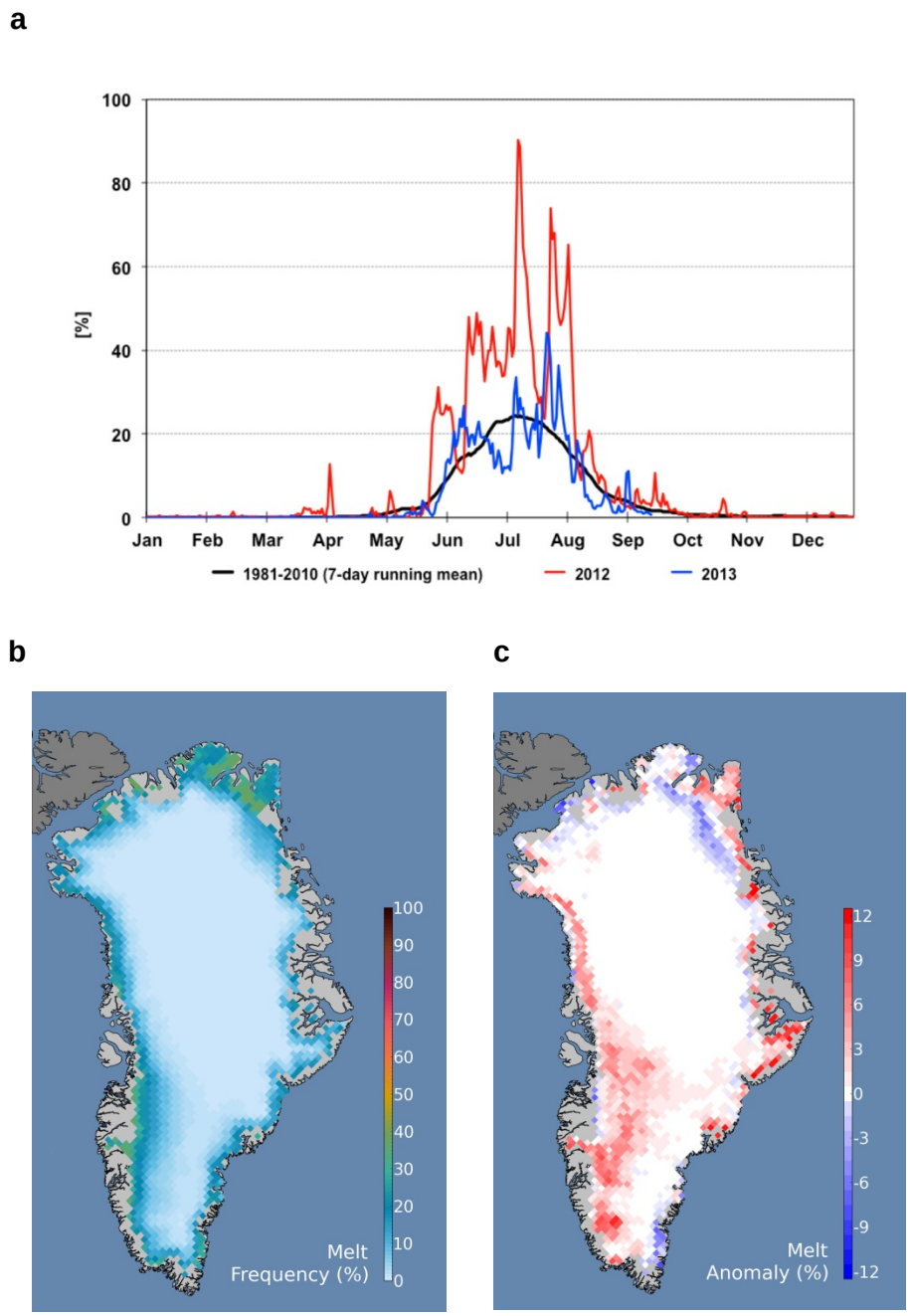

Fig. 54. Melting at the surface of the Greenland ice sheet. (a) Annual cycle of melt extent (expressed as a percentage of the ice sheet where melting is detected) illustrated by the 1981-2010 average and the 2012 and 2013 melt seasons. (b) Melt duration (total number of days of melting) anomaly between 1 January and 23 September, 2013, expressed as a percentage of the average melt duration for the period 1981-2010. (c) Melt frequency (how often melting occurred) anomaly between 1 January and 23 September, 2013, expressed as a percentage of the average melt frequency for the period 1981-2010. Source: National Snow and Ice Data Center, USA.

The cumulative spatial extent of melt across the Greenland ice sheet during 2013 closely followed the long-term average of 1981-2010 (**Fig. 54b**, updated through 23 September 2013, when melting can be considered to have ceased). Consistent with the long-term average, melting during 2013 occurred in excess of 100 days in some locations along the southwestern

margin of the ice sheet. The frequency of melting was slightly higher than the 1981-2010 average along the western and northwestern coasts along but less frequent than average along the southern and southeastern coasts (**Fig. 54c**).

Surface Mass Balance and Runoff

Since measurements began in 1990, there has been a trend of decreasing surface mass balance (mass loss increasing) at the 'K-transect' (lowest elevation located ~20 km east from Kangerlussuaq between 340 m and 1500 m above sea level, a.s.l.; van de Wal et al. 2005, 2012) in west Greenland (**Fig. 55a**). In 2013 (red box, **Fig. 55a**), measurements made at individual points along the transect (**Fig. 55b**) indicate that there was slightly less melting in the lower ablation zone compared to the 1990-2010 average, particularly near the ice margin. The estimated equilibrium line altitude (the highest altitude at which winter snow survives) in 2013 on the K-transect was close to the long-term average position of 1500 m a.s.l. (in contrast to its upslope migration to ~2700 m in 2012, when record mass losses occurred at high elevations during an exceptionally warm summer, e.g., Tedesco et al. 2013b).

a

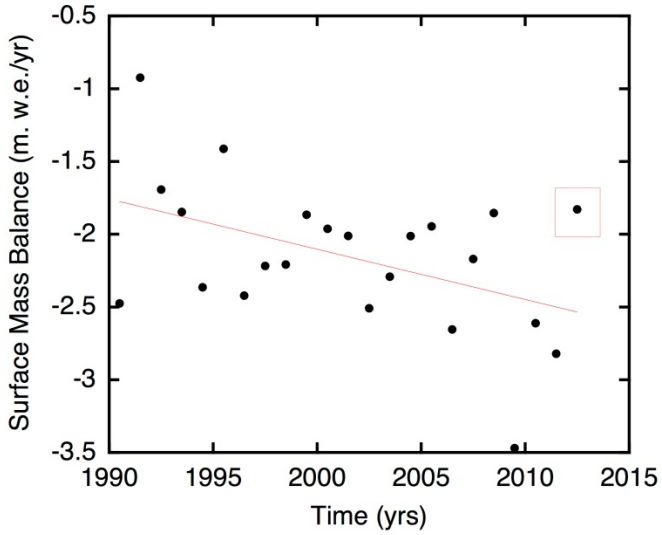

b

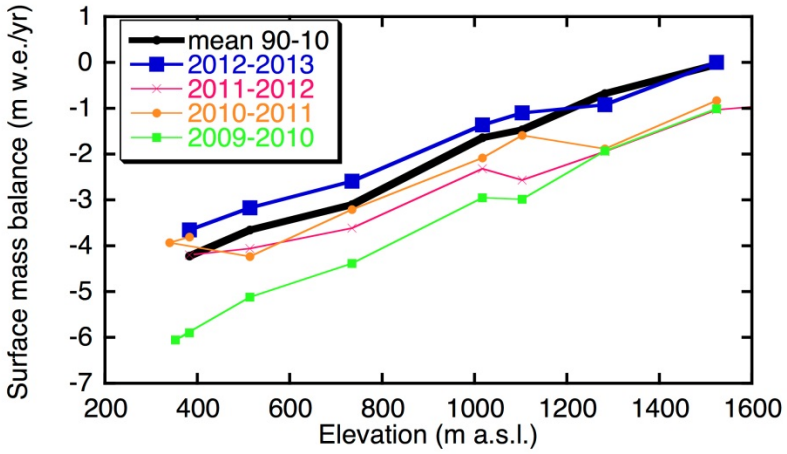

c

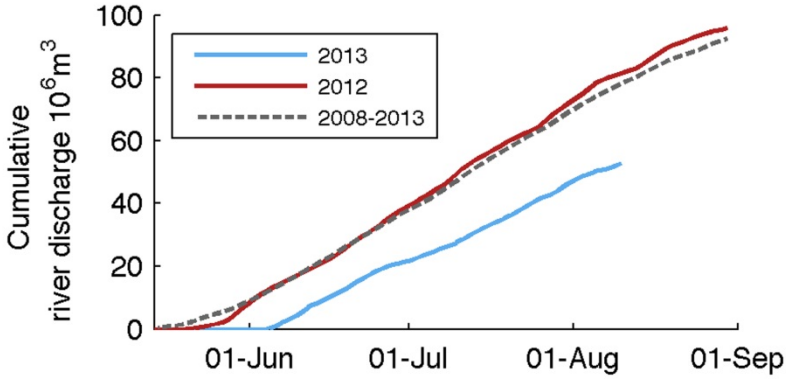

d

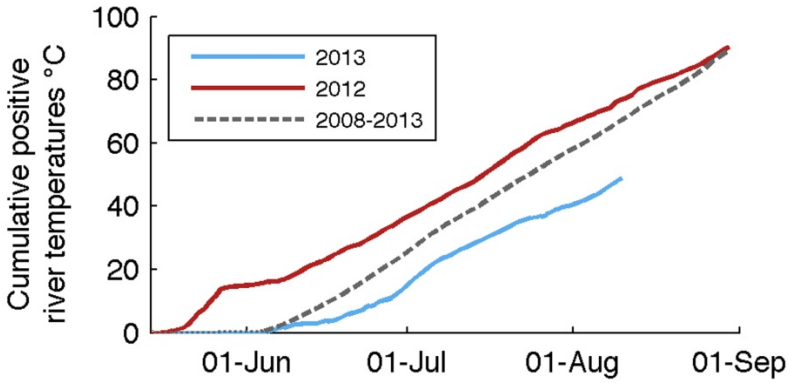

Fig. 55. (a) Average surface mass balance since 1990 for seven sites in the elevation range 390-1500 m a.s.l. along the K-transect (the red box identifies the 2013 value; each value is a simple arithmetical average that ignores the spatial extent of each site). (b) Surface mass balance (in meters of water equivalent per year) as a function of elevation along the K-transect for the last four years and the 20-year average for the period 1990-2010. (c) Cumulative river discharge and (d) Cumulative positive stream temperatures from the AK4 catchment (~20 km east of Kangerlussuaq) in west Greenland in 2013 compared with 2012 and the 2008-2012 average.

Rivers draining from the ice sheet transport meltwater runoff to the ocean, but are currently monitored at only a few sites around Greenland (Rennermalm et al. 2013a). Consistent with surface mass balance estimates at the K-transect, river discharge observations of a small basin (with an estimated ice catchment area of ~31-60 km^2 and altitude of 400-850 m a.s.l.; Rennermalm et al. 2012, Rennermalm et al. 2013b) of the Kangerlussuaq catchment (largely including the K-transect) reveal a later melt season onset in 2013 and lower flow conditions compared to previous years. Cumulative river discharge (e.g., ice sheet meltwater export, **Fig. 55c**) in 2013 was the lowest recorded during the instrumental record for this site (2008-2013). Also, consistent with the lower air temperatures reported below, meltwater temperatures were considerably lower than the 2008-2013 average (**Fig. 55d**). While runoff from this single catchment cannot be extrapolated to other parts of the ice sheet, this short record suggests that meltwater runoff from the ice margin for this area of southwestern Greenland was lower than previous years.

Total Ice Mass

GRACE satellite gravity data (Velicogna and Wahr 2006) are used to estimate monthly changes in the total mass of the Greenland ice sheet (**Fig. 56**). Unfortunately, GRACE mass loss estimates are not available for August and September 2013, when the K-band ranging system was switched off to preserve battery life. The next estimate, for October 2013, will be available in early 2014. Nevertheless, there are sufficient GRACE data to provide some information about the total mass of the ice sheet in 2013 relative to previous years.

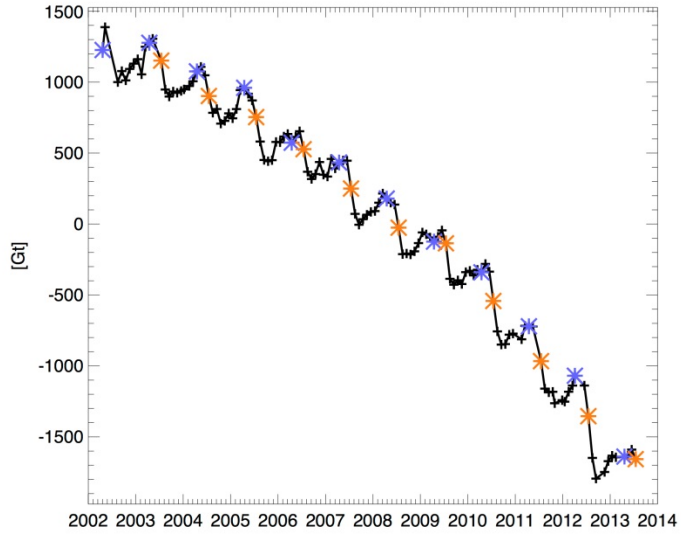

Fig. 56. Monthly changes in the total mass (in Gigatonnes) of the Greenland ice sheet estimated from GRACE measurements since 2002. The blue and orange asterisks denote April and July values, respectively.

From the end of April 2012 through the end of April 2013, which corresponds reasonably well to the period between the beginning of the 2012 and 2013 melt seasons, the cumulative ice sheet loss was 570 Gt, over twice the average annual loss rate of 260 Gt y^{-1} during 2003-2012. The 2012-2013 mass loss is the largest annual loss rate for Greenland in the GRACE record, mostly reflecting the large mass loss during the summer of 2012 (Tedesco et al. 2013b). The mass loss

during the 2013 summer melt season is likely to be considerably smaller than during 2012, based on other evidence such as the reduced surface melt extent, surface mass balance and runoff described above. A lower mass loss during summer 2013 can also be inferred from the much smaller difference between the April (blue asterisks) and July 2013 mass values (orange asterisks), particularly relative to each of the three previous years (**Fig. 56**).

Ice Albedo

The average ice sheet-wide albedo derived from the Moderate-resolution Imaging Spectroradiometer (MODIS, e.g., Box et al. 2012) during summer 2013 was the highest since 2008 (**Fig. 57a**), interrupting a period of increasingly negative and record albedo values (Box et al. 2012, Tedesco et al. 2011, 2013a). Overall, albedo for the period JJA 2013 was well above the 2000-2011 average along the southwest, northwest and northeast regions and coasts of the ice sheet, but it was below the average for the east and southeast regions (**Fig. 57b**).

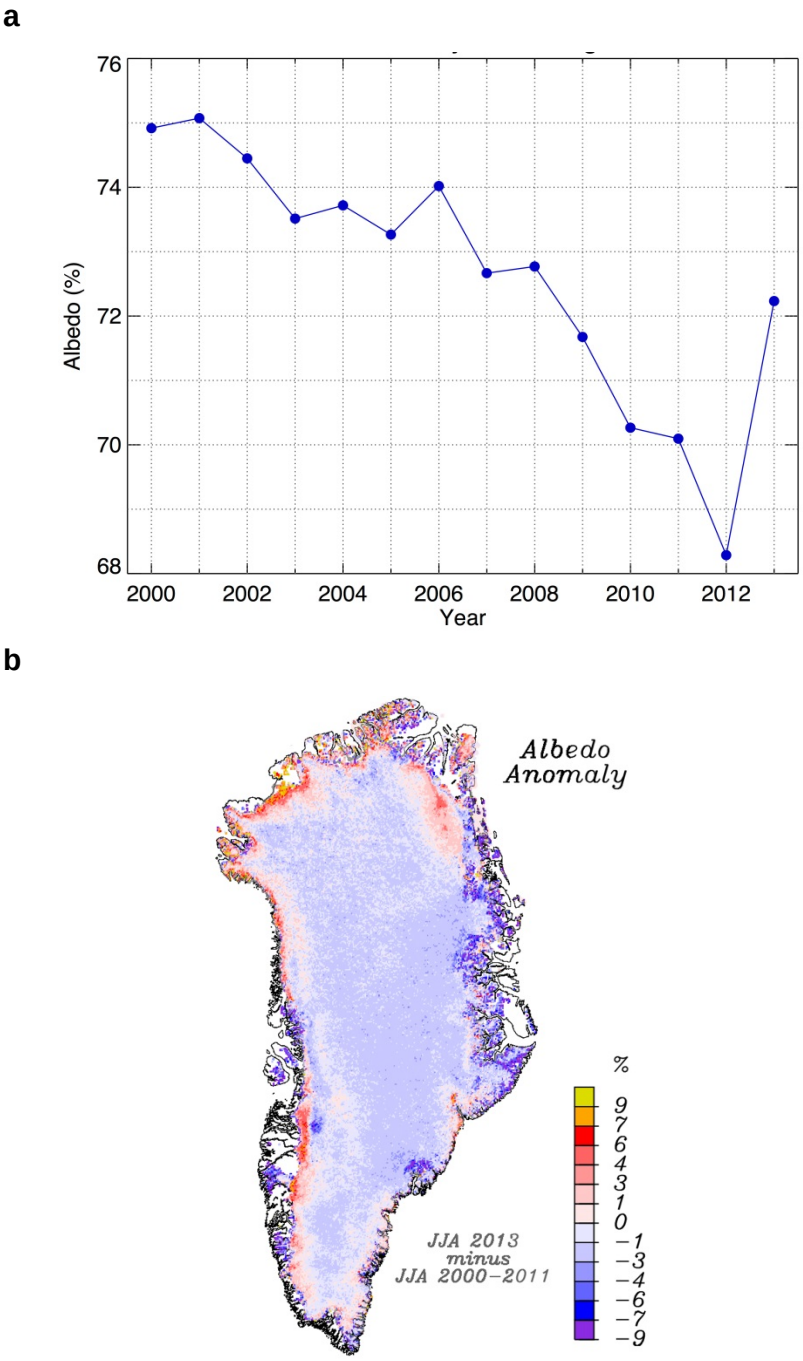

Fig. 57. Greenland ice sheet albedo in summer (June, July, August) derived from MODIS (Moderate-resolution Imaging Spectroradiometer). (a) Average ice sheet-wide albedo from 2000 to 2013. (b) Spatial variation of albedo anomaly relative to the 2000-2011 average.

Meteorological Conditions

Near surface air temperature (NSAT) data recorded by automatic weather stations (Cappelen 2013, http://www.dmi.dk/fileadmin/Rapporter/TR/tr13-04.pdf) indicate that the outstanding surface temperature feature for calendar year 2013 was a consistent warm anomaly along the

west Greenland coast during March (see **Fig. 3b** in the essay on *Air Temperature*). A record warm March was recorded at Pituffik/Thule AFB, where the NSAT anomaly relative to 1981-2010 baseline was +7.7°C, the warmest on record since 1948. Similarly, the Upernavik and Kangerlussuaq March NSAT anomalies were +7.7°C and +8.6°C, respectively.

In contrast to the previous six summers, summer 2013 was characterized by a positive North Atlantic Oscillation (NAO) and persistently lower-than-normal 500 hPa geopotential heights. Consequently, warm, southerly air masses were diverted eastward away from Greenland and cool northerly airflow in west Greenland (see **Fig. 4** in the essay on *Air Temperature*) promoted cooler, wetter and cloudier weather than normal, and less melting than in recent years, as reported above. This is reflected in the NSAT data (**Table 7**), which show that during the summer months (June, July, August) NSAT values were generally near or below one standard deviation of anomalies relative to the 1981-2010 baseline period, indicating that summer 2013 NSATs were "normal" with respect to that period. Wide-area air temperature anomalies (**Fig. 3d** in the essay on *Air Temperature*) are broadly consistent with the data for individual stations (**Table 7**).

Table 7. Near-surface air temperature (NSAT) anomalies in °C relative to the period 1981-2010 for the months of June, July and August 2013, and the average anomaly for June through August (JJA). Values in the parentheses indicate number of standard deviations the anomaly is from the 1981-2010 average.

Station Name (lat., °N; lon., °W)	June	July	August	JJA
Pituffik/Thule (75.9, 68.8)	-1.0 (-0.6)	-0.8 (-0.5)	-0.4 (-0.4)	-0.8 (-0.6)
Upernavik (72.2, 56.2)	0.7 (1.1)	0.7 (1.10)	-0.2 (0.2)	0.4 (1)
Kangerlussuaq (66.4, 50.7)	1.4 (1)	0.5 (0.4)	-0.6 (-0.8)	0.4 (0.4)
Ilulissat (68.5, 51.1)	0.8 (1.1)	-0.4 (0.1)	-1.1 (-0.5)	-0.3 (0.4)
Aasiaat (68.0, 52.8)	1.2 (1.0)	0.4 (0.3)	0.5 (0.4)	0.7 (0.7)
Nuuk (63.5, 51.8)	0.4 (0.3)	0.9 (0.9)	0.9 (0.7)	0.7 (0.7)
Paamiut (61.3, 49.7)	-1.1 (-0.7)	0.0 (0.0)	-0.2 (-0.1)	-0.4 (-0.4)
Narsarsuaq (60.5, 45.4)	-0.8 (-0.3)	-0.7 (-0.5)	-0.1 (-0.1)	-0.5 (-0.4)
Qaqortoq (60.1, 46.0)	-1.3 (-1.1)	-1.1 (-0.9)	-0.6 (-0.4)	-1 (-1)
Danmarkshavn (76.1, 18.8)	0.7 (0.7)	0.8 (1.10)	0.8 (0.9)	0.8 (1.2)
Illoqqortoormiut (69.8, 22.0)	1.3 (1.6)	1.1 (1.4)	1.2 (1.5)	1.2 (1.6)
Tasiilaq (64.9, 37.6)	0.7 (0.3)	0.5 (0.2)	-0.3 (-0.2)	0.3 (0.2)
Prince Christian Sund (59.3, 43.2)	0.5 (0.3)	0.1 (0.6)	0.5 (1.2)	0.8 (0.8)
Summit (71.9, 38.5)	0.3 (0.1)	0.1 (-0.1)	-2 (-0.9)	-0.5 (-0.4)

Marine-Terminating Glaciers

Marine-terminating glaciers are the outlets via which the inland ice sheet discharges to the ocean. When in balance, the rate of iceberg calving (by area) is balanced by the seaward motion of the ice. LANDSAT and ASTER images of 17 of the widest marine-terminating glaciers

in summer 2013 indicate a net area change of -11.3 km^2 since summer 2012. This retreat is the 4th lowest in the 13-year period of observations (2000-2013) and equivalent to 13% of the trend of -84 $km^2\ yr^{-1}$ for the period (**Fig. 58**). The largest increases in area between 2012 and 2013 occurred at Petermann (+15.9 km^2) and Nioghalvfjerdsbrae/79 (+3 km^2) glaciers. The largest area loss occurred at the Zachariae glacier (-15.6 km^2).

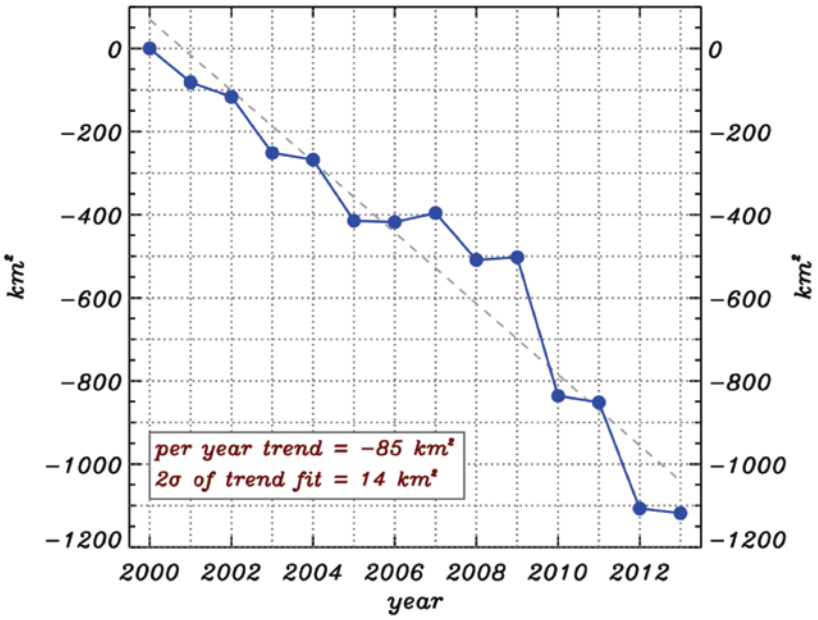

Fig. 58. Cumulative annual net area change of 17 of the widest marine-terminating glaciers of the Greenland ice sheet (after Box and Decker 2011). The dashed line is a least squares regression: y = -85.4099km^2x + 170889 (r = -0.96, p>0.999).

References

Box, J. E., X. Fettweis, J. C. Stroeve, M. Tedesco, D. K. Hall, and K. Steffen, 2012: Greenland ice sheet albedo feedback: thermodynamics and atmospheric drivers. *The Cryosphere*, 6, 821-839, doi:10.5194/tc-6-821-2012.

Box, J. E., and D. T. Decker, 2011: Greenland marine-terminating glacier area changes: 2000-2010. *Ann. Glaciol.*, 52, 91-98, http://dx.doi.org/10.3189/172756411799096312.

Cappelen, J., 2013: Greenland - DMI Monthly Climate Data Collection 1768-2012, Denmark, The Faroe Islands and Greenland. *Dansk Meteorol. Inst. Tech. Rap.*, 13-04, 75 pp.

Mote, T. L., and M. R. Anderson, 1995: Variations in melt on the Greenland Ice Sheet based on passive microwave measurements. *J. Glaciol.*, 41, 51-60.

Mote, T. L., 2007: Greenland surface melt trends 1973-2007: Evidence of a large increase in 2007. *Geophys. Res. Lett.*, 34, L22507, doi:10.1029/2007GL031976.

Nghiem, S. V., and 8 others, 2012: The extreme melt across the Greenland ice sheet in 2012. *Geophys. Res. Lett.*, 39, doi: 10.1029/2012GL053611.

Rennermalm, A. K., L. C. Smith, V. W. Chu, R. R. Forster, J. E. Box, and B. Hagedorn, 2012: Proglacial river stage, discharge, and temperature datasets from the Akuliarusiarsuup Kuua River northern tributary, Southwest Greenland, 2008-2011. *Earth Sys. Sci. Data*, 4, 1-12.

Rennermalm, A. K., and 11 others, 2013a: Understanding Greenland ice sheet hydrology using an integrated multi-scale approach. *Environ. Res. Lett.*, 8, 015017.

Rennermalm, A. K., L. C. Smith, V. W. Chu, J. E. Box, R. R. Forster, M. R. Van den Broeke, D. Van As, and S. E. Moustafa, 2013b: Evidence of meltwater retention within the Greenland ice sheet. *The Cryosphere*, 7, 1433-1445.

Tedesco, M., and 7 others, 2011: The role of albedo and accumulation in the 2010 melting record in Greenland. *Environ. Res. Lett.*, 6, 014005 doi:10.1088/1748-9326/6/1/014005.

Tedesco, M., X. Fettweis, T. Mote, J. Wahr, P. Alexander, J. E. Box, and B. Wouters, 2013a: Evidence and analysis of 2012 Greenland records from spaceborne observations, a regional climate model and reanalysis data. *The Cryosphere*, 7, 615-630, doi:10.5194/tc-7-615-2013.

Tedesco, M., and 8 others, 2013b: [Arctic] Greenland ice sheet [in "State of the Climate in 2012"]. *Bull. Amer. Meteor. Soc.*, 94, S121-S123.

van de Wal, R. S. W., W. Greuell, M. R. van den Broeke, C.H. Reijmer, and J. Oerlemans. 2005: Surface mass-balance observations and automatic weather station data along a transect near Kangerlussuaq, West Greenland. *Ann. Glaciol.*, 42, 311-316.

van de Wal, R. S. W., W. Boot, C. J. P. P. Smeets, H. Snellen, M. R. van den Broeke, and J. Oerlemans, 2012: Twenty-one years of mass balance observations along the K-transect, West Greenland. *Earth Sys. Sci. Data*, 5, 351-363, doi:10.5194/essdd-5-351-2012.

Velicogna, I., and J. Wahr. 2006: Acceleration of Greenland ice mass loss in spring 2004. *Nature*, 443, 329-331. doi:10.1038/Nature05168.

Lake Ice

C. Duguay[1], L.C. Brown[2], K.-K. Kang[1], H. Kheyrollah Pour[1]

[1]Interdisciplinary Centre on Climate Change & Department of Geography and Environmental Management, University of Waterloo, Waterloo, ON, Canada
[2]Climate Research Division, Environment Canada, Downsview, ON, Canada

November 21, 2013

Highlights

- Freeze-up in 2012 and break-up in 2013 both occurred earlier than the 2004-2012 average in most regions of the Arctic.
- Ice cover duration was shorter by ~1-4 weeks in regions adjacent to Hudson Bay, as well as in the western portion of the Canadian Arctic Archipelago, northern Alaska, Siberia and northern Scandinavia.
- Ice cover duration was longer by ~1-4 weeks for most parts of central to western Arctic Canada, southern Alaska, western Russia, southern Scandinavia and Baffin Island.

Lake ice is a sensitive indicator of climate variability and change. Lake ice phenology, which encompasses freeze-up (ice-on) and break-up (ice-off) dates, and ice cover duration, is largely influenced by air temperature changes and is therefore a robust indicator of regional climate conditions (Duguay et al. 2006, Kouraev et al. 2007). Long-term trends in ground-based observational records reveal increasingly later freeze-up and earlier break-up dates, closely corresponding to increasing air temperature trends, but with greater sensitivity at the more temperate latitudes (Brown and Duguay 2010, Prowse et al. 2011). Broad spatial patterns in these trends are also related to major atmospheric circulation patterns originating from the Pacific and Atlantic oceans such as the El Niño-La Niña/Southern Oscillation, the Pacific North American pattern, the Pacific Decadal Oscillation and the North Atlantic Oscillation/Arctic Oscillation (Bonsal et al. 2006, Prowse et al. 2011). Despite the robustness of lake ice as an indicator of climate change, a dramatic reduction in ground-based observational recordings has occurred globally since the 1980s (Lenormand et al. 2002, Duguay et al. 2006, IGOS 2007, Jeffries et al. 2012). Consequently, satellite remote sensing has assumed a greater role in observing lake ice phenology (Latifovic and Pouliot 2007, Brown and Duguay 2012, Kropáček et al. 2013, Surdu et al., 2013).

Ice phenology dates (freeze-up/ice-on and break-up/ice-off dates) and ice cover duration are derived from the NOAA Interactive Multisensor Snow and Ice Mapping System (IMS) 4 km resolution grid daily product for the 2012-2013 ice season over the Arctic, and are compared to average conditions for the length of the available satellite historical records. The IMS (Helfrich et al., 2007) incorporates a wide variety of satellite imagery, derived mapped products and surface observations. Ice-on and ice-off dates as well as ice duration were derived at the pixel level from this product. Freeze-up and break-up dates and ice-on and ice-off dates have the same meaning in this report.

Freeze-Up

Freeze-up (FU) in 2012-2013 occurred earlier than the 2004-2012 average by ~1-3 weeks for most regions of the Arctic (**Fig. 59**). Notable exceptions include lakes Ladoga and Onega (western Russia) and lakes of smaller size in southern Norway and adjacent areas of Sweden (~4-5 weeks earlier). Arctic-wide, a very few lakes experienced later FU than normal (~1-2 weeks later), and lakes in a small, localized region of lakes in southern Sweden experienced notably later FU than normal (~2-5 weeks). This is in contrast to the 2011-2012 ice season when FU occurred almost a full month later for most lakes located in the southern portion of northern Europe and part of the central portion of Arctic Canada (i.e., Great Slave Lake and Lake Athabasca regions) (Duguay et al. 2013).

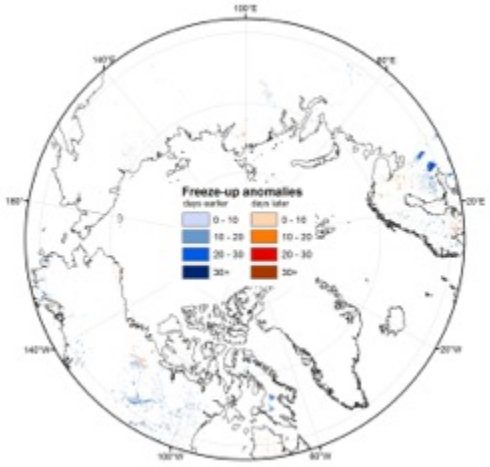

Fig. 59. Lake ice freeze-up anomalies in 2012-2013 relative to the 2004-2012 average from the NOAA IMS 4 km product.

Break-Up

Break-up (BU) dates in 2013 occurred ~1-3 weeks earlier than the 2004-2012 average over much of the Arctic, with the exception of Baffin Island and Ellesmere Island (Canada) (~1-4 weeks later) and the southern part of Scandinavia and western Russia (~1-5 weeks later) (**Fig. 60**). Lakes showing the largest BU anomalies with earlier dates (~3-4 weeks earlier) in 2013 are found in Siberia, consistent with spring-time positive air temperature anomalies and early snow cover loss (see the essays of *Air Temperature* and *Snow*). Break-up was also particularly early (by ~2-3 weeks) in the western Hudson Bay and Victoria Island regions of Canada. Earlier BU anomalies of the same magnitude were reported throughout Siberia in 2012 (Duguay et al. 2013).

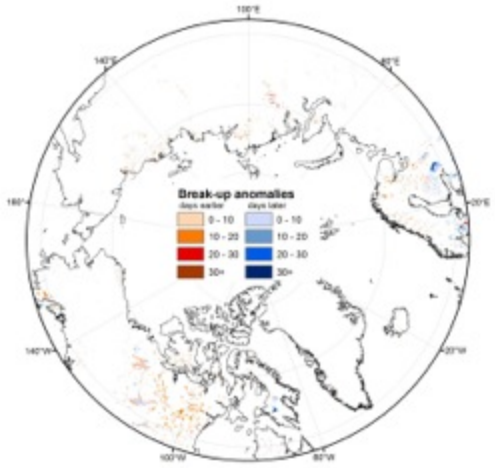

Fig. 60. Lake ice break-up anomalies in 2012-2013 relative to the 2004-2012 average from the NOAA IMS 4 km product.

Ice Cover Duration

In general, the spatial pattern of ice cover duration (ICD, **Fig. 61**) anomalies followed closely that of BU anomalies. ICD for 2012-2013 was shorter by ~1-4 weeks in regions adjacent to Hudson Bay, as well as in the western section of the Canadian Arctic Archipelago (CAA), northern Alaska, Siberia and northern Scandinavia. ICD was longer by ~1-4 weeks for most parts of central to western Arctic Canada, southern Alaska, western Russia, southern Scandinavia, and on Baffin Island. A few exceptions include: (1) Canadian lakes Amadjuak and Nettilling (the largest lakes of Baffin Island) and Lake Hazen on Ellesmere Island, which experienced longer ICD by ~40-70 days, and (2) north European lakes Onega and Ladoga (western Russia), as well as smaller lakes to their south, and lakes in southern Norway. ICD was longer by ~50-80 days in 2012-2013 compared to the 2004-2012 average for these Russian and Norwegian lakes.

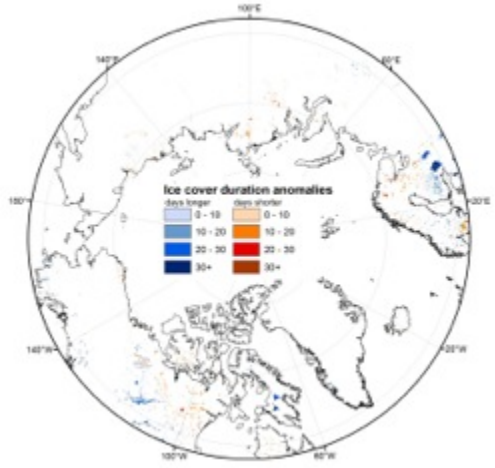

Fig. 61. Lake ice duration anomalies in 2012-2013 relative to the 2004-2012 average from the NOAA IMS 4 km product.

References

Bonsal, B. R., T. D. Prowse, C. R. Duguay, and M. P. Lacroix, 2006: Impacts of large-scale teleconnections on freshwater-ice duration over Canada. *J. Hydrol.*, 330, 340-353.

Brown L. C., and C. R. Duguay, 2010: The response and role of ice cover in lake-climate interactions. *Prog. Phys. Geogr.*, 34, 671-704.

Brown, L. C., and C. R. Duguay, 2012: Modelling lake ice phenology with an examination of satellite detected sub-grid cell variability, *Adv. Meteorol.*, 2012, Article ID 529064, 19 pages, doi:10.1155/2012/529064.

Duguay, C., L. Brown, K.-K. Kang, and H. Kheyrollah Pour, 2013: [The Arctic] Lake ice [In "State of the Climate in 2012"]. *Bull. Am. Meteorol. Soc.*, 94, S124-S126.

Duguay, C. R., T. D. Prowse, B. R. Bonsal, R. D. Brown, M. P. Lacroix, and P. Ménard, 2006: Recent trends in Canadian lake ice cover. *Hydrol. Processes*, 20, 781-801.

Helfrich, S. R., D. McNamara, B. H. Ramsay, T. Baldwin, and T. Kasheta, 2007: Enhancements to, and forthcoming developments in the Interactive Multisensor Snow and Ice Mapping System (IMS). *Hydrol. Processes*, 21, 1576-1586.

IGOS, 2007: *Integrated Global Observing Strategy Cryosphere Theme Report - For the Monitoring of our Environment from Space and from Earth*. World Meteorological Organization, WMO/TD-No. 1405, 100 pp.

Jeffries, M. O., K. Morris, and C. R. Duguay, 2012: Floating ice: lake ice and river ice. *Satellite Image Atlas of Glaciers of the World - State of the Earth's Cryosphere at the Beginning of the 21st Century: Glaciers, Global Snow Cover, Floating Ice, and Permafrost and Periglacial Environments*, R. S. Williams, Jr. and J. G. Ferrigno, Ed., U.S. Geological Survey Professional Paper 1386-A, A381-A424.

Kouraev, A. V., S. V. Semovski, M. N. Shimaraev, N. M. Mognard, B. Légresy, and F. Remy, 2007: Observations of Lake Baikal ice from satellite altimetry and radiometry. *Remote Sens. Environ.*, 108, 240?253.

Kropáček, J., F. Maussion, F. Chen, S. Hoerz, and V. Hochschild, 2013: Analysis of ice phenology of lakes on the Tibetan Plateau from MODIS data. *The Cryosphere*, 7, 287-301.

Latifovic, R., and D. Pouliot, 2007: Analysis of climate change impacts on lake ice phenology in Canada using the historical satellite data record. *Remote Sens. Environ.*, 16, 492-507.

Lenormand, F., C. R. Duguay, and R. Gauthier, 2002: Development of a historical ice database for the study of climate change in Canada. *Hydrol. Processes*, 16, 3707-3722.

Prowse, T., K. Alfredsen, S. Beltaos, B. Bonsal, C. Duguay, A. Korhola, J. McNamara, W. F. Vincent, V. Vuglinsky, and G. A. Weyhenmeyer, 2011: Past and future changes in lake and river ice. *Ambio*, 40 (S1), 53-62.

Surdu, C., C. R. Duguay, L. C. Brown, and D. Fernández Prieto, 2013: Response of ice cover on shallow lakes of the North Slope of Alaska to contemporary climate conditions (1950-2011): radar remote sensing and numerical modeling data analysis, *The Cryosphere Discussion*, 7, 3783-3821.

Permafrost

V.E. Romanovsky[1], S.L. Smith[2], H.H. Christiansen[3,4], N. I. Shiklomanov[5], D.A. Streletskiy[5], D.S. Drozdov[6], N.G. Oberman[7], A.L. Kholodov[1], S.S. Marchenko[1]

[1]Geophysical Institute, University of Alaska Fairbanks, Fairbanks, Alaska, USA
[2]Geological Survey of Canada, Natural Resources Canada, Ottawa, ON, Canada
[3]Geology Department, University Centre in Svalbard, UNIS, Norway
[4]Institute of Geography and Geology, University of Copenhagen, Denmark
[5]Department of Geography, George Washington University, Washington, DC, USA
[6]Earth Cryosphere Institute, Tyumen, Russia
[7]MIRECO Mining Company, Syktyvkar, Russia

November 26, 2013

Highlights

- In 2013, new record high temperatures at 20 m depth were measured at two northernmost permafrost observatories on the North Slope of Alaska, in the Brooks Range, Alaska, and in the High Canadian Arctic, where measurements began in the late 1970s.
- During the last fifteen years (1998-2012), active-layer thickness has increased in the Russian European North, northern East Siberia and Chukotka.
- In 2012 in west Siberia, the active-layer thickness was the greatest observed since 1996, and in the Russian European North it was the greatest observed since measurements began in 1998.

Introduction

The most direct indicators of changes in permafrost state are temperature and active layer thickness (ALT). Permafrost is ground that remains frozen for two or more years. The active layer is the top layer of soil and/or rock that thaws during the summer and freezes again during the fall. Permafrost temperature at a depth where seasonal temperature variations cease to occur can be used as an indicator of long-term change. This depth varies from a few meters in warm, ice-rich permafrost to 20 m and more in cold permafrost and in bedrock (Smith et al. 2010, Romanovsky et al. 2010a). Where continuous, year-round temperature measurements are available, the mean annual ground temperature (MAGT) at any depth within the upper 15 m of permafrost can be used as a measure of permafrost change. Such measurements can be obtained from boreholes, which now number ~600. A borehole inventory, including MAGTs for most of the boreholes are available online at http://nsidc.org/data/g02190.html.

Permafrost Temperature

Alaska: In 2013, new record high temperatures at 20 m depth were measured at some permafrost observatories on the North Slope of Alaska and in the Brooks Range (**Fig. 62a**), where measurements began in the late 1970s and early 1980s (**Fig. 62b**). The 20 m temperatures in 2013 were higher than in 2012 by 0.03°C at West Dock and Deadhorse (**Fig. 62b**) on the North Slope and by 0.06°C at Coldfoot (**Fig. 62c**) in the southern foothills of the Brooks Range. Permafrost temperatures at the other North Slope sites were exactly the same

as in 2012, except for Happy Valley, where lower (by 0.06°C) temperatures than in 2012 were observed. At a depth of 20 m, temperature has increased since 2000 by +0.44°C per decade at West Dock, by +0.47°C per decade at Deadhorse, and by ~ +0.28°C per decade at Franklin Bluffs and Happy Valley (**Fig. 62b**). Permafrost temperatures in Interior Alaska (**Fig. 62a**) continued to decrease in 2013 (**Fig. 62c**), a cooling that dates back to 2007. Consequently, temperatures in 2013 at some sites in Interior Alaska were lower than those located further north, e.g., temperatures at College Peat and Birch Lake are now lower than at Old Man and Chandalar Shelf in the Brooks Range (**Fig. 62**). During the late 1980s, temperatures at College Peat and Birch Lake were 0.7°C higher than at Old Man and Chandalar Shelf, respectively.

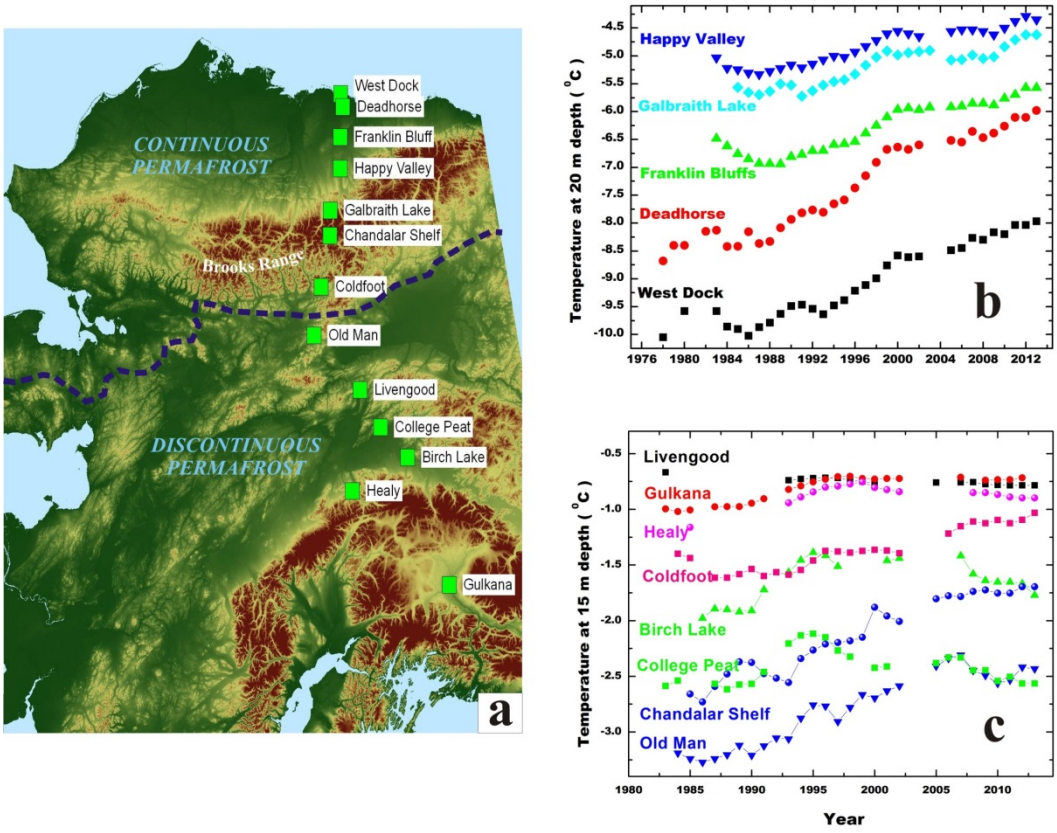

Fig. 62. (a) Map of Alaska showing the continuous and discontinuous permafrost zones (separated by the broken blue line) and location of a north-south transect of permafrost temperature measurement sites; (b) and (c) time series of mean annual permafrost temperature at depths of 20 m and 15 m, respectively, below the surface at the measurement sites (updated from Romanovsky et al. 2012).

Canada: In 2012 (the most recent year for which data are available), temperatures in the upper 25 m of ground at Alert, northernmost Ellesmere Island, were the highest since measurements began in 1978 (**Fig. 63**). At a depth of 15 m in borehole BH5, temperature has increased by ~ +1.5°C per decade since 2000, which is about +1°C higher than the rate for the entire record (**Table 8**). Even at a depth of 24 m, temperature has increased since 2000 at a rate approaching +1°C per decade (**Table 8**). Note that the rate of warming at Alert is greater than on the North Slope of Alaska.

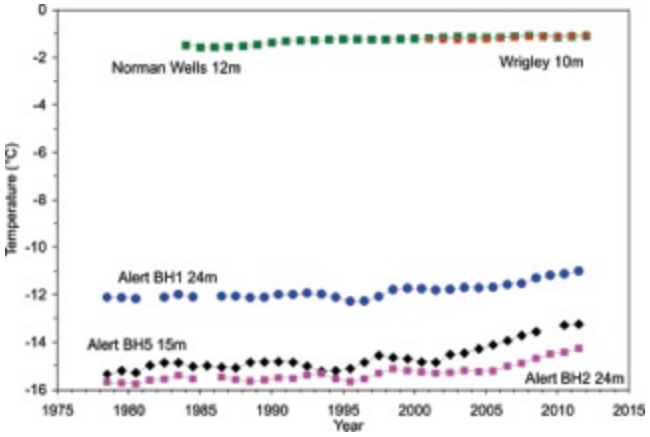

Fig. 63. Time series of mean annual permafrost temperatures at 10 and 12 m depth at Wrigley (red squares) and Norman Wells (green squares), respectively, in the discontinuous permafrost zone of the central Mackenzie River Valley, Northwest Territories, Canada, and at 15 m and 24 m depth in continuous permafrost at CFS Alert, Nunavut, Canada (updated from Smith et al. 2010, 2012). The method described in Smith et al. (2012) was used to address gaps in the data and produce a standardized record of mean annual ground temperature.

Table 8. Rate of temperature change in boreholes at Alert, northernmost Ellesmere Island, and at Norman Wells and Wrigley in the Mackenzie River Valley.

Location	Rate of change (°C/decade)	Rate of change (°C/decade)
Alert BH1 (24m)	0.28°C (1978-2012)	0.74°C (2000-2012)
Alert BH2 (24m)	0.32°C (1978-2012)	0.98°C (2000-2012)
Alert BH5 (15m)	0.48°C (1978-2012)	1.58°C (2000-2012)
Norman Wells (12 m)	0.17°C (1984-2012)	0.07°C (2000-2012)
Wrigley (10 m)	Insufficient data	0.2°C (2001-2012)

Permafrost in the central Mackenzie River Valley in northwestern Canada continues to warm, but much more slowly than at Alert (**Fig. 63**, **Table 8**). Note also that permafrost in this region is much warmer than it is at Alert (**Fig. 63**). At depths of 10-12 m, ground temperature at Norman Wells and Wrigley has risen by 0.07-0.2°C per decade since 2000. At Norman Wells, the rate of warming has decreased during the last decade (**Table 8**).

Russia: Permafrost temperature has increased by 1-2°C in northern Russia during the last 30 to 35 years (Romanovsky et al. 2010b). This is similar to the warming observed in Alaska during the same period. In the Polar Ural, for example, temperatures at 15 m depth at colder permafrost sites have been increasing by ~ +0.5°C per decade since the late 1980s (**Fig. 64**, ZS-124, R-92, and R57 sites). At the same time, at the warmer permafrost site, KT-16A, the warming has been much less pronounced (**Fig. 64**). At some warmer permafrost sites a slight cooling has been observed since 2009 (sites ZS-124 and KT-16a (**Fig. 64**).

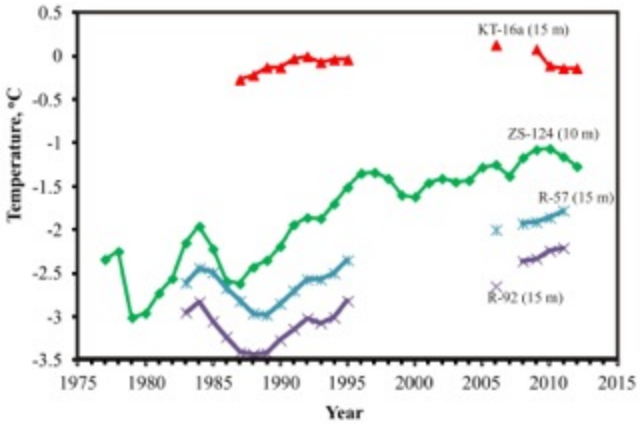

Fig. 64. Time series of mean annual permafrost temperature at 10 m and 15 m depth at four research sites in the Polar Ural, Russia.

Nordic area: There are limited long-term permafrost temperature records for the Nordic area. A few of these were initiated at the end of the 1990s, and since then temperature has increased at rates of +0.4 to +0.7°C/decade in the highlands of southern Norway, northern Sweden and Svalbard, with the largest warming in Svalbard and in northern Scandinavia (Isaksen et al. 2011; Christiansen et al. 2010).

Active Layer Thickness

In 2012 (the most recent year for which data are available), a majority of Alaska and Russian regions reported higher ALT values relative to the 1995-2012 average (**Fig. 65**). On the North Slope of Alaska, for example, ALT was on average 6% higher than the 1995-2012 average of 0.47 m. Compared to 2011, however, it was about 2% lower. In Interior Alaska ALT has been relatively unchanged since 2007, when it reached a maximum; the 2012 ALT values were slightly higher than 2011 and close to those of 2007-2010. Sites on the Seward Peninsula, westernmost Alaska mainland, showed much lower (by 20%) ALT values in 2012 relative to the long-term mean of 1999-2012.

Fig. 65. Active-layer change in six different Arctic regions according to the Circumpolar Active Layer Monitoring (CALM) program (http://www.gwu.edu/~calm/). The data are presented as annual percentage deviations from the mean value for the period of observations (indicated in each graph). The number of CALM sites within each region varies and is indicated in each graph. Thaw depth observations from the end of the thawing season were used. Availability of at least ten years of continuous thaw depth observations through the 2012 thawing season was the only criterion for site selection. Solid red lines show mean values for the regions. Dashed grey lines represent maximum and minimum values for the region.

A large increase in ALT was observed in West Siberia during 2009-2012, with 2012 ALT values being the highest (10% higher than 1995-2012 mean or 1.2 m) since 1996. A more or less continuous thickening of the active layer has been reported for Russian European North locations (Kaverin et al. 2012), where ALT in 2012 was the highest since observations began in 1998. Central Siberian locations also report the highest ALT values since observations began, in this case in 2005. In 2012 in eastern Siberia, ALT was 10% lower than in 2011 and all sites had lower ALT than the 1996-2012 average of 0.6 m. In 2012 in Chukotka (Russian Far East), ALT values were about 3% higher than in 2011, but overall there has been a progressive decrease in ALT since 2007, when it reached a maximum since observations began in 1994.

A progressive increase in ALT has been observed in some Nordic countries, e.g., in the Abisko area of Sweden since the 1970s, with an accelerated rate after 1995 that resulted in disappearance of permafrost in several mire landscapes (e.g., Åkerman and Johansson 2008, Callaghan et al. 2010). The increase in thaw propagation ceased during 2007-2010, coincident with drier summer conditions (Christiansen et al. 2010). Increases in ALT since the late 1990s have been observed on Svalbard and Greenland, but these are not spatially and temporally uniform (Christiansen et al. 2010).

References

Åkerman, H. J., and M. Johansson, 2008: Thawing permafrost and thicker active layers in sub-arctic Sweden. *Permafr. Periglacial Proc.*, 19, 279-292.

Callaghan, T. V., F. Bergholm, T. R. Christensen, C. Jonasson, U. Kokfelt, and M. Johansson, 2010: A new climate era in the sub-Arctic: Accelerating climate changes and multiple impacts, *Geophys. Res. Lett.*,37, L14705, doi:10.1029/2009GL042064.

Christiansen, H. H., and 17 others, 2010: The Thermal State of Permafrost in the Nordic area during the International Polar Year, *Permafr. Periglacial Proc.*, 21, 156-181.

Isaksen, K., R. S. Oedegård, B. Etzelmüller, C. Hilbich, C. Hauck, H. Farbrot, T. Eiken, H. O. Hygen, and T. F. Hipp, 2011: Degrading mountain permafrost in southern Norway: spatialand temporal variability of mean ground temperatures, 1999-2009, *Permafr. Periglacial Proc.*, 22, 361-377.

Kaverin, D., G. Mazhitova, A. Pastukhov, and F. Rivkin, 2012: The Transition Layer in Permafrost-Affected Soils, Northeast European Russia. *10th International Conference on Permafrost, Salekhard, Russia*, June 25 - 29, 2012, Vol. 2, 145-148.

Romanovsky, V. E., S. L. Smith, and H. H. Christiansen, 2010a: Permafrost Thermal State in the Polar Northern Hemisphere during the International Polar Year 2007-2009: a synthesis. *Permafr. Periglacial Proc.*, 21, 106-116.

Romanovsky, V. E., and 11 others, 2010b: Thermal State of Permafrost in Russia. *Permafr. Periglacial Proc.*, 21, 136-155.

Romanovsky, V., N. Oberman, D. Drozdov, G. Malkova , A. Kholodov, and S. Marchenko, 2012: Permafrost, [in "State of the Climate in 2010"]. *Bull. Amer. Meteor. Soc.*, 93 (7), S137-S138.

Smith, S. L., V. E. Romanovsky, A. G. Lewkowicz, C. R. Burn, M. Allard, G. D. Clow, K. Yoshikawa, and J. Throop, 2010: Thermal State of Permafrost in North America—A Contribution to the International Polar Year. *Permafr. Periglacial Proc.*, 21, 117-135.

Smith, S. L., J. Throop, and A. G. Lewkowicz, 2012: Recent changes in climate and permafrost temperatures at forested and polar desert sites in northern Canada. *Can. J. Earth Sci.*, 49, 914-924.